UNIVERSIDAD AUTÓNOMA DE MADRID
DEPARTAMENTO DE BIOQUÍMICA

Understanding the mechanisms of chemoresistance and modeling tumor growth in glioblastoma

Álvaro Curiel García
PhD thesis

Madrid, 2019

Universidad Autónoma de Madrid
Facultad de Medicina
Departamento de Bioquímica

Understanding the mechanisms of chemoresistance and modeling tumor growth in glioblastoma

Doctoral thesis submitted to the Universidad Autónoma de Madrid for the degree of Doctor of Philosophy by M.Sc. in Biomedicine research

Alvaro Curiel García

Thesis Director: Dr. Massimo Squatrito

Seve-Ballesteros Foundation Brain Tumor Group
Molecular Oncology Programme
Spanish National Cancer Research Centre

This thesis submitted for the degree of Doctor of Philosophy at the Universidad Autónoma de Madrid, has been complied in the Seve Ballesteros Foundation – Brain Tumor Group at the Spanish National Cancer Research Centre (CNIO), under the supervision of Dr. Massimo Squatrito.

The last part of this work was recently published in the journal *Nature Communications:*

OLDRINI, B.*, **CURIEL-GARCÍA, Á**.*, MARQUES, C., MATIA, V., ULUÇKAN, Ö., GRAÑA-CASTRO, O., TORRES-RUIZ, R., RODRIGUEZ-PERALES, S., HUSE, J. T. & SQUATRITO, M. 2018. Somatic genome editing with the RCAS-TVA-CRISPR-Cas9 system for precision tumor modeling. Nature Communications 9, 1466. *equal contribution

In addition, the following work was published in *Nature Communications* as a collaborative project:

OLDRINI, B., HSIEH, W. Y., ERDJUMENT-BROMAGE, H., CODEGA, P., CARRO, M. S., **CURIEL-GARCIA, A.**, CAMPOS, C., POURMALEKI, M., GROMMES, C., VIVANCO, I., ROHLE, D., BIELSKI, C. M., TAYLOR, B. S., HOLLMANN, T. J., ROSENBLUM, M., TEMPST, P., BLENIS, J., SQUATRITO, M. & MELLINGHOFF, I. K. 2017. EGFR feedback-inhibition by Ran-binding protein 6 is disrupted in cancer. Nat Commun, 8, 2035.

These publications are attached at the end of this thesis

This work was supported by the following grant:

- Severo Ochoa PhD Fellowship by the Ministry of Economy and Competitiveness 2013 Call – Alvaro Curiel

A mis padres

No basta examinar; hay que contemplar: impregnemos de emoción y simpatía las cosas observadas; hagámoslas nuestras, tanto por el corazón como por la inteligencia.

Santiago Ramón y Cajal

"No se consigue nada sin esfuerzo, y lo que se consigue sin esfuerzo, ni lo aprecias, ni lo valoras"

Severiano Ballesteros

Acknowledgments

Acknowledgments

The content of this thesis is the result of 4 years of intense research. It would not have been possible without the support of many great people.

First of all, I want to thank Dr. Massimo Squatrito for giving me the opportunity to perform my PhD thesis work in his laboratory. I want to thank you all your support, patience and guidance over these years. I am very grateful about the scientific discussions we shared in these years.

I am also grateful for the support of all the current and former members of Seve Ballesteros Foundation – Brain tumors group as well as the Cancer Cell Biology program. Thanks all of you for your scientific input.

I am thankful for having met so many amazing scientists during my time in Madrid and I am happy about the wonderful friendships I have made.

Quisiera dedicar unas palabras a todos los pacientes, familiares y amigos que luchan cada día por ganar esta "batalla". En mi caso, acordarme especialmente de Felisa Molledo, Mª del Pilar Martínez, Emilio García, y Celedonio García; sin olvidarme de Seve Ballesteros, a quién su Fundación da nombre al laboratorio en el CNIO y gracias a su generoso apoyo nos permite avanzar en entender esta enfermedad. Vuestra lucha y ganas de vivir despertaron mi pasión por la investigación.

No quiero acabar sin agradecer a mi familia, amigos y muy especialmente a Rut por su apoyo incondicional en todo momento, que tanto me ha servido para seguir adelante.

A todos vosotros, gracias de corazón.

Summary

Summary

Glioblastoma is the most common and malignant brain tumor. Standard of care for GBM includes resection of the tumor mass, followed by concurrent radiotherapy and chemotherapy with the alkylating agent Temozolomide (TMZ) However, TMZ is not effective in long-term and patients develop resistance and, consequently, recurrence in the disease.

In order to identify genes that modulate TMZ resistance, we have performed a forward genetic screen using the PiggyBac transposon system for an insertional mutagenesis screen in human haploid cells (Hap1). We were able to identify and validate the mismatch repair (MMR) component MSH6, which is known to be related to resistance to TMZ. MSH6 inactivating mutations are found in 20% of the patients resulting in chemotherapy failure. We then performed a compound screening with 120 drugs either FDA-approved or under clinical trials looking for MMR synthetic lethality. After a pilot study, we were not able to validate any candidate compound and further experiments will be needed in order to identify possible drugs that sensitize the MMR-deficient cells. Drug resistance and the ability of the drug to cross the blood brain barrier are the main limitations of treating GBM patients. It is also important the development and/or testing of new compounds that prolong the survival. We have tested the efficacy of a by-alkykating agent Val-083, currently in clinical trials. Preliminary data show better efficacy as compared to TMZ in GBM cells (even in those cells that are resistant to TMZ). Moreover, we observed an additive effect in combination with TMZ both *in vitro* and *ex vivo*.

Finally, the identification of the molecular alterations that occur in GBM opens a new window for the study of the disease as well as for the validation of novel therapies. Consequently, animal models will be needed to recreate these alterations that occur in patients. One of the most widely mouse model used for the study of gliomas is the RCAS-TVA-based somatic gene transfer system. We have developed a new RCAS/Tva-CRISPR/Cas9 mouse model combining the advantages (feasible, versatile, resemble human GBM features) of the RCAS/Tva system and the genome editing capacity of the CRISPR/Cas9. We have been able to recreate, in a time-controlled manner, different genetic alterations of tumor suppressor genes (TSGs) that have a known role in gliomagenesis. As a result, we have developed a powerful tool that can recapitulate molecular features found in GBM patients.

Resumen

El glioblastoma (GBM) es tumor cerebral más común y maligno. Su tratamiento incluye cirugía, radio y quimioterapia utilizando un agente alquilante llamado Temozolomida (TMZ). Sin embargo, la TMZ muestra una baja eficiencia a largo plazo y los pacientes desarrollan resistencia y un relapso de la enfermedad.

Para poder identificar genes que puedan estar modulando la respuesta a TMZ, realizamos un "*screening"* genético mediante el sistema de transposones "PiggyBac" en células haploides humanas. Validamos el gen MSH6, un gen relacionado con la ruta de reparación de los errores de apareamiento de bases durante la replicación del ADN (genes MMR). Es bien conocido el papel de MSH6 con la resistencia a TMZ. Se ha visto que los genes MMR se encuentran alterados en un 20% de los pacientes con GBM que desarrollaron resistencia a TMZ, indicando la importancia de desarrollar terapias alternativas a las actuales. Realizamos otro *"screening"* con 120 compuestos aprobados por la FDA o en ensayos clínicos en busca de letalidad sintética con células deficientes de la vía MMR. Estudios preliminares mostraron que ningún compuesto candidato era más eficaz en estas células y nuevos experimentos serán necesarios para poder identificar compuestos que generen letalidad sintética en estás células.

La resistencia al tratamiento convencional y la capacidad de los compuestos en atravesar la barrera hematoencefálica son factores limitantes para los pacientes con GBM. Uno de los objetivos actuales es el desarrollo de nuevos compuestos que prologuen su supervivencia. Así, hemos testado la eficacia de otro agente alquilante, denominado Val-083, observando mayor eficacia que la TMZ en células de GBM, y un efecto sinérgico en combinación con TMZ *in vivo* y *ex vivo*.

La identificación de alteraciones moleculares en gliomas abre nueva ventana en el estudio de esta enfermedad. Así, modelos animales precisos que recreen las alteraciones descritas en pacientes se antojan necesarios. Uno de los modelos murinos más usados para el estudio de gliomas es el sistema de transferencia génica RCAS/Tva. Desarrollamos un nuevo modelo RCAS/Tva-CRISPR/Cas9 que combina las ventajas del sistema RCAS/Tva (versátil, recapitulación de las características de los GBM humanos) con el sistema de edición génica CRISPR/Cas9. Generamos gliomas deficientes en genes supresores de tumores que se sabe tienen un papel relevante en el desarrollo de gliomas. De esta forma, tenemos una potente herramienta que nos puede permitir recrear de manera eficaz diferentes alteraciones encontradas en pacientes con GBM.

Table of contents

Table of contents

Table of contents

Table of contents

Abbreviations

AIC	5-aminoimidazole-4-carboxamide
ALV-A	Avian Leukosis virus subgroup A
AML	Acute myeloid leukemia
ATP	Adenosine triphosphate
ATRX	Alpha thalassemia/mental retardation syndrome X linked
BBB	Blood brain barrier
BER	Base excision repair
BLI	Bioluminescence analysis
CIOMS	Council for International Organizations of Medical Sciences
Cas9	CRISPR associate protein 9
CNS	Central Nervous System
CSCs	Cancer stem cells
CT	Computerized axial tomography
CRISPR	clustered regularly interspaced short palindromic repeats
DBS	DNA double strand break
DF1	Chicken fibroblast cell line
DMEM	Dulbecco´s Modified Eagle´s Medium
D-2-HG	D-2 hydroxyglutarate
EGFR	Epidermal growth factor receptor
EXO1	Exonuclease 1
FBS	Fetal bovine serum
FDA	Food and Drug Administration
FELASA	Federation of European Laboratory Animal Science Associations
Fluc	Firefly luciferase
GBM	Glioblastoma Multiforme
gDNA	Genomic DNA
GEMMs	Genetically engineered mouse model
GFAP	Glial fibrillary acidic protein
GSCs	Glioma stem cells
GTva	GFAP/Tva
HAP1	Human haploid cells
HDR	Homology directed repair
HR	Homologous recombination

HTS	High-Throughput Screening
IDH1/2	Isocitrate Dehydrogenase 1/2
IFP	Intermediate filament protein
IHC	Immunohistochemistry
ITRs	Inverted terminal repeat sequences
IR	Ionizing radiation
KO	Knock-out
LTR	Long terminal repeat
MCS	Multiple cloning site
MDM2	Mouse double minute 2
MGMT	O^6-Methylguanine DNA Methyltransferase
mi-RNA	micro-RNA
MLH	MutL homologs proteins
MMR	DNA Mismatch repair
mNS	Mouse neurospheres
MRI	Magnetic resonance imaging
MSH	Mut S homologs proteins
MSH6	Mut S homologs 6
MTIC	5-(3-methyltriazen-1-yl)-imidazole-4-carboxamide
NHEJ	Non-homologous end joining
NT	Non targeting
MTIC	Monomethyl triazene 5-(3-methyltriazen-1-yl)-imidazole-4-carboxamide
NTva	Nestin/Tva
N^7-MeG	N^7 - methylguanine
N^3-MeA	N^3 - methyladenine
O^6-MeG	O^6 - methylguanine
OS	Overall survival
OV	Oncolytic viruses
PAM	Protospacer-associated motif
PB	PiggyBac
PDGFA	Platelet-derived growth factor A
PDGFB	Platelet-derived growth factor B

PDGFRa	Platelet-derived growth factor receptor alpha
PD1	Programmed cell death-1 receptor
PD-L1	Programmed cell death-1 ligand
PAM	Protospacer-associat-ed motif
PFA	Paraformaldehyde
PI	Propidium iodide
PMS	Post meiotic segregation proteins
PTEN	Phosphatase and tensin homolog
RCAS	Replication Competent ALV LTR with a splice acceptor
RNAi	RNA interference
RT-PCR	Real-time PCR
sgRNA	Small-guide RNA
shRNA	Short hairpin RNA
sp-PCR	Splinkerette-PCR
SVZ	Subventricular zone
TALENs	Transcription activator-like proteins
TMZ	Temozolomide
TSG	Tumor suppressor gene
TTFields	Tumor treating fields
Tva	Tumor Virus A
VAL-083	1,2:5,6-Dyanhydrogalactitol
WHO	World Health Organization
ZFN	Zinc finger nucleases

Introduction

1. Central Nervous System tumors

Central nervous system (CNS) tumors include both non-malignant and malignant tumors of the brain and spinal cord. These brain tumors are the second cause of cancer in children and adolescents. However, in adults, they are rare disease associated with a high rate of morbidity and mortality, especially in patients between 55 to 64 years of age (Siegel et al., 2018).

2. Gliomas

In 1863, Rudolf Virchow described a tumor that “arises from the glial cells within the brain”, using the term glioma for the first time (David, 1988). These tumors are a highly heterogenous and, every year, around 80% of all newly diagnosed primary brain tumors are gliomas. There are about 18,000 new cases in the United States of America with an incidence of 3-4 case per 100,000 individuals (American Cancer Society, 2017) and a median age at diagnosis of 64 (Ostrom et al., 2017). In Spain, primary CNS tumors represent 2% of total cancer in adults and up to 15% in children under 15 years of age; proving that it is, at least in adults, a rare tumor with higher incidence in men than women (SEOM, 2017).

The incidence of gliomas increases with age and the 60-year-old population has the highest probability to develop the malignant form of glioma, glioblastoma multiforme (GBM). (Ohgaki & Kleihues, 2005). Many environmental factors have been studied, being therapeutic doses of ionizing radiation (IR) the only definite factor recognized as a causative agent (Ostrom & Barnholtz-Sloan, 2011; Weller et al., 2015). Although biologically relevant, known genetic predisposition syndromes including Cowden, Turcot, Li-Fraumeni, neurofibromatosis type 1 and type 2, tuberous sclerosis, or familial schwannomatosis account for only < 1% of all gliomas (Weller et al., 2015).

Finally, clinical epidemiologic data on patients with gliomas are limited due to not only the low incidence, but also to their high morbidity, heterogeneity and mortality (Rasmussen et al., 2017).

2.1. Glioma classification

Different types of gliomas have been classified according to the histological appearance under the light microscope. However, it is now clear that different molecular profiles of the tumor lead to different responses to treatment (Ramaswamy & Taylor. 2016). The World Health Organization (WHO) classification system of brain tumors has recently been updated and some tumors have been re-defined by a combination of microscopic, morphologic, molecular and genetic factors (Louis et al., 2016).

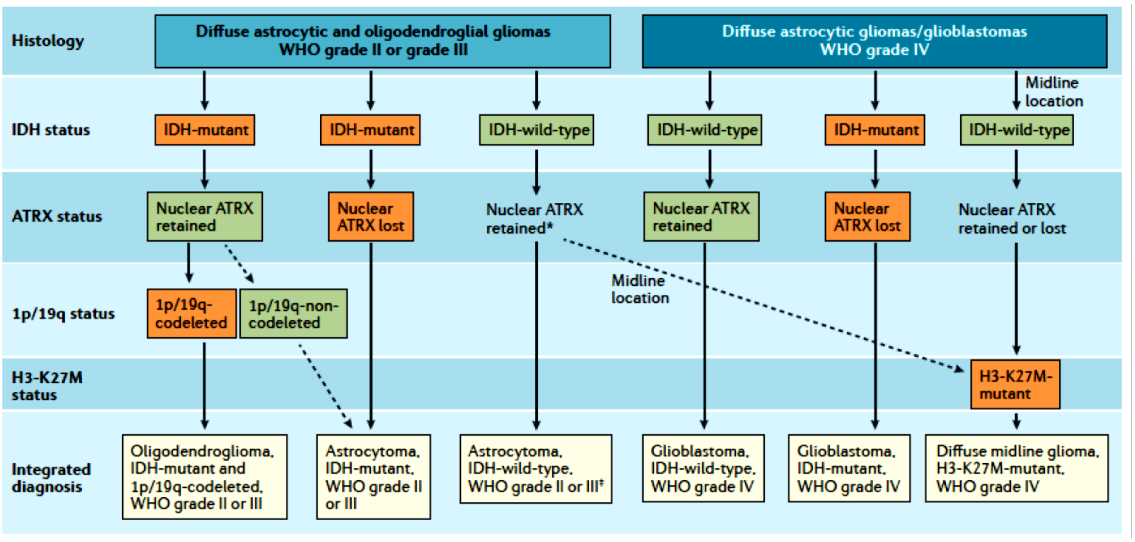

Figure 1: 2016 WHO Classification of Tumors of the CNS in adults. In addition to histological appearance, diffuse gliomas are evaluated for isocitrate dehydrogenase 1 or 2 (IDH)-mutation status. Evaluation of the 1p/19q codeletion is performed in patients with IDH-mutant tumors with ATRX null expression to further characterize these tumors. IDH-wild-type gliomas located in midline structures (thalamus, brainstem, or spinal cord) are additionally tested for histone-H3K27M mutations. Dashed lines indicate smaller subgroups of tumors with the respective diagnoses. (Reifenberger et al., 2017)

This is a novel concept in which, for the first time in the classification of the CNS tumor entities in adults, histological features are combined with the incorporation of molecular parameters (Figure 1). In an evidence-based manner for low-grade gliomas, gliomas can be now distinguished by analyzing the presence of IDH mutations (either in IDH1 or IDH2). These alterations have been associated with patients diagnosed with low-grade gliomas (WHO grade II) (Parsons et al., 2008). However, there is a small subset of patients with secondary GBM (progressing from lower grade) with IDH mutations (Parsons et al., 2008). In these cases, the

prognosis is better than IDH wild-type tumors (Louis et al., 2016) (Figure 1). The alpha thalassemia/mental retardation syndrome X linked (ATRX) gene mutations in glioma is primarily seen in tumors with IDH mutations (Louis et al., 2016; Bush & Butowski, 2017) (Figure 1). ATRX inactivation within gliomas can be due to mutations, deletions or gene fusions having better prognosis perhaps due to the glioma-CpG island methylated phenotype (Wiestler et al., 2013; Cancer Genome Atlas, 2015). Another genetic hallmark identified in low-grade glioma is the loss of the short arm of chromosome 1 and the long of chromosome 19 (Reifenberger et al., 1995). These tumors carry a favorable prognosis and good response to chemotherapy in comparison to similar grade tumors without codeletion (Kaloshi et al., 2007; Louis et al., 2016) (Figure 1). It is critical to evaluate the presence of this codeletion in GBM patients to ensure an accurate diagnosis (Yip et al., 2008). Around 90% of GBM patients are IDH wild-type and retain nuclear ATRX expression although a small fraction of GBM patients share these molecular characteristics in concomitance with mutations involving histone H3 (Schwartzentruber et al., 2012) (Figure1). These mutations are mainly present in pediatric gliomas and they are not associated with worse survival (Picca et al., 2018).

The main goal of this new classification was to define more heterogeneous categories with greater prognostic value. It would also lead to improved patient management and more accurate determinations of prognosis and treatment response (Louis et al., 2016). This undoubtedly constitutes a paradigm shift and represents a clear advance in tumor classification.

Additionally, GBM can be divided in primary and secondary GBMs. Primary GBMs, which is the most aggressive form, arise de novo without clinical and histological evidences of precursor lesion. Secondary GBMs, produced in patients of 45 years of age or younger, progress slowly from preexisting lower-grade astrocytoma (Smith & Ironside, 2007; Agnihotri et al., 2013). Hallmark alterations of primary GBM include epidermal growth factor receptor (EGFR) gene mutation and amplification, overexpression of mouse double minute 2 (MDM2), TERT promoter mutation or loss of tensin homolog (PTEN). Other alterations such as mutations in IDH1/2, TP53 and ATRX have been found in

secondary GBMs (Alifieris & Trafalis, 2015; Wilson et al., 2014; Young et al., 2015). Moreover, four GBM subtypes have been identified (classical, pro-neural, neural, and mesenchymal), having each of them with distinctly different patterns of disease progression and survival outcomes (Verhaak et al., 2010; Brennan et al., 2013; Wang et al., 2015).

3. Glioblastoma multiforme: epidemiology, pathology, prognosis and molecular biology

GBM is the most common malignant form of primary brain tumor in adults, accounting for over 80% of all primary gliomas (Ostrom et al., 2017). Approximately 0.59 to 3.69 GBM cases per 100,000 are diagnosed annually worldwide (Ohgaki & Kleihues, 2005), and the number of deaths is more than breast and lung cancer (Burnet et al., 2005). The lethality of the disease is associated with an aggressive clinical course (poor prognosis), with a median overall survival (OS) of 15 months (Stupp et al., 2005). In particular, only 17-30% of patients with newly diagnosed GBM survive after 1 year and 3-5% after 5 years (Ohgaki et al., 2004).

GBM signs and symptoms can change depending on the affected regions. These may develop rapidly and can sometimes be confused with other pathologies. Necrotic areas produced by tumor malignancy destroy the brain tissue and generate focal neural deficit and cognitive impairments (Omuro & DeAngelis, 2013). Moreover, tumor size can produce an increase of the intracranial pressure and edema resulting in headache (Borsook, 2012). Around 20-40% of the patients present seizures usually with a focal onset (Omuro & DeAngelis, 2013). Thus, the most frequent location for GBM is the cerebral hemispheres. 95% of these tumors arise in the supratentorial regions, and only low percentage of tumors occur in cerebellum, brainstem or spinal cord (Nakada et al., 2011).

The diagnostic technique used is magnetic resonance imaging (MRI). Its superior soft tissue contrast allows better visualization of the complexity and the heterogeneity of the tumor lesion than computerized axial tomography (CT) scan

(Nelson & Cha, 2003). Tumors are usually unifocal but can also be multifocal (Omuro & DeAngelis, 2013).

GBMs are morphologically heterogeneous tumors characterized by considerable cellularity and mitotic activity, poorly differentiated neoplastic astrocytes, angiogenesis, and the presence of necrotic areas (Theeler et al., 2011). However, despite being highly infiltrative, they are typically confined to the CNS and do not metastasize.

As first-line of treatment, patients with newly diagnosed GBM undergo maximal surgical resection of the tumor bulk, when possible. Following surgery, patients are also treated with radiotherapy (IR) and concomitant and adjuvant chemotherapy using a DNA alkylating agent called temozolomide (TMZ). A randomized phase 3 trial performed by Stupp and colleagues showed that the combination of IR and TMZ increased not only the median survival (from 12.1 to 14.6 months), but also the two-year survival rate as compared to IR alone (Stupp et al., 2005) (Figure 2A). It has also been shown that epigenetic silencing of O^6-Methylguanine-DNA Methyltransferase (MGMT) by promoter methylation confers benefit in patients treated with TMZ (Hegi et al., 2005) (Figure 2B). Although MGMT is expressed in normal tissues, around 50% of GBM display unmethylated MGMT promoter and respond better to TMZ (Hegi et al., 2005) (Figure 2B). Regardless, all GBM patients receive TMZ independently of the MGMT expression.

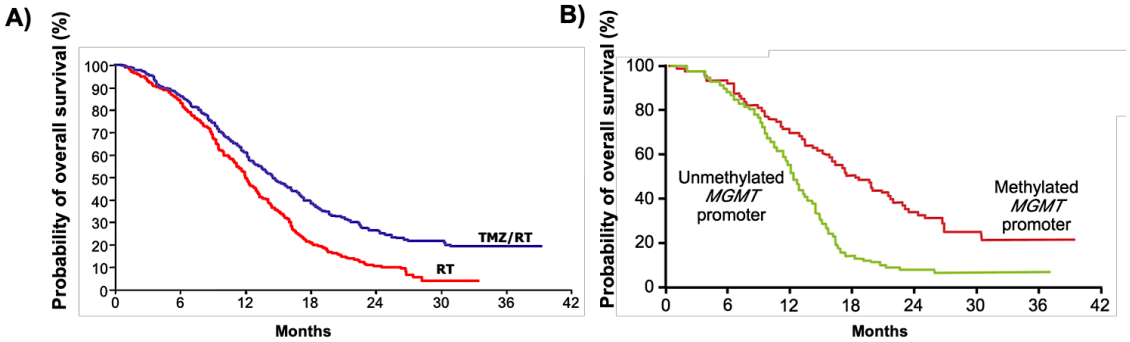

Figure 2: Overall survival of GBM patients based on treatment (A) or MGMT status (B) (Stupp et al., 2005; Hegi et al., 2005).

3.1. Temozolomide: mechanism of action

TMZ is an alkylating agent derived from dacarbazine, stable at a pH less than five and able to cross the blood brain-barrier (BBB) (Reid et al., 1997; Moody & Wheelhouse, 2014). It has been previously reported that TMZ is active against some human cancers such as melanomas and astrocytomas (Middelton et al., 2000; Hart et al., 2013). It was approved by the US Food and Drug Administration (FDA) for adult patients diagnosed with refractory anaplastic astrocytoma in 1999 and for newly diagnosed in 2005 (Yung et al., 1999; Middleton et al., 2000). Since multiple administrations of TMZ are more effective than a single dose (Newlands et al., 1992), newly diagnosed GBM patients tend to be given 75 mg/m2/day of TMZ for 6 weeks concomitantly with focal radiotherapy (60 Gy). Afterwards, they receive 6 cycles of TMZ alone, receiving 150 mg/m2 once daily for 5 days in a row followed by 23 days without treatment prior to the next cycle (Brock et al., 1998). Secondary effects of TMZ have been described such as mild nauseas, vomiting, and dose limiting myelosuppression (Newlands et al., 1992).

At pH lower than seven, TMZ rapidly decomposes to form monomethyl triazene 5-(3-methyltriazen-1-yl)-imidazole-4-carboxamide (MTIC) and reacts with water to form 5-aminoimidazole-4-carboxamide (AIC) and the cation methyldiazonium. This cation is the responsible for the addition of methyl groups to the DNA, at positions N^7 of guanine in guanine-rich regions (N^7-MeG), N^3 adenine (N^3-MeA), and O^6 guanine residues (O^6-MeG) (Denny et al., 1994) (Figure 3).

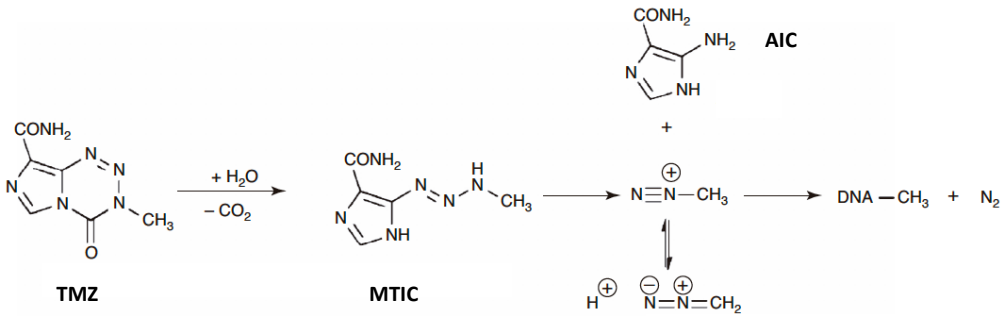

Figure 3: Structure and activation of temozolomide and production of the active compound 5-(3-methyltriazen-1-yl)-imidazole-4-carboxamide (MTIC) and DNA methylation. Adapted from Messaoudi et al., 2015

Although N^7-MeG and N^3-MeA are the main DNA adducts induced by TMZ, the most cytotoxic and mutagenic product is the O^6-MeG (Denny et al., 1994; Zhang et al., 2012). These can be directly repaired in the cell by the action of the MGMT enzyme, which removes the methyl adduct in a one-step alkyl transfer reaction restoring guanine and inactivating MGMT (Figure 4). It is important to know that one MGMT molecule can repair only one alkyl adduct, therefore the repair of O^6-MeG adducts is dependent on the number of MGMT molecules per cell and on the rate of MGMT regeneration (Kaina et al., 2007). Low expression or inactive form of MGMT leads changes in the O^6-MeG. This methylation alters the normal hydrogen bonding of guanine with cytosine resulting in mispairing of O^6-MeG with thymine during DNA replication (Loveless A. 1969) (Figure 4). In the cell, the DNA mismatch repair (MMR) pathway is the responsible of maintaining the genomic stability (Modrich & Lahue, 1996) and recognizes the mispaired repairing the daughter strand. However, this machinery cannot repair the template strand generating repeated attempts by the MMR pathway in a process called futile cycling. Thus, futile cycles of the MMR pathway occur in the context of DNA replication and result in activation of ATR/Chk1 and replication-associated DNA double-strand breaks (DBSs) (Hirose et al., 2001). This damage can be repaired by homologous recombination, although unrepaired DBSs result in cell cycle arrest at G2/M phase and, finally, cell death by apoptosis or autophagy (Roos et al., 2007) (Figure 4). Consequently, cytotoxicity from TMZ is directly dependent on an intact MMR pathway and low levels of MGMT. Lastly, the cytotoxic effect of TMZ is hindered at N7-MeG and N3-MeA since these sites are rapidly repaired by DNA base excision repair (BER) pathway (Horton & Wilson, 2007) (Figure 4).

3.2. Mechanisms of chemoresistance

Patients that respond to TMZ treatment at first, succumb to the disease due to the development of drug resistance and subsequent tumor recurrence (Lee, 2016). Intrinsic or acquired resistance to TMZ remains the greatest obstacle to successful treatment for GBM patients, and a variety of mechanisms of drug resistance have been identified.

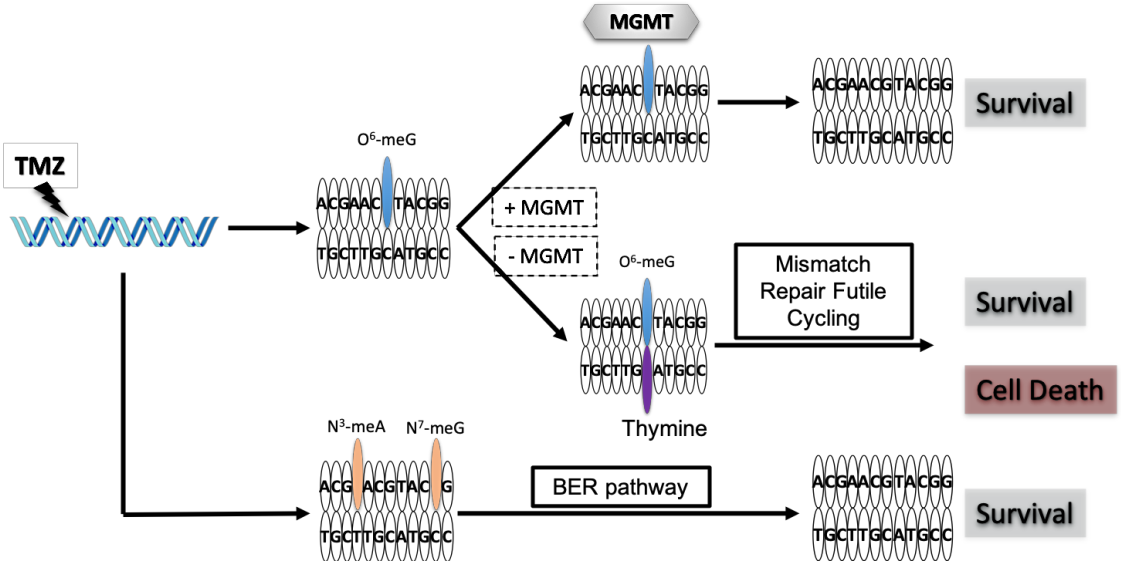

Figure 4: Mechanism of action of TMZ. TMZ modifies DNA at N^7 and O^6 sites on guanine and the N^3 on adenine by the addition of methyl groups. The methylated sites can remain mutated, be fixed by DNA mismatch repair (MMR), be removed by base excision repair (BER) or by the action of a demethylating enzyme such as O6-methylguanine methyltransferase (MGMT).

3.2.1. MGMT promoter hypermethylation

MGMT expression is the main mechanism of GBM resistance and the unique biomarker accepted in clinics. The levels of MGMT vary widely according to the type of tumor and within the same type of tumor (Esteller et al., 2000) and its expression correlates to the methylation profile of the MGMT promoter (Silber et al., 2012). MGMT inhibitors such as O6-benzylguanine (O6-BG) have been tested in clinical trials before TMZ treatment (Verbeek et al., 2008). These pseudosubtrates increased TMZ activity in tumor cells expressing high levels of MGMT both *in vitro* and *in vivo,* but their high toxicity when combined with TMZ against normal cells is an obstacle for the use of these molecules in patients (Hansen et al., 2007).

3.2.2. DNA Mismatch Repair alterations

The MMR pathway is composed by different protein complexes: Mut S homologs (MSH) (MSH2, MSH3, and MSH6), MutL homologs (MLH) (MLH1, MLH3), and post meiotic segregation (PMS) (PMS1, PMS2) (Evans & Alani, 2000). MutSα heterodimer is important for the repair of the mismatch. MSH2 and MSH6 are members of the complex that recognize the mispaired nucleotides. Subsequently, this recognition leads to the recruitment of MutLα (MLH1 and PMS2),

displacement of the DNA polymerase and PCNA, and the recruitment of an exonuclease (EXO1) (Li, 2008) (Figure 5).

In case of GBM patients, loss of MMR pathway mediates directly TMZ resistance when MGMT levels are low (Ghosal & Chen, 2013). However, clinical studies examining pre-existing MMR mutations have failed to show that these MMR deficiencies occur before TMZ treatment (Yip et al., 2009). Analysis of samples pre and post exposure to alkylating agents showed that MMR mutations were not present in pre-treatment samples; indicating that these mutations arose as a result of therapy (Yip et al., 2009). Surviving tumor cells are likely to have acquired MMR mutations in around 20% of cases, resulting in acquired tolerance to further TMZ therapy: a situation typical of GBMs in the clinic. Recently, Wang et al have probed that hypermutant genotype was associated with mutations in the MMR genes, only detected at the recurrence of the diseas (Wang et al., 2016).

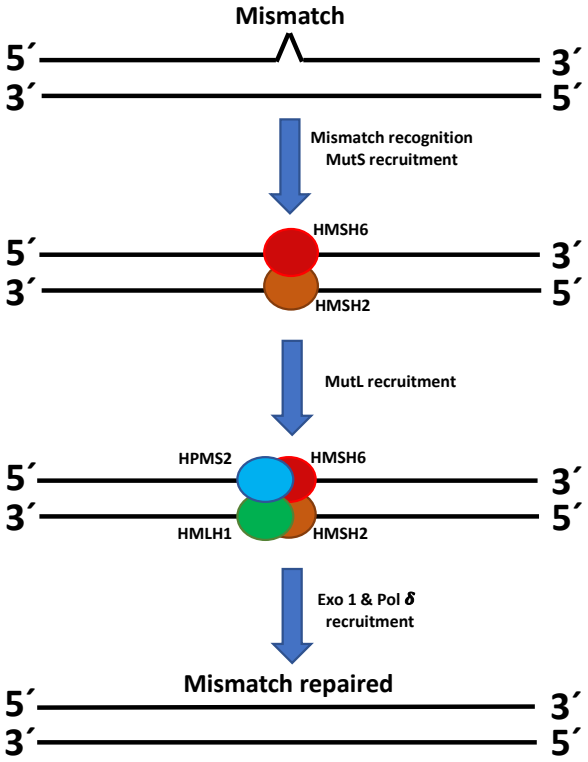

Figure 5: Mechanism of mismatch repair. The canonical MMR pathway recognizesbase-base mismatches and insertion/deletion loops that occur during DNA replication. The repair of these errors primarily involves three steps; recognition, excision and resynthesis (Adapted from Guillotin & Martin, 2014).

3.2.3. Other mechanisms involved in chemoresistance

In the recent years, many authors have described different mechanisms involved in TMZ resistance. For example, several studies suggest that micro-RNAs (miRNA) may act as novel class of oncogenes or tumor suppressor genes (TSG) (Babashah & Soleimani, 2011). In GBM cells, some miRNAs have been identified to be up or downregulated affecting TMZ response (Shi et al., 2010; Ujifuku et al., 2010). EGFR is another protein involved in TMZ resistance. Its activity results in the activation of Ras/Raf/MAPK (Guha et al., 1997) or PI3K/AKT/mTOR (Narita et al., 2002) signaling pathways. These pathways are strongly activated in GBM, inhibiting cell autophagy and apoptosis, responsible for the decrease of TMZ efficiency (Furuta et al., 2004). Different EGFR inhibitors have been proposed to be evaluated in the TMZ context with disappointing results in most of cases (Combs et al., 2006; Neyns et al., 2009). Other studies have shown that the relapse and the agressiveness of the GBM tumors treated with TMZ-treated GBM tumors is due to the enrichment of cancer stem cells (CSCs) (Bleau et al., 2009; Beier et al., 2012b;). The role of CSCs has been described in GBM (Singh et al., 2004; Galli et al., 2004) and the glioma stem cells (GSCs) are enriched after chemoradiation, suggesting that they may serve as a repository for tumor recurrence (Sanai et al., 2005). In mouse models, GSCs induced tumor recurrence following TMZ treatment (Chen et al., 2012). Nevertheless, these studies are not extensive and may not represent all the complexity of TMZ resistance. Genetic analysis using genome-wide approaches can offer a better understanding of the resistance mechanisms. This could ultimately lead to the development of effective therapeutic strategies to overcome resistance.

4. Novel treatment strategies for glioblastoma

Despite advances in the understanding of molecular basis of GBM, patients have not yet benefited from more effective treatments. Several factors may limit the efficacy of novel therapeutic strategies, including molecular heterogeneity, invasion of tumor cells beyond the bulk tumor core delineated by imaging, and the blood–brain barrier (BBB) (van Tellingen et al., 2015). The BBB is responsible for nutrient transport, homeostasis, and communication between the body and the brain and also prevents foreign substances from reaching the brain. It also

provides both physical and biochemical barriers to drug delivery into normal brain (Abbott, 2013). It has been observed that all GBM patients have tumor regions with an intact BBB with limits brain distribution of many oncologic drugs, including monoclonal antibodies, antibody-drug conjugates, and hydrophilic molecules (Oberoi et al., 2016; Parrish et al., 2015; Sarkaria et al., 2018). However, in the last few years new and promising therapies have been developed that can help GBM patients by extending their quality of life and life expectancy.

4.1 Tumor Treating Fields (TTFields)

TTFields are a novel cancer treatment modality that uses alternating electric fields of intermediate frequency (~100-500 kHz) and low intensity (1-3 V/cm). TTFields disrupt cell division by interaction with key molecules during mitosis (Stupp et al., 2012; Stupp et al., 2015). TTFields are delivered to the patients by transducer arrays that are placed on the head close to the tumor and act regionally and non-invasively to inhibit tumor growth. TTFields therapy was recently approved by the FDA for GBM treatment (both newly diagnosed in combination with TMZ and recurrent GBM), and it is under clinical trials for other cancer types testing their safety and efficacy (Mehta et al., 2017).

4.2 Immunotherapy

Immunotherapy is offering promising options for treating lethal cancer such as melanoma. It starts from the concept that T lymphocytes are able to recognize antigens expressed by cancer cells. However, programmed cell death (PD)-1 receptor and its ligand (PD-L1), can suppress the activity of T lymphocytes by inducing apoptosis in activated immune cells (Xue et al., 2017). Blocking of PD-1 and PD-L1 is already used for treating melanoma and non-small cell lung cancer (Hamid et al., 2013; Rizvi et al., 2014). For GBM patients, preclinical studies in mice have given promising results. A number of clinical studies are ongoing to test the effect of PD-1 and PD-L1 blocking both alone or in combination with other agents (bevacizumab, TMZ). The results of these studies will be available in a few years (Paolillo et al., 2018). Oncolytic viral vectors are under clinical development for cancer therapy. Oncolytic viruses (OV) are native or modified viruses that directly kill tumor cells but spare normal tissue inducing host antitumor immunity (Parato et al., 2005). It represents a unique class of

cancer therapeutics with distinct mechanisms of action. Typically, OV can be distinguish in 2 classes: 1) viruses that naturally replicate preferentially in cancer cells and are non-pathogenic in humans often due to elevated sensitivity to innate antiviral signaling or dependence on oncogenic signaling pathways; 2) viruses that are genetically-manipulated for use as vaccine and/or those genetically-engineered with mutations/deletions in genes required for replication in normal, but not cancer cells (Cattaneo et al., 2008). Recently, Tejada et al showed a genetically modified OV was capable of not only to infect and kill glioma cells, but also to stimulate an anti-tumor immune response (Tejada et al., 2018). A variant of this OV is now under clinical trials for patients with recurrent GBM.

Lastly, clinical trials of various vaccine therapies using autologous tumor antigens or tumor-associated/specific antigen peptides with adjuvants have been performed to treat GBM patients (Terasaki et al., 2011; Del Vecchio et al., 2012; Pollack et al., 2014). One of the main targets used for these vaccines is the EGFRvIII mutation (Winograd et al., 2016) although no survival benefit has been observed (nor alone neither in combination with TMZ) so far (Weller et al., 2017).

5. Novel research approaches to study the biology and chemoresistance of GBM

5.1. Forward genetic screens

In the context of deciphering the mechanism of resistance to TMZ, people have tried to develop TMZ-resistant cell lines and then they tried to trace-back the resistance mechanism (Yan et al 2016). It is now evidence that drug resistance is a consequence of the impact of many genes advances in experimental genetic screening systems have been used to better understand these mechanisms (Hu & Zhang, 2016). Forward genetic screens are an attractive approach to determine the genetic basis responsible for the phenotype of interest. These screenings have been used for a long time to identify genes involved in a specific biological pathway or process. This is possible by the analysis of populations of cells or animals that contain random modifications throughout the genome that can be screened for phenotypic effects (Lawson & Wolfe, 2011) (Figure 6). RNAi technology is a great system in which the population cells are knocked-down

looking for specific phenotypes (Sheng et al., 2010). Another interesting approach is the insertional mutagenesis screen by piggybac (PB) transposons, a movable genetic element that can be inserted into the genome by a “cut and paste” mechanism (Wu et al., 2006). This system has been in use for the past few years, especially in haploid cells because it can generate loss-of-function phenotypes (Carette et al., 2009). Previous screens using this strategy have been performed to find novel drug-resistant candidates. Pettitt et al showed that Parp1 is a mediator of olaparib toxicity in haploid cells (Pettitt et al., 2013). Moreover, this strategy has been also implemented for the identification of mutations that confer drug sensitivity in haploid mouse embryonic stem cells (Pettitt et al., 2017).

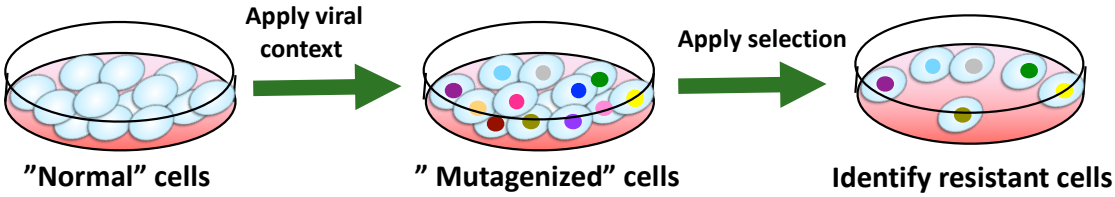

Figure 6: Outline of forward genetic screens. Cells are transduced with a viral plasmid to generate a library of mutant cells where resistant cells are identified after drug selection.

5.2 Genome editing approach for pathological studies and therapeutic treatment

Different tools such as Zinc finger nucleases (ZFNs) or transcription activator-like proteins (TALENs) have been developed to edit the genome. However, the CRISPR/Cas9 (clustered regularly interspaced short palindromic repeats/CRISPR associate protein 9) technology has emerged as an easy and efficient alternative to ZFNs and TALENs for inducing targeted genetic alterations. This system was described in bacteria as protective against invading foreign DNA via RNA-guided DNA cleavage (Wiedenheft et al., 2012). It is composed by two main molecules that introduce an alteration into the DNA: on the one hand, the endonuclease called Cas9 who acts as ‘scissors’ that can cut the two strands of DNA at a specific location in the genome so that bits of DNA can then be added or removed. On the other hand, a small piece of pre-designed RNA sequence (about 20 bases long), called small guide RNA (sgRNA) located

within a longer RNA scaffold. The scaffold binds to the DNA and the pre-designed sequence 'guides' Cas9 to the right area of the genome in order to cut at the desired region in the genome. The double-stranded endonuclease activity of Cas9 also requires a short-conserved sequence, (2–5 base pairs) known as protospacer-associat-ed motif (PAM), that follows immediately 3´- of the sgRNA complementary sequence (Jinek et al., 2012; Nihisamu et al., 2014) (Figure 7A). This cut produces DSBs which can be repaired by the cellular non-homologous end joining (NHEJ) pathway, resulting in insertions and/or deletions (indels) which disrupt the targeted locus. Alternatively, if a donor template with homology to the targeted locus is supplied, the DSB may be repaired by the homology-directed repair (HDR) pathway allowing for precise replacement mutations to be made (Gong et al., 2005; Overballe-Petersen et al., 2013) (Figure 7B).

Thanks to its efficiency and efficacy in generating genomic silencing, point mutations and genetic rearrangements, this is now a routine approach in many genetic and molecular laboratories for *in vitro* and *in vivo* experiments. In GBM, Zuckermann and colleagues generated GBM in mouse brain thanks to the deletion of TP53, Pten and NF1 simultaneously by CRISPR/Cas9 (Zuckermann et al., 2015). Moreover, Cook and collaborators were also able to generate gene fusion events showed in GBM patients (Cook et al., 2017).

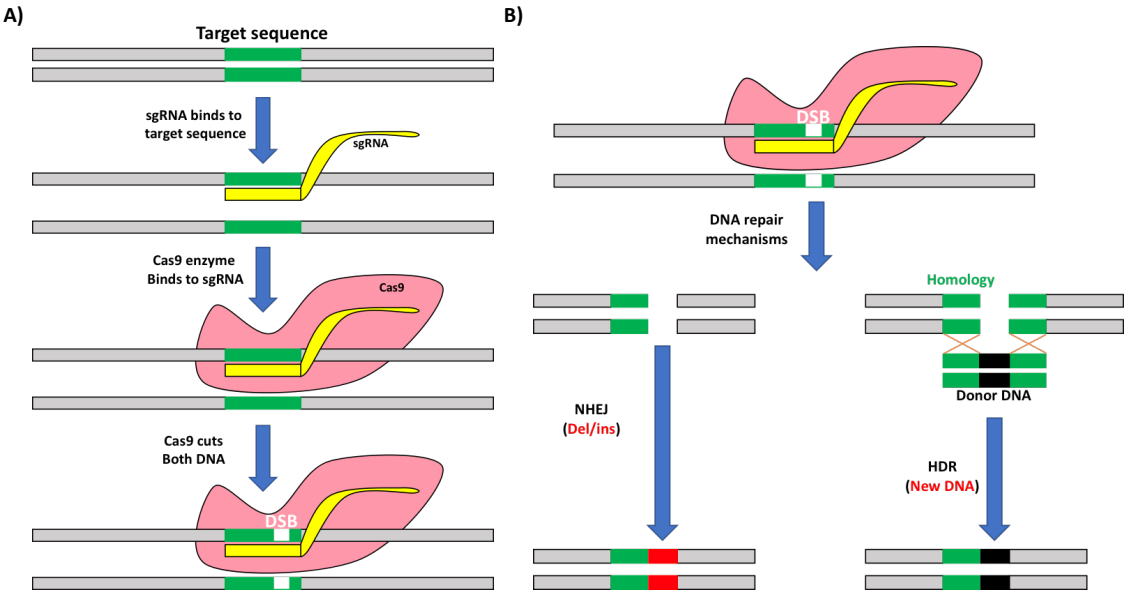

Figure 6: Scheme about how the CRISPR-Cas9 editing tool works. A) The sgRNA containing specific nucleotides is able to target a specific sequence by complementarity. Once the sgRNA finds this sequence, it will attach allowing the Cas9 protein to produce DSBs. **B)** Wild-type Cas9 nuclease specifically cleaves DBSs activating double-strand break repair machinery. In the absence of a homologous repair template NHEJ can result in indels disrupting the target sequence. Alternatively, precise mutations and knock-ins can be made by providing a donor template and exploiting the HDR pathway.

5.3 Modeling glioblastoma: the RCAS/Tva System

In vivo models are used to recapitulate different hallmarks of human cancer that cannot be modeled *in vitro*. It is also important to mimic tumor microenvironment to assess drug safety profiles and reduce clinical trial failure (Sergalis et al., 2018).

Genetically engineered mouse model (GEMMs) are excellent as *in vivo* GBM models since they allow the analysis of the cell-intrinsic and cell-extrinsic processes. GEMMs are useful to validate cancer target genes, oncogenes, determine cell-of-origin, study the contribution of tumor microenvironment in tumor homeostasis or metastasis (Kersten et al., 2017). One of the most widely used models for the study of gliomas is the somatic transfer system called RCAS/Tva (Holland & Varmus, 1998). This is an efficient, quick, feasible and flexible technique composed by 2 components:

The first element of the RCAS/Tva system is the Tumor Virus A (Tva) receptor, a glycoprotein conserved in avian species that allows the efficient infection by subgroup A Avian Leukosis Virus (ALV-A) (Snitkovsky & Young., 2000). Transgenic mice that express Tv-a receptor under control of tissue-specific promoter Nestin (NTva) or glial fibrillary acidic protein (GFAP/GTva) were generated for the study of brain tumors (Holland & Varmus, 1998) (Figure 7A). Nestin is a type VI intermediate filament protein (IFP) that is mostly expressed in different type of cells including nerve cells during embryonic development (Michalczyk & Zima, 2005). In adult brain its expression is repressed and mostly localized in the subventricular zone (SVZ) (Parlakian et al., 2016). GFAP is the main astrocytic filament, highly expressed in the CNS, preferentially expressed by neurogenic astrocytes in the subventricular zone (Yang & Wang, 2015).

The second component of the RCAS-Tva system is the RCAS retroviral vector (Replication Competent ALV LTR with a Splice acceptor). The virus produced by

the RCAS plasmid enters only in cells via the Tv-a receptor, which mammalian cells do not natively express (Fisher et al. 1999). Following entry into the host cell, a cDNA copy of the viral genome is made and after cell division the viral cDNA copy is incorporated into the host genome. This RCAS virus retains all of the necessary viral genes for replication (Ahronian & Lewis, 2014). The immortalized chicken fibroblast cell line (DF1) is normally used to propagate RCAS viruses in culture (Himly et al., 1998; Schaefer-Klein et al. 1998) (Figure 7B). Expression of the inserted genes can be driven by either the viral long terminal repeat (LTR) or an appropriate internal promoter (Petropoulos & Hughes, 1991; Du et al., 2006). RCAS viruses can readily deliver dominant-negative versions of tumor-suppressor proteins, shRNAs, miRNAs, and other noncoding RNAs (Du & Li, 2007; Bromberg-White et al., 2004). Inserts in the RCAS retrovirus are stable up to 2.8 kb but less stable when >2.8 kb. It is common beyond this insert size that the RCAS will lose its insert, generate truncation mutants, or produce low-titer virus. The limited carrying capacity of RCAS viruses is one of the major drawbacks of the RCAS-Tva system.

Injection of DF1 cells carrying the RCAS plasmid into transgenic mice (either pups or adults) produces efficient *in vivo* infection of specific mouse cells engineered to express the Tv-a receptor (Figure 7C). As a result, the retroviral RCAS infection enables the introduction of a gene of interest into a specific cell type or tissue.

This unique approach represents a powerful method to model cancer initiation and progression. It is well-known that most of human cancers, including GBM, are very heterogenous from a genetic point of view and the development of novel *in vivo* models to recapitulate this genetic complexity is needed. The genome editing capacity of CRISPR/Cas9 is a powerful tool able to generate most of the alterations produced in cancer and many authors have used it for cancer modeling (Zuckerman et al., 2015; Cook et al., 2017; Oldrini et al., 2018).

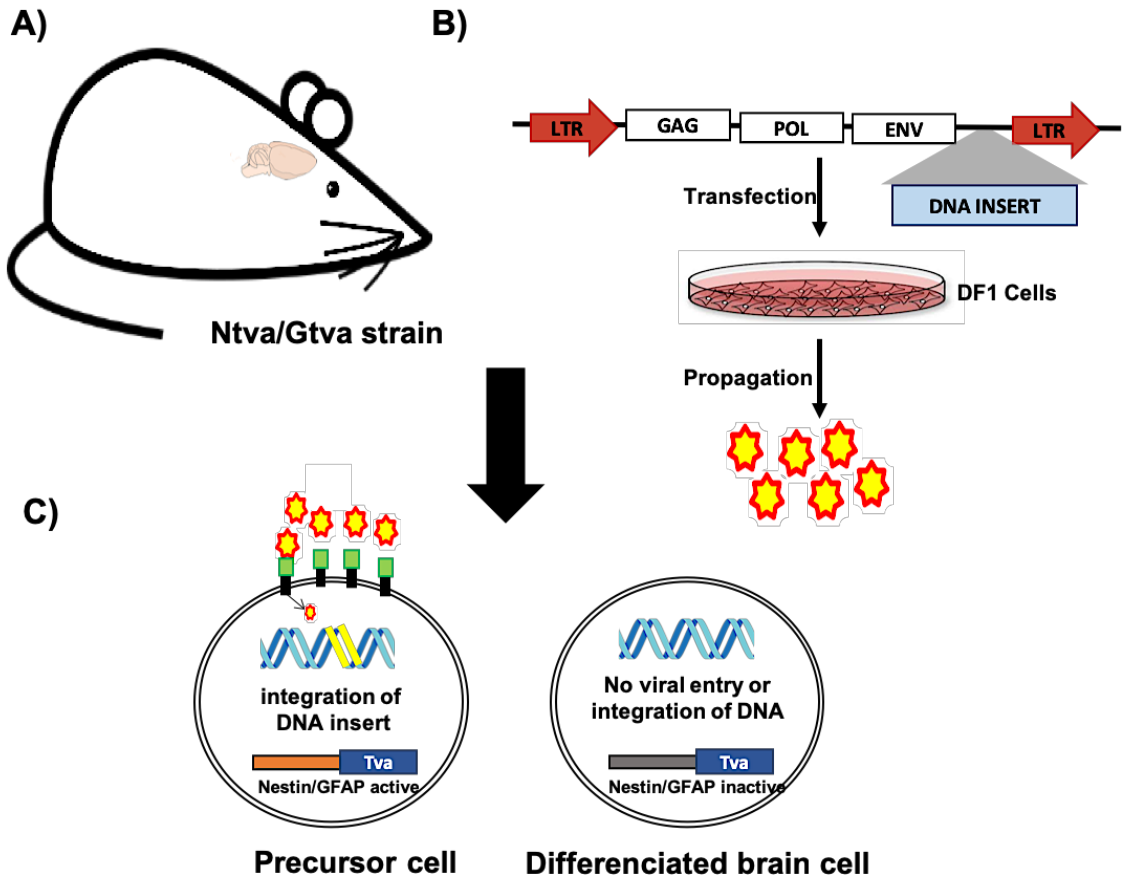

Figure 7: Schematic representations of the RCAS/Tva glioma mouse model. (A) Transgenic mice were generated expressing the Tv-a receptor under control of the tissue-specific nestin/GFAP promoter. **(B)** DF1 cells are transfected with RCAS constructs that propagate and release RCAS virions into the culture media. (C) DF1 cells are injected into transgenic pups/adult mice. The RCAS virions only bind to the Tv-a positive cells integrating the DNA insert to produce stable gene expression changes leading to tumor formation (adapted from Ahronian et al., 2014).

Objectives

The experimental work developed in the present PhD project can be included in three main blocks:

1) **Explore the mechanisms of resistance to TMZ.** Despite the low efficacy of chemotherapy treatment in GBM patients, TMZ remains the unique option. Our first goal was the study TMZ resistance. To do this, we performed a forward genetic screen using a PiggyBac (PB) transposon-mediated mutagenesis approach in human haploid cells (Hap1). Specifically:
   a) Forward genetic screen using PB transposon-mediated insertional mutagenesis in Hap1 cells.
   b) Validation of candidate genes in Hap1 and different GBM cell lines using CRISPR/Cas9 genome editing.
   c) Identification and validation of antitumoral compounds in MMR-deficient GBM cell line.
2) **Test the effectiveness of Val-083 in GBM cells.** Based on the limited efficacy of TMZ for GBM patients, which retains a poor prognostic value, many strategies are under clinical trials. The priority is to prolong overall survival and enhancing quality of life for these patients. Thus, in our laboratory we are evaluating the efficacy of a novel compound called Val-083 as compared to TMZ. In particular:
   a) Compare the efficacy of Val-083 with TMZ.
   b) Analyze the effects of Val-083 in MMR-deficient cells.
   c) Evaluate its effect in combination with TMZ.
3) **Development of new murine model for the study of gliomas.** In the recent year, the advances produced in genetics have allowed a better understanding of the multiple events that occur in the GBM formation. For this reason, the development of new *in vivo* models that can recreate alterations in an efficient way seems indispensable for the study of tumor biology as well as the development of new therapies. In this last part of the project we aimed:
   a) Generation of a new murine model by combining the somatic gene transfer RCAS/Tva model and the genome editing capacity by CRISPR/Cas9 system.
   b) Test the efficacy of the model by recreating different genetic alterations found in GBM patients.

Objetivos

El trabajo experimental generado en esta tesis doctoral se puede englobar en tres grandes bloques:

1) **Explorar los mecanismos de resistancia a Temozolomida.** A pesar de la baja eficacia de la quimioterapia en el tratamiento de GBM, la TMZ permanece como la única opción para los pacientes. Así, nuestro primer objetivo fue estudiar la resistencia a TMZ a través un cribado genético mediante el sistema de transposones PiggyBac en células haploides humanas (Hap1). De manera específica:
    a. Realizar un cribado genético en células Hap1 en respuesta a TMZ
    b. Validación de los genes candidatos en las células Hap1 así como en diferentes líneas celulares de GBM mediante el sistema CRISPR/Cas9
    c. Identificación y validación de compuestos antitumorales en células de GBM carentes de la ruta de MMR
2) **Testar la eficacia del Val-083 en células de GBM.** Dada a la poca eficacia de la TMZ en pacientes con GBM es muy limitada, manteniendo un mal factor pronóstico, diferentes estrategias se encuentran actualmente en ensayos clínicos. En nuestro laboratorio estamos evaluando la eficacia del compuesto Val-083 en comparación a TMZ. En concreto
    a. Comparar la eficacia del Val-083 respecto a TMZ
    b. Analizar los efectos del Val-083 en células carentes de MMR
    c. Evaluar sus efectos en combinación con TMZ
3) **Desarrollo de un nuevo modelo murino para el estudio de gliomas.** Los avances producidos en los últimos años en genética han permitido un mejor entendimiento de los diferentes eventos que se producen en la formación de gliomas. Nuevos modelos que recreen estas alteraciones de manera eficaz se antojan necesarios para el estudio de la biología tumoral, así como el desarrollo de nuevas terapias. En nuestro caso queremos:
    a. Generar un nuevo modelo murino combinando el modelo de glioma de transferencia de genes RCAS/Tva y la edición génica mediante el sistema CRISPR/Cas9
    b. Testar la eficacia del modelo recreando diversas alteraciones genéticas halladas en pacientes con GBM

Materials & methods

1. Ethic Statement

Investigation has been conducted in accordance with the ethical standards and based on the Declaration of Helsinki and according to national and international guidelines.

2. Cell lines, transfections and infections

Haploid cells (Hap1) were kindly provided by the Genomic Instability group (Spanish National Cancer Research Centre – Madrid) and grown in IMDM (Invitrogen #12722F) with 15% Fetal Bovine Serum (FBS -Sigma #F524) and 1% penicillin/streptomycin (pen/strep – Gibco #15140).
The following GBM cell lines U251-MG, U87-MG, T98G and were provided by Memorial Sloan Kettering Cancer Centre and cultured in Dulbecco´s Modified Eagle´s Medium – high glucose (DMEM – Sigma #D5796) supplemented with 10% FBS and 1% pen/strep. Cells were maintained under standard incubation conditions (+37ºC, 5%CO2).

Retrovirus or lentivirus were generated by co-transfection of retroviral or lentiviral plasmids and the packaging VSVg for retrovirus and the 2nd generation packaging plasmids pMD2G and psPAX2 for lentivirus in Gp2-293 using Fugene®6 (Promega #E269A) in a ratio 1:3. Subsequently, different cell lines were infected with lentivirus and Cas9 expressing cells were selected using 7 μg/ml Blasticidin S HCl (Thermo Fisher #A1113903) while sgRNA or shRNA-expressing cells were selected using 2 μg/ml of Puromycin (Sigma #P8833).
The DF-1 chicken fibroblast cell line (ATCC, CRL-12203) was transfected with different RCAS plasmids using Fugene®6 in a ratio 1:3 according to manufacturer's protocol and selected using 1,5 μg/ml of Puromycin.

3. Plasmids, siRNA and sgRNA design and cloning strategy

Human-specific MSH6 hairpin (Table 1) was designed and cloned into the mirE-based retroviral MLP vector (kindly provided by Scott Lowe). For the genome editing approach, all sgRNA provided in table 1 were designed using a "CRISPR design" tool from Zhang lab (http://crispr.mit.edu) and cloned into the pKLV-U6gRNA(BbsI)-PGKpuro2ABFP plasmid (Addgene #50946). Primers containing

the BbsI site and the specific sgRNA sequence were cloned into the pKLV-U6gRNA(BbsI)-PGKpuro2ABFP as described previously using the MIT CRISPR design tool (http://www.genome-engineering.org/crispr/)

Primer name	Sequence 5´ → 3´
shRenilla	TGCTGTTGACAGTGAGCGCAGGAATTATAATGCTTATCTATAGTGAAGCCACAGATGTATAGATAAGCATTATAATTCCTATGCCTACTGCCTCGGA
shMSH6	TGCTGTTGACAGTGAGCGCAAGAGTGAAGAAGATAATGAATAGTGAAGCCACAGATGTATTCATTATCTTCTTCACTCTTATGCCTACTGCCTCGGA
sgRNA-NT-Fw	CACCGTGCTTTTCCGACACGGTCGCGT
sgRNA-NT-Rv	TAAAACGCGACCGTGTCGGAAAAGCA
sgRNA-MSH6-Fw	CACCGGAACATTCATCCGCGAGAAGT
sgRNA-MSH6-Rv	TAAAACTTCTCGCGGATGAATGTTCC
sgRNA-MSH6.2-Fw	CACCGATAGAGTGTTTACTAGACTGT
sgRNA-MSH6.2-Rv	TAAAACAGTCTAGTAAACACTCTATC
sgRNA-PTGES3-Fw	CACCGGATTCCAAGCATAAAAGAAGT
sgRNA-PTGES3-Rv	TAAAACTTCTTTTATGCTTGGAATCC
sgRNA-PTGES3.2-Fw	CACCGTCCTGAGTTGATAGCTCTAAGT
sgRNA-PTGES3.2-Rv	TAAAACTTAGAGCTATCAACTCAGGA
sgRNA-PSMD1-Fw	CACCGTCAATTCATACCTTAAGCTGGT
sgRNA-PSMD1-Rv	TAAAACGCGGGCGTCGGGACGCAAAGC
sgRNA-PSMD1.2-Fw	CACCGAGGCTGCAAACTGCCGACTCGT
sgRNA-PSMD1.2-Rv	TAAAACGAGTCGGCAGTTTGCAGCCT
sgRNA-SMS-Fw	CACCGTTTCAACACTTTCATTGAGGT
sgRNA-SMS-Rv	TAAAACCTCAATGAAAGTGTTGAAAAC
sgRNA-SMS.2-Fw	CACCGAGCACGCTCGACTTCATGCTGT
sgRNA-SMS.2-Rv	TAAAACAGCATGAAGTCGAGCGTGCT
sgRNA-PEX5L-Fw	CACCGGAATTAGTGGCTCCGACTCGT
sgRNA-PEX5L-Rv	TAAAACGAGTCGGAGCCACTAATTCC
sgRNA-PEX5L.2-Fw	CACCGAAATCATCCTCATCTAGAACGT
sgRNA-PEX5L.2-Rv	TAAAACGTTCTAGATGAGGATGATTT
sgRNA-IPO7-Fw	CACCGCACTTCTTGCATTTCCACCAGT
sgRNA-IPO7-Rv	TAAAACTGGTGGAATGCAAGAAGTGC
sgRNA-IPO7.2-Fw	CACCGATGATCGACCTGAGTTACCAGT
sgRNA-IPO7.2-Rv	TAAAACTGGTAACTCAGGTCGATCATC

sgRNA-ERF-Fw	CACCGCCAACCCCACATCAATGAAGT
sgRNA-ERF-Rv	TAAAAGTTCATTGATGTGGGGTTGGC
sgRNA-ERF.2-Fw	CACCGCCAACCCCACATCAATGAAGT
sgRNA-ERF.2-Rv	TAAAAGTTCATTGATGTGGGGTTGGC
sgRNA-c11orf85.1-Fw	CACCGCCAACTACCTGAGTTGGGTGT
sgRNA-c11orf84.1-Rv	TAAAACACCCAACTCAGGTAGTTGGC
sgRNA-c11orf85.4-Fw	CACCGTGGTGGTGGCCGTAATTCCGT
sgRNA-c11orf85.4-Rv	TAAAACGGAATTACGGCCACCACCAC
sgRNA-AHSA1.1-Fw	CACCGCCAGTGCCAGTTGTTGACGGT
sgRNA-AHSA1.1-Rv	TAAAACCGTCAACAACTGGCACTGGC
sgRNA-AHSA1.2-Fw	CACCTAAGAGTGATCTTACAAGTGT
sgRNA-AHSA1.2-Rv	TAAAACACTTGTAAGATCACTCTTAC

Table 1: List of shRNA, sgRNA oligos used and the primers for PCR amplification.

For the *in vivo* experiments, the insert that contains hU6 promoter; 2 BbsI cloning sites followed by the gRNA scaffold; PGK promoter; Puro and BFP was amplified from the pKLV-U6gRNA (BbsI)-PGKpuro2ABFP plasmid and aTTB sites to sublcone into the Gateway® pDONR™221 vector were generated by PCR using PlatinμM Pfx Kit (Invitrogen, #11708-013) and the following oligos (Table 2). The new plasmid pDONR_sgRNA has a Gateway® pDONR™221 vector backbone with the following features between the aTTL sites: hU6 promoter; 2 BbsI cloning sites followed by gRNA scaffold; PGK promoter; Puro and BFP as a selection marker. To obtain the pDONR_sgRNA, BP reaction was prepared following the suggestions in the Gateway reagent protocol (Invitrogen, #11789-020).

The final plasmid pDONR_sgRNA was obtained after removing the BbsI site by site-directed mutagenesis kit according to the PCR mutagenesis protocol with Pfu UltraHF polymerase (Agilent, Ref.200521-5) and the following oligos (Table 2). pDONR221 plasmid was modified using the PDGFB_BbsI_mut in order to remove the extra BbsI site and verified by Sanger sequencing. The sgRNA listed in table 2 were obtained from Weber et al., 2015 and Ruiz S et al., 2016 and then cloned into the pDONR transferred from the pDONR_sgRNA into RCAS-DV using the Gateway™ LR Clonase™ II Enzyme mix (Invitrogen, ref. 11791-020), following the manufacturer's instructions. 1μl of the reaction was transformed

using a bacteria strain with a lower frequency of homologous recombination Stbl-3 in house prepared.

Primer name	Sequence 5´ → 3´
PDGFB_BbsI_mut-Fw	AGGCCACGGTGACGCTGGAGGATCACCTGGCATGCAAGTG
PDGFB_BbsI_mut-Rv	CACTTGCATGCCAGGTGATCCTCCAGCGTCACCGTGGCCT
sgRNA-Trp53-Fw	CACCCGAGTGAAGCCCTCCGAGTGTCGT
sgRNA-Trp53-Rv	TAAAACGACACTCGGAGGGCTTCACTC
sgRNA-Cdkn2a-Fw	CACCGTGGTGAAGTTCGTGCGATCCGT
sgRNA-Cdkn2a-Rv	TAAAACGGATCGCACGAACTTCACCA
sgRNA-Pten-Fw	CACCGAAAGACTTGAAGGTGTATACGT
sgRNA-Pten-Rv	TAAAACGTATACACCTTCAAGTCGGGC
PCR-Trp53-Fw	GGAGGCCAGCCTGGGATAAG
PCR-Trp53-Rv	CACGAAAGACAACTCCCCGG
PCR-Cdkn2a-Fw	ATGGGCGTGGAGCAAAGATG
PCR-Cdkn2a-Rv	TAAGCCGAAGGGGGAAAGCG
PCR-Pten-Fw	GCCTCAGTCGCGTATTCTG
PCR-Pten-Rv	CATCCAGTGACGCATCCAG

Table 2: List of oligos used for the *in vivo* experiments.

4. Clones isolation

Clones were isolated from the selected population using “cloning cylinders” (Merck #TR1004) and the protocol suggested by Sigma webpage.

5. Forward genetic screen, Reversion phenotype assay and Splinkerete – PCR

Hap1 cells transduced with a PiggyBac (PB) transposon-mediated mutagenesis were treated with TMZ (Sigma #T2577) at the specified concentration for 1 week in two independent experiments. Media containing TMZ was changed every 3 days.

To isolate revertants, isolated clones were electroporated with the hyPBase expression plasmid and cultured for three days without selection. 10^5 transfected and non-transfected cells were then plated separately in 6-well plates and treated with 500 μM of TMZ.

Genomic DNA from ten clones isolated from the pB-mutagenized library was extracted and used to map the integration sites. Host sequences flanking piggyBac insertions were amplified using the Splinkerette – PCR protocol previously described (Potter et al., 2010) and sent for Sanger sequencing.

6. RNA isolation, Quantitative real-time reverse transcriptase PCR analysis and RNAseq analysis

mRNA from the same clones isolated was extracted and purified using RNeasy Mini Kit (Qiagen #74104). cDNA was synthetized with the SuperScript II First-Strand Synthesis System (Invitrogen, #18064014). The PCR amplification mix contained 500 ng of cDNA, SYBR Green I Master Mix buffer (Applied Biosystem, #4472908) and 20 μM from the forward and reverse primers (Table 4).
Details for performing RNAseq analysis can be found in the material and methods described in Mayor et al., 2017.

Primer name	Sequence 5´ → 3´
p21-Fw	TCCACAGCGATATCCAGACA
p21-Rv	GGACATCACCAGGATTGGAC
Puma-Fw	ACGACCTCAACGCGCAGTA
Puma-Rv	CGGTGTCGATGCTGCTCTT
Mdm2-Fw	GGAAGATGCGCGGGAAGTA
Mdm2-Rv	CCGCTCGCCCAGCAG
Noxa-Fw	AGGAAGGAAGTTCCGCCG
Noxa-Rv	AGCGTTTCTCTCATCACATCACA

Table 4: List of qPCR oligos used

7. Immunobloting

Cell pellets were lysed with RiIPA lysis buffer (50mM HEPES, 150mM NaCl, 1% Glycerol, 1% Triton X-100, 1.5mM MgCl2, 5mM EGTA) and protein concentrations were determined by DC™ protein assay kit (Biorad, #500-0115) using the manufacture´s protocol. Proteins were separated on house-made SDS-

PAGE gels and transferred to nitrocellulose membrane (Amersham). Membranes were incubated in blocking buffer (5% milk, 0.1% Tween, 10 mM Tris at pH 7.6, 100 mM NaCl) during 1 hour and then with primary antibody overnight at 4ºC according to the antibody datasheet. Antibodies used: p53 (1:1000, Cell Signaling Technologies, #2524), PTEN (1:1000, Cell Signaling Technologies, #9188), MSH6 (1:1000, BD Biosciences, #610919), Vinculin (1:10000, Sigma, #V9131), MGMT (1:1000, Sta Cruz, #sc8825), p-CHK1 (1:1000, Cell Signaling Technologies, #2344S) and p-CHK2 (1:1000, Cell Signaling Technologies, #2661S). Anti-mouse or rabbit-HRP conjugated antibodies (Jackson Immunoresearch) were used to detect desired protein by chemoluminescence with ECL (Amersham).

8. Genomic DNA isolation and TA Cloning strategy

Genomic DNA was isolated by proteinase K/isopropanol/ethanol. Cell pellets were incubated in lysis buffer (10 mM Tris-HCl ph 8, 100mM NaCl, 0.5 mM EDTA, 10% SDS and proteinase K) for 4h at 55°C. DNA was precipitated using isopropanol (ratio V/V 1:1). The aqueous phase was recovered to fresh tubes and washing in 70% cold ethanol as performed. Samples were centrifuged at 15000 rpm for 25 min. After draining and dissolving in water, genomic DNA was quantified using nanodrop. 100ng of DNA were amplified with the specific primers listed in table 2 using PlatinμM Pfx Kit with the following conditions: 2 min at 94º for initial denaturing, 30 cycles of 15 s at 94º denaturing, 30 s at 59º annealing and 30 s at 60º extension. PCR products were cloned into the multiple cloning region from pGEM®-T Easy vector within the coding region for the α-peptide of β-galactosidase. Insertional inactivation of the α-peptide allows recombinant clones to be visually identified by color screening (blue/white) on LB-ampicillin plates containing X-Gal/IPTG. White colonies were amplified, plasmid was isolated using QIAprep Spin Miniprep Kit (Qiagen, #27104) and submitted to sequence.

9. Clonogenic assay

$1x10^4$ cells were plated in 6-well plate and treated 3 hours later with TMZ and/or Val-083 in duplicates. Medium containing the drug was changed every 3 days. 10 days after, medium was removed, and cells were stained with crystal violet.

10. CRISPR-sgRNA library: design, amplification and screening

For the generation of the sgRNA library, four sgRNAs per gene and nine non-targeting (NT) sgRNAs were designed. This library was prepared, subcloned and amplified and sublconed into the pKLV-U6gRNA (BbsI)-PGKpuro2ABFP plasmid following the instructions from the agilent surevector library cloning kit (Agilent #G7556A).

U251^{Cas9} cells (1 x 10^6) were plated on a 100-mm dish and transduced with the lentiviral protocol described above. Transduced cells were selected on media containing 2 µg/mL puromycin. For the screening, 3 days after selection 1x10^5 cells were plated and treated with 100 or 400 µg/mL of TMZ.

11. Highthroughput sequencing: preparation of the libraries and analysis

After ten days on treatment, genomic DNA was isolated for analysis by next generation sequencing. In order to amplify the region containing the sgRNA from the lentiviral plasmid a first PCR was performed using the oligos listed in table 4 and the Kappa HiFi PCR Kit (KappaBiosystems, #KK2101) with the following conditions: 1 min at 95º for initial denaturing, 3 cycles of 20 s at 98º denaturing, 20 s at 66º annealing and 20 s at 72º extension, 5 cycles of 20 s at 98º denaturing, 20 s at 63º annealing and 20 s at 72º extension and 12 cycles of 20 s at 98º denaturing, 20 s at 60º annealing and 20 s at 72º extension. PCR products were loaded in a 2% agarose gel, purified using the Quiakit PCR purification kit (Quiagen #28104) and sent to Illumina NovaSeq 6000 for sequencing. The screening data was analyzed using the RStudio software v.1.1.383.

Primer name	Sequence 5´ → 3´
pKLV_U6gRNA_Fw	AATGATACGGCGACCACCGAGATCTaatggactatcatatgcttaccgtaact
pKLV_U6gRNA_Rv_Idx3	CAAGCAGAAGACGGCATACGAGATgcctaaGTGACTGGAGTTCA GACGTGTGCTCTTCCGATCaagTgcatgctccagactgc
pKLV_U6gRNA_Rv_Idx8	CAAGCAGAAGACGGCATACGAGATtcaagtGTGACTGGAGTTCA GACGTGTGCTCTTCCGATCaagTgcatgctccagactgc

Table 4: PCR oligos used for the CRISPR-sgRNA library experiments

12. Compound library and screening

The Experimental Therapeutics Program at CNIO, ETP-CNIO, owns a compound library of about 120 single compounds either FDA-approved or under clinical trials. 1500 U251-MG cells were seeded into 96-well plates and 2,5 μM of each compound form library was added using a robotic platform (Beckman 96 tip). Cells were cultured for 3 days and cell viability was analyzed using the CellTiter-Glo cell viability assay (Promega, #G7570) to measure cell viability by luminescence measurement of adenosine triphosphate (ATP) consumption. The ATP reagent was added to each well of a 96-well plate, and the intensity of luminescence was measured using the EnVision plate reader (PerkinElmer) 30 min after the addition of the reagent. To measure cell viability, the percentage of activity or inhibition was calculated and represented.

13. Dose-response and proliferation assays

For compound validations and experiments regarding Val-083, dose-response assays were performed, and 1500 U251-MG cells were plated in 96-well plates. Candidate compounds, as well as Val-083 (Clinisciences S.L., # A15269-513914), were selected and specific concentrations were used for the validations. 96 hours after treatment, cell viability was determined by MTT (3-(4,5-Dimethylthiazol-2-yl)-2,5-diphenyltetrazolium bromide) assay (Roche). Adherent cultured cells were plated in 96-well culture plates (1000 cells/well) in 100μl of their medium, in absence/presence of TMZ (Sigma, # T2577) and/or VAL-083. 96 hours later, 10 μl of MTT (2.5 mg/ml) were added and cells were further incubated for 4h, followed by the addition of 100 μl solubilization buffer and incubation overnight. Spectrophotometric absorbance was measured at 570 nm and percentage of cell growth was calculated and represented using Prism software.

14. Flow cytometer

To analyze the percentage of γH2AX-positive cells, GBM cells were incubated with TMZ and/or Val-083, trypsinized, fixed in suspension by the addition of cold 70% ethanol and maintained at -20ºC at least for 24h. Cells were suspended in 0.25% Triton X-100 in PBS, and incubated on ice for 15 min. After centrifugation,

the cell pellets were suspended in PBS containing 1% BSA and antibodies recognizing 53BP1 (NB, #100-304) and γH2AX (Millipore, #05-636). Secondary antibodies conjugated with Alexa-647 or Alexa-488 (Life Technologies) were used at a dilution of 1:250. DNA content was visualized with either propidium iodide (PI) or Cell Cycle blue-405.

GBM cells were incubated with TMZ and/or Val-083 for the indicated time and 20μM EdU was added during the last hour of incubation. Trypsinized cells were fixed with 4% paraformaldehyde (PFA) for 10 minutes and EdU was detected by the Click-iT™ EdU Alexa Fluor® Imaging kit (Invitrogen/Molecular Probes). Acquisition was conducted on a FACSCanto II (BD) and data was analyzed using RStudio v.1.1.383.

15. High-throughput fluorescence microscope analysis

To analyze the percentage of 53BP1 and γH2AX-positive cells, 2.000 cells/well were plated on an opaque 96 well plate and cells were treated with TMZ and or Val-083 for 48 hours. Cells were fixed with PFA 4%, permeabilized for 15 minutes with BSA 0.2% + Triton X-100 0.5% and then blocked with BSA 3% for 1 hour.The primary antibodies used for immunofluorescence were α-γ-H2AX (Millipore, #05-636) and α-53BP1 (NB, #100-304) diluted 1:1000 or 1:3000 respectively in BSA 3%. After incubation overnight at 4ºC with the primary antibodies, cells were washed twice with PBS 1x and then incubated for 1 hour with the secondary antibodies Donkey α-Mouse 555 and Donkey α-Rabbit 488 (both diluted 1:400 in BSA 3%). Cells were washed twice with PBS 1x and then stained with DAPI (1:4.000) for 5 minutes.

To measure EdU incorporation, 2.000 cells/well were plated on an opaque 96 well plate and cells were treated with TMZ and/or Val083 for 48 hours. Cells were incubated with EdU 10 μM for 1 hour at 37 ºC and fixed with PFA 4%. Cells were then permeabilized with BSA 0.2% and Triton X-100 0.5% for 20 minutes and blocked with BSA 3% for 1 hour. Finally,cells were incubated with the Click iT Reaction Cocktail (Click-iT EdU Imaging Kit - Invitrogen) for 45 minutes and then washed with BSA 3%. Finally, cells were stained with DAPI (1:4.000) for 5 minutes.

Acquisition was conducted on a confocal microscopy system using Opera (Pelkin Elmer) and data was analyzed using R programming.

16. Cell cycle analysis

Cultured cell lines were fixed in 70% ethanol on ice for 30 minutes, rehydrated in PBS, treated with RNase A (100μg/ml) (Qiagen, #10109142001) and stained with propidium iodide (50μg/ml). Acquisition was conducted on a FACSCanto II (BD) and data was analyzed using FlowJo v.10.4.2.

17. Immunohistochemistry

Tissue samples were fixed in 10% formalin, paraffin-embedded and cut in 3 μm sections. Tissues were deparaffinized in xylene and re-hydrated through a series of graded ethanol until water. For histopathological analysis, sections were stained with hematoxylin and eosin (H&E). For immunohistochemistry (IHC), paraffin sections underwent first an antigenic exposure process, then endogenous peroxidase was blocked, and the slides were then incubated in blocking solution (2.5% BSA, 10% goat serum, with or without MOM IgG, according to the species of primary antibody, in PBS). Incubation with the appropriate primary antibodies was carried out for 3 hours as detailed: PTEN (1:100, Cell Signaling Technology, #9559), p19ARF (1:100, Santa Cruz Biotechnology, sc-32748), p21 (1:10, CNIO monoclonal antibody core, clone 291H/B5), cleaved caspase-3 (1:750, Cell Signaling Technology, #9661,). After that, all slides were incubated with appropriate secondary antibodies and the visualization system AB solution (AB solution-Vector, #PK-6100). The immunohistochemistry for p53 (1:100, CNIO monoclonal antibody core, clone POE316A), Ki67 (undiluted, Master Diagnostica, #0003110QD), Cas9 (1:100, Cell Signaling Technology, #14697), p-S6 (S240/244) (1:500, Cell Signaling Technology, #92991), p-AKT (S473) (1:175, Abcam, # ab81283) and p16INK4a (CNIO monoclonal antibody core, clone AM-33B, ready to use) was performed using an automated immunostaining platform (Ventana discovery XT, Roche).

18. Mouse strains and husbandry

Nestin-Tva and GFAP-Tva mice were generously provided by Eric Holland. The Rosa26-LSL-Cas9 knockin mouse strain was purchased from The Jackson Laboratory (# 024857). Nestin-Cre and GFAP-Cre, hUBC-CreERT2 transgenic lines were kindly provided by various researchers at the Spanish National Cancer Research Centre (Marcos Malumbres, Mariano Barbacid and Maria Blasco). Mice were housed in the specific pathogen-free animal house of the Spanish National Cancer Research Centre under conditions in accordance with the recommendations of the Federation of European Laboratory Animal Science Associations (FELASA). All animal experiments were approved by the Ethical Committee (CEIyBA) and performed in accordance with the guidelines stated in the International Guiding Principles for Biomedical Research Involving Animals, developed by the Council for International Organizations of Medical Sciences (CIOMS).

19. Generation of murine gliomas

For the RCAS-mediated gliomagenesis, newborns or 4–6-week-old mice were injected intracranially with $2x10^5$ DF1 carrying the RCAS-PDGFB and $2x10^5$ DF1 transduced with different RCAS-sgRNA expressing cells. Adult mice were anaesthetized by 4% isofluorane and then injected with a stereotactic apparatus (Stoelting) as previously described (Hambardzumyan et al., 2009). For the inducible model (NTva; LSL-Cas9; hUBC-CreERT2), 2 weeks after cells injection, mice either received intraperitoneal injections of 4-Hydroxytamoxifen (Sigma-Aldrich, Cat. H6278) (2 mg/injection, 3 times/week) or were fed *ad libitum* with tamoxifen-containing pellets. After intracranial injection, mice were checked until they developed symptoms of disease (lethargy, poor grooming, weight loss, macrocephaly).

20. Organotypic tissue cultures

Organotypic slice cultures from adult nude mouse brain were processed and prepared as previously described (Valiente et al., 2014). Briefly, mice injected with GBM cells expressing a luciferase reporter were anesthetized with isofluorane. They were then injected retro-orbitally with d-luciferin (150 mg per kg) and imaged with an IVIS Xenogen machine (Caliper Life Sciences).

Bioluminescence analysis (BLI) was performed using Living Image software, version 3.

Brain slices were imaged to confirm the presence of glioma cells using BLI. Growth rate was obtained by comparing the fold increases between day7 and day 0. Treatment on brain slices was replaced at day 4 of the experiment (10 µM/25 µM of TMZ and/or 0,5 µM of Val-083) by adding them to the media.

Results

1. Forward genetic screen using PiggyBac transposon-mediated insertional mutagenesis in human haploid cells for the identification of genes related to modulation of TMZ response

1.1 Haploid cells express MGMT and tolerate high doses of TMZ

The development of resistance to TMZ represents a major obstacle for the successful treatment and eradication of GBM in patients. Although some progress has been made in the understanding of the biology of the tumor origin, there is a limitation in the understanding of the mechanisms of resistance to current therapies. In this regard, the identification of the relevant targets in resistance pathways, remains challenging. The identification of resistance genes has focused largely on forward genetic approaches, such as RNAi library screens (Meijer et al, 2006). Mobile genetic elements like PB-transposons provide a powerful alternative method for gene discovery that can overcome many of the limitations of forward genetic screens (Chew et al, 2011).

The PB-transposon is a mobile genetic element that can efficiently swap between vectors and chromosomes via a "cut and paste" mechanism. For the first part of this project, we decided to use a PiggyBac (PB) transposon system for an insertional mutagenesis screen in human haploid (Hap1) cells, a nearly haploid cell line derived from leukemia cells (Kotecki et al., 1999). In this system, the PB can precisely complete excision and reinsertion in chromosomes. After the reinsertion, the transgene is inserted into the genome at TTAA regions. No DNA synthesis occurs during the PB transposition, and the target gaps caused by transposition are sealed simply by ligation, making the transposition of PB precise (Mitra et al., 2008). One advantage of the PB system is the possibility to re-express the silenced gene by expression of the PB transposase (Zhao et al., 2016; Figure 8A). Genomes containing an inserted PB vector can be re-transfected with a specific PB transposase expression vector, removing the transposon from the genome and leaving intact the DNA (Figure 8A). This approach has been described by Pandzic *et al.* for the identification of resistance mechanisms for the chemotherapeutic drug fludarabine in chronic lymphocytic leukemia (Pandzic et al., 2016).

Using the PB system in haploid cells, transposon integrations can lead to a complete loss-of-function phenotypes. Our first objective was to use a library of mutant cells generated in Hap1 cells for a forward genetic screen in order to identify genes related to TMZ response.

First of all, a clonogenic assay was performed in Hap1 cells by treating with increasing doses of TMZ. We noticed that these cells are quite resistant to TMZ and they express MGMT (Figure 8B). Then, Hap1 cells transduced with a PB transposon were subsequently treated for 2 weeks with 500 μM of TMZ, in two independent replicates, and TMZ-resistant clones were observed (Figure 8C).

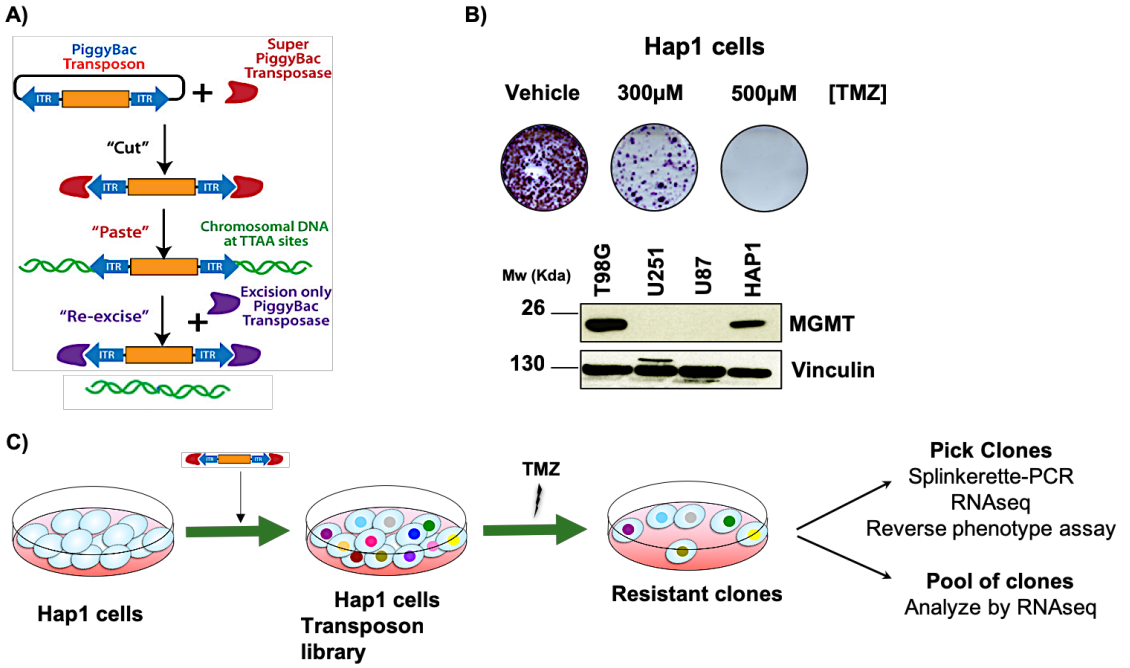

Figure 8: **Workflow of the PB-transposon system and forward genetic screen in Hap1 cells. A)** PB-transposon system approach. During transposition, the PB-transposase recognizes transposon-specific inverted terminal repeat sequences (ITRs) located on both ends of the transposon vector and efficiently moves the contents from the original sites and integrates them into specific TTAA chromosomal sites. Then, PB-transposon can be easily removed from the genome by specific PB-transposase (adapted from biosciences). **B)** *Top panel*: Clonogenic assay performed in Haploid cells to determine the lethal dose for TMZ. Cells were treated with increasing doses of TMZ. Notice that Hap1 need high doses of TMZ to kill all the cells. *Bottom panel*: immunoblot showing that Hap1 cells express MGMT. **C)** Strategy for the forward genetic screen. Hap1 cells were transduced with the PB-transposon vector to generate the transposon library and treated with TMZ. Some of the resistant clones were isolated for deeper analysis by Splinkerette-PCR, reverse phenotype assay and RNAseq. The rest of the clones were collected as a pool and analyzed by RNAseq.

1.2 PB screen in Hap1 cells revealed 43 candidate genes that could be related to TMZ resistance

Ten clones were isolated independently, and the rest of the clones were harvested as a pool for their analysis. In order to map the location of the integrations sites, thus finding the gene responsible of the resistance, the isolated clones were analyzed by Splinkerette-PCR (spPCR). This technique allows the sequencing of the genomic regions flanking the PB insertions (Shao et al., 2012). Briefly, genomic DNA from the resistant clones containing the PB transposon were digested with Sau3AI restriction enzyme. Digested DNA was then ligated with specific splinkerette oligonucleotide with a stable hairpin loop. This was followed by two rounds of nested PCR that contained the flanking genomic DNA between the transposable element insertion site and the genomic digestion site. By Sanger sequencing we were able to map the integration site of the PB transposon (Figure 9; See material & methods for details). Moreover, both the clones and the pool were sent for RNAseq for more in-depth analysis (Figure 8C).

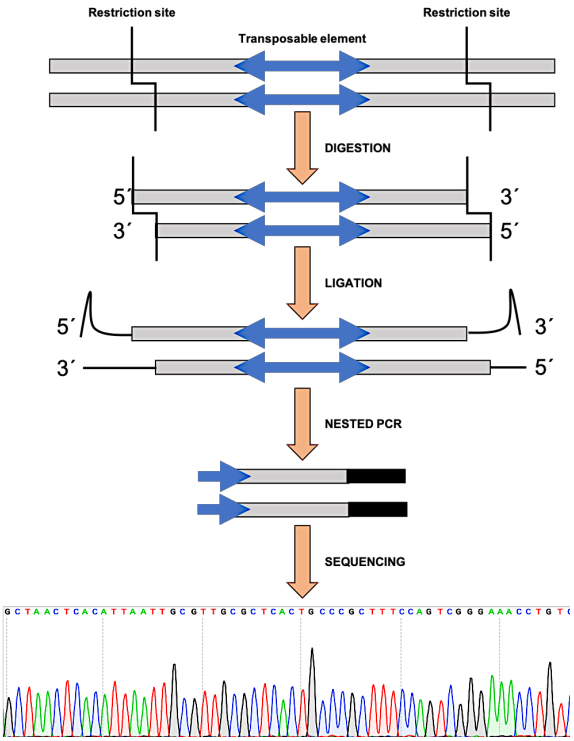

Figure 9. Schematic for the splinkerette PCR method. Genomic DNA (gDNA) is isolated from the isolated clones to be mapped. The genomic DNA is digested by Sau3A1 restriction enzyme that produces sticky ends. A specific double stranded splinkerette oligonucleotide compatible with sticky ends is ligated to the digested gDNA. After two rounds of nested PCR the fragment generated contains the flanking gDNA between the transposable element insertion site. Specific primer directed against the transposon is used for Sanger sequencing. Adapted from Potter et al., 2010.

We were able to identify 43 different integration sites corresponding to 43 different ´candidate´ genes (Table 5) that could modulate the resistance to TMZ. Interestingly, we identified MSH6, an MMR component known to be involved in the repair of TMZ-induced DNA damage. (Cahill et al., 2008; Yip et al., 2009; Nguyen et al., 2014). We also identified this gene in other screenings performed in our laboratory in the context of TMZ-resistance. This suggests that PB-transposon system is a valid system for the identification of TMZ-modulator genes. In addition, the proteasome component PSMD1 was previously described to modulate the sensitivity to alkylating agents in Drosophila cells (Amaravadi et al., 2009).

GENE	DETECTION METHOD	GENE	DETECTION METHOD
C11orf84	Splinkerette-PCR / RNA SEQ	**VPS13D**	Splinkerette-PCR
SMS	Splinkerette-PCR / RNA SEQ	**ENO1**	RNA SEQ
PEX5L	Splinkerette-PCR	**HDAC9**	RNA SEQ
PSMD1	Splinkerette-PCR / RNA SEQ	**MEGF9**	RNA SEQ
MSH6	Splinkerette-PCR RNA SEQ	**NDC80**	RNA SEQ
NUP98	Splinkerette-PCR	**ACTN4**	RNA SEQ
PTGES3	Splinkerette-PCR / RNA SEQ	**ACY1**	RNA SEQ
MAP1B	RNA SEQ	**AHSA1**	RNA SEQ
TBCD	RNA SEQ	**ANKLE2**	RNA SEQ
ERF	RNA SEQ	**AURKA**	RNA SEQ
HNRNPA1	RNA SEQ	**CREBBP**	RNA SEQ
FBXO5	RNA SEQ	**DNAJC25**	RNA SEQ
IPO7	Splinkerette-PCR / RNA SEQ	**DPPA4**	RNA SEQ
MCOLN1	Splinkerette-PCR	**EXOSC9**	RNA SEQ
PTPN4	Splinkerette-PCR	**PSMD2**	RNA SEQ
SIPAL1L	Splinkerette-PCR	**RCC1**	RNA SEQ
DIAPH3	Splinkerette-PCR	**RPS6**	RNA SEQ
NUCKS1	Splinkerette-PCR / RNA SEQ	**DOCK3**	RNA SEQ
ITSN2	Splinkerette-PCR	**EZR**	RNA SEQ
RIOK2	Splinkerette-PCR	**NFATC3**	RNA SEQ
PPFIA2	Splinkerette-PCR	**SRPK 1**	Splinkerette-PCR
		CHORDC1	Splinkerette-PCR

Table 5: Resistant genes detected by RNAseq and/or Splinkerette-PCR.

1.3 Transposon integration induces TMZ resistance in Hap1 cells

The PB-transposon inserted into the genome can be removed by PB-transposase, leaving the locus in an intact wild-type sequence configuration and re-sensitizing the cells to the drug. Thus, it is easy to verify whether the transposon integration is responsible for the phenotype (Fraser et al., 1996; Elick, 1996). A reversion phenotype assay was performed in the isolated clones that were then treated with TMZ before and after removing the transposon (Figure 10A). The resistance to TMZ was reverted once the transposon was eliminated in the ten isolated clones (Figure 10B). The interpretation of these results is very intuitive: the insertion of PB was responsible for the phenotype whereas precise excision of PB abolished it. Our data indicate that the resistance to TMZ was dependent on the specific integration site and not from random mutations produced by TMZ in the genome.

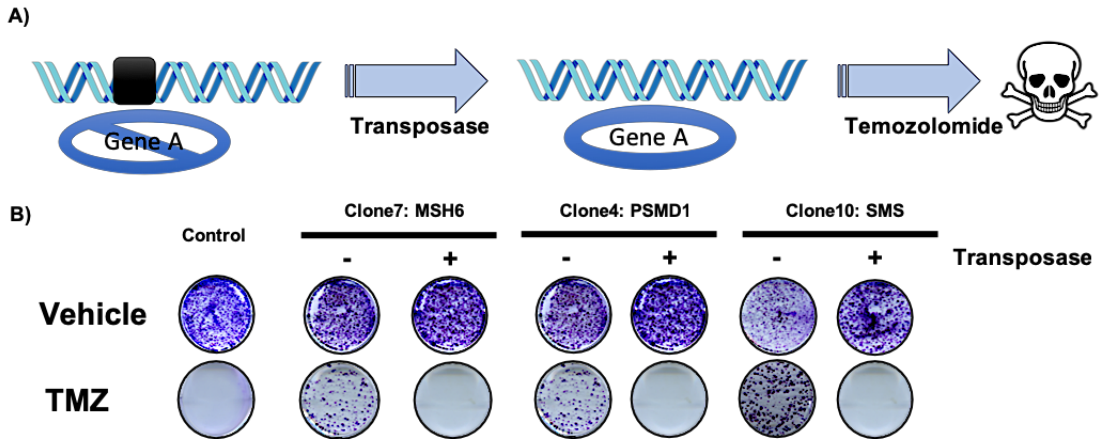

Figure 10: Reversion phenotype assay analysis. A) Strategy of reversion phenotype. Specific PB-transposase is used to remove the insertion of the PB-transposon into the genome leaving intact the locus and re-sensitizing the cells to the drug. **B)** Example of this assay in 3 different isolated clones. 10^4 cells were plated in a 6-well plate and treated with 500 μM of TMZ in the presence or absence of the PB-transposon for 10 days and then stained with crystal violet. Note: all the isolated clones were positive for this assay.

1.4 Inactivation of the MMR component MSH6, but not of other HAP1 candidate genes, generates resistance in GBM cell lines.

Next, to validate the candidate genes we used the CRISPR/Cas9-based genome editing in Hap1 and in different GBM cell lines (U251-MG and U87-MG). These cells were first infected with a lentiviral Cas9 vector for a constitutive expression

of Cas9. Thus, different sgRNA for MSH6, PSMD1, IPO7, PTGES3, PEX5L, SMS and ERF as well as a non-targeting sgRNA (Table 1) were designed and cloned into the pKLV-U6sgRNA PGK2ABFP lentiviral vector. These vectors were used to infect the three different cell lines. Finally, the KO cells generated for the candidate genes were tested in clonogenic assay and showed that they were resistant upon TMZ treatment in Hap1^{Cas9} (Figure 11A). However, except for MSH6-defficient cells, we could not observe similar results neither in U251^{Cas9} nor in U87^{Cas9} GBM cells (Figure 11B).

The efficacy of the cut in the CRISPR/Cas9 system remains a limitation and may have its basis in the different Cas9 functions, like efficient DNA-scanning (Sternberg et al., 2014), PAM detection (Nishimasu et al., 2014; Jinek et al., 2014), or nuclease domain activation (Sternberg et al., 2015). Recently, it has been described that nucleotide composition of the sgRNA may produce changes in genome editing efficacy (laubuhn et al., 2018). To test the sgRNA efficacy, genomic DNA (gDNA) was extracted from some of cells generated, before and after TMZ treatment, and the efficacy of cutting was analyzed by Sanger Sequencing. PCR products containing the CRISPR locus were subcloned into the multiple cloning site (MCS) in the pGEM-T® Easy Vector. Successfully cloned colonies were selected by β-galactosidase and picked for plasmid isolation. The cloned fragment of interest was analyzed by Sanger sequencing. As expected, only TMZ-treated cells contained indels in the locus indicating that those cells without editing were died because of the treatment. Nevertheless, we could identify wild type sequences in the control cells (Figure 11C)

A)

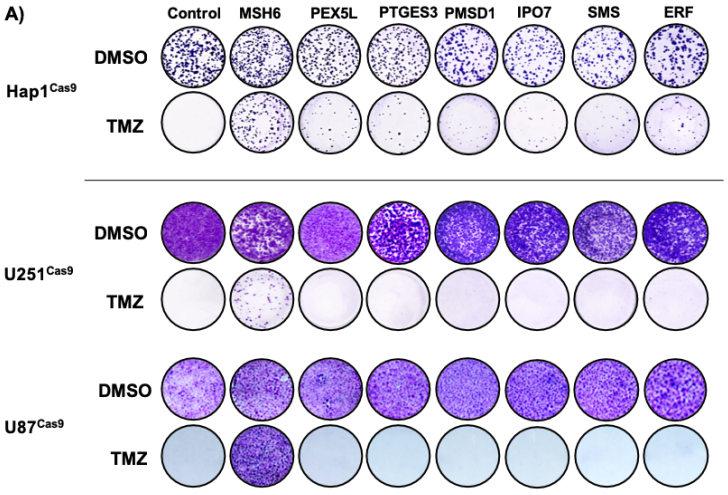

B)

GENE	DMSO	TMZ
ERF	WT (4/8) Big deletions	Del8nt Del5nt Del11 Del44 Del12(x2)
MSH6	WT (x1) Del1nt Del5nt Del11 Del2(x2)	Del1nt (x3) Del8nt Del5nt Insertion 1nt
PEX5L	WT (5/7) Del1nt Big deletions	Del8nt Del22nt Del2nt Del6nt (x2) Del14nt

Figure 11: Validations in Hap1 and GBM cells. Hap1^{Cas9} **(A)** and U251^{Cas9} or U87^{Cas9} cells **(B)** were infected and selected with the different sgRNAs cloned into a lentiviral plasmid. 10^4 cells were plated and treated with lethal doses of TMZ for 10 days and then stained with crystal violet. **C)** Indel analysis of ERF, MSH6 and PEX5L genes identified in Hap1 cells.

Despite these discouraging results observed in the first set of validations in GBM cells, we decided to perform a low-throughput secondary screening by designing and generating a sgRNA library with the genes (all but MSH6) previously identified. The library was composed by four different sgRNAs per gene identified and nine non-targeting sgRNAs as internal controls. U251^{Cas9} GBM cells were transduced with the CRISPR-sgRNA library and treated with low (100μM) and high (400μM) doses of TMZ for 10 days. Regrettably, we were not able to detect any resistant clones in the highest dose and the cell survival upon the lowest dose in the library-containing cells was similar to the control cells. Regardless, the cells were collected, processed and analysed by HiSeq in order to see whether there were sgRNAs enriched in the treated samples.

Based on the results obtained on the non-treated cells, we could confirm the presence of each sgRNA from the library in the original cell population (Figure 12A). One sgRNA for c11orf84, a SPIN1-docking protein related to histone methylation ability, was present 5 times more in the treated cells than in the non-treated control. In addition, another sgRNA for the same gene was detected in the top 15 sgRNAs with the highest fold-change (Figure 12B). Moreover, there was another gene represented by 2 different sgRNAs in the top 15: AHSA1, a co-chaperone of Hsp90AA1. We decided to clone only those sgRNAs for c11orf84 and AHSA1 into the lentiviral plasmid for validations in a different set of GBM cell lines. However, none of sgRNAs were validated after clonogenic assay in U251^{Cas9} cells (Figure 12C).

A)

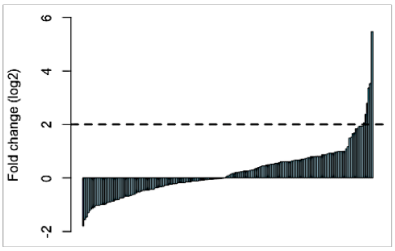

B)

sgRNA - name	sgRNA - Sequence	Log2 Fold-change
C11orf84_4	GTGGTGGTGGCCGTAATTCC	5.47
SRPK1_3	GTCATCAAATCCAATTATCA	3.53
EZR_1	GCAAACTTACCAGGGACCAG	3.37
NUP98_2	GATATGAAAGCAAGTCACTA	2.8
SMS_3	GTTACCACCCATAGTGCGAG	2.37
ANKLE2_1	GAAGCGTATCCGTTACGTGG	2.06
C11orf84_1	GCCAACTACCTGAGTTGGGT	1.95
AHSA1_1	GCCAGTGCCAGTTGTTGACG	1.94
DOCK3_1	GAGTACCTATTCGGATCACA	1.92
CHORDC1_1	GCTTCTAGACTCTCTAGACC	1.85
MEGF9_2	GAGCAGTCGCCCAAAGAGGG	1.84
HDAC9_4	GTTTCCCTCTAAAGTAACAT	1.67
IPO7_1	GATGATCGACCTGAGTTACC	1.65
ITSN2_4	GTCTGGAGATATAATTCAGG	1.51
AHSA1_2	GTAAGAGTGATCTTACAAGT	1.49

C)

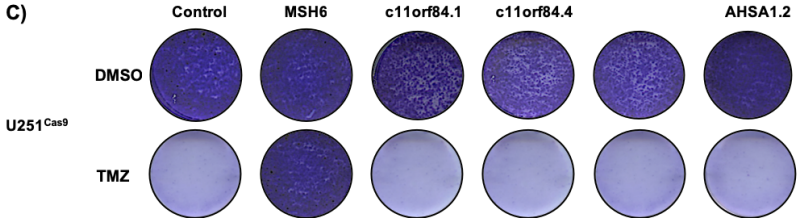

Figure 12: Analysis of CRISPR-sgRNA library showed an enrichment of some sgRNAs upon TMZ treatment. A) Barplot showing differential changes by log2 fold change and normalized to non-treated cells of the CRISPR-sgRNA library in U251^{Cas9} cells treated with 100μM of TMZ for 10 days. **B & C)** List of top 15 sgRNAs identified in the screening. Noticed that c11orf84 and AHSA1 genes are represented by 2 different sgRNAs. Clonogenic assay in U251^{Cas9} for the top 2 genes enriched (2 or more sgRNAs). Cells were plated and treated with 100μM of TMZ for 10 days. None of the sgRNA led to resistance to TMZ.

The signal for a positive selection (TMZ resistance) is strong promoting the enrichment of sgRNAs which allows for the easy detection of resistant cells. However, the identification of false-positives may result when the CRISPR/Cas9 system modifies off-target genomic sites with sequence similarity to the intended CRISPR target site (Tsai & Joung, 2016). In our case, the identification of enriched sgRNAs in our library that do not validate individually may be explained by the detection of false positives.

2. Compound screening in MMR-defective GBM cells

MSH6 is a member of the MMR pathway that dimerizes with MSH2 and forms a MutSα in charge of detecting single nucleotide mismatches. Upon detection, subsequent corrective actions are undertaken by complexes of other MMR family members (Kunkel & Eurie., 2015). As mentioned in the introduction, MSH6 mutations are involved in the recurrence of GBM patients. Around 20% of the patients treated with TMZ acquire mutations in this gene resulting in chemotherapy failure (Yip et al., 2009). Thus, alterations in MSH6 (mutations or deletions) lead to resistance to TMZ and reinforce the importance of developing additional therapies to deal with MSH6-deficient glioma.

In most cancers, the standard therapies are directed to block specific pathways for cell survival (Pagliarini et al., 2015). However, resistance to therapies is a common outcome in different tumor types and it has been shown found that targeting a second signaling pathway in combination with a cell-specific mutation, could result in synthetic lethality (Bunting et al., 2010; Bian et al., 2014). Cells with gene A or B mutated may not produce cell death (Figure 13B). A synthetic lethal interaction when the inactivation of gene B (either genetically or by a drug) will produce cell death in those cells that have a mutation in gene A, and vice versa (Figure 13C) (Nagel et al., 2016). Consequently, the inhibition of A or B is selectively lethal to cancer cells with mutations in the other gene. This would promote favorable combination of therapeutic treatment, to which only tumor cells that contain the mutation would be sensitive. Furthermore, these interactions could expand the treatments for lethal cancers, since they could facilitate the indirect targeting of non-druggable cancer mutations through the identification of second-signaling pathways that may be druggable.

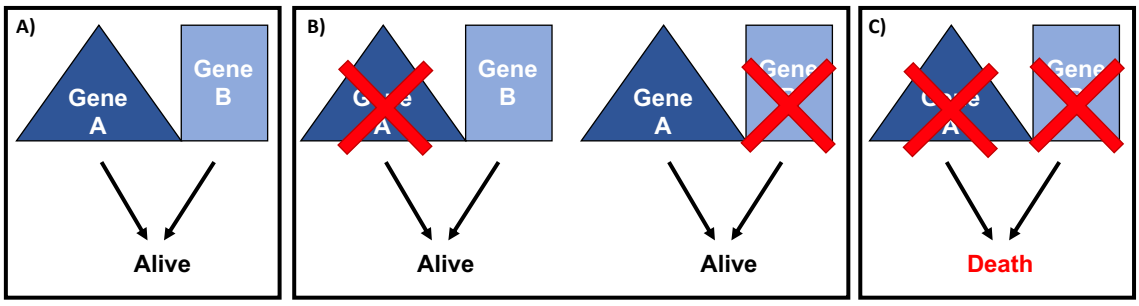

Figure 13: The concept of synthetic lethality. A) In normal conditions, the expression of gene A and B does not alter cell growth. **B)** Loss or the inhibition of either gene A or B alone sometimes does not affect cell viability. **C)** Mutation or pharmacological inhibition of the gene B in cells with a mutation of gene A results in non-viable cell (synthetic lethality). (Adapted from Nijman, 2011)

2.1 MSH6-defective GBM cells might me more sensitive to anti-mitotic drugs

Considering that MSH6 is the only gene that we have validated and the relationship between MMR deficiency and TMZ resistance, our next goal was to identify compounds that are more effective in MSH6-deficient cells as compared to normal cells. In order to do so, we performed a compound screening in U251 GBM cells, either MMR-proficient or deficient, using 120 antitumoral drugs that are FDA -approved or under clinical trials.

For this screening, we used the RNA interference (RNAi) technique in U251 cells infected to silence the expression of MSH6 using short hairpin RNAs (shRNA) (figure 14A). These cells were treated with 2,5μM of every compound of the library and 3 days after treatment, proliferation was measured. Preliminary data suggested that MMR defective cells might be more sensitive to anti-mitotic drugs (microtubules activity and Aurora Kinase inhibitors) (Figure 14B and C).

A)

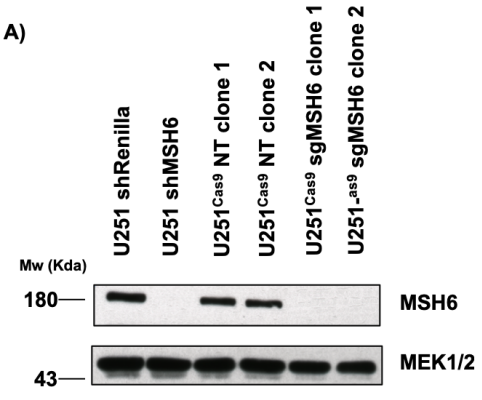

B)

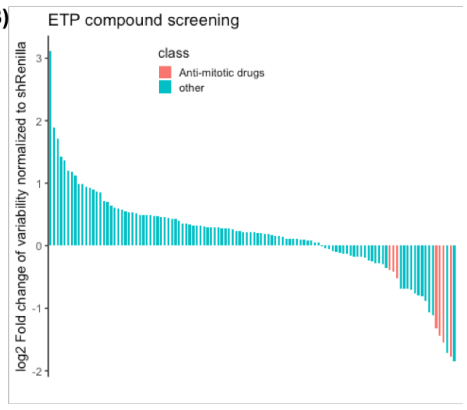

C)

Compound	Name	Function
ETP-51799	GSK461364	PLK1i. Selective agains isoforms
ETP-51634	Alisertib	Selective Aurora A inhibitor
ETP-51636	Mesylate	Selective Aurora A, B and C inhibitor
ETP-61631	Dovitinib	Multitarget RTK inhibitor
ETP-51637	Tozasertib	Aurora A inhibitor
ETP-39817	Etoposide	Anticancer, topoisomerase I inhibitor
ETP-45335	Docetaxel	Antimitotic micotubule destabilizer
ETP-39816	Irinotecan	Topoisomerase I inhibitor
ETP-45229	Taxol	Microtubule polymer stabilizer
ETP-45337	Gemcitabine	Antimetabolite
ETP-48208	BK120	PI3K inhibitor
ETP-45338	Vincristine	Inhibitor of polymerization of microtubules by binding to tubulin

Figure 14: Compound screening results in U251 shRenilla/shMSH6 cells. A) Immunoblot showing the efficiency for silencing MSH6 gene by using the RNAi or genome editing systems in U251 GBM cells used for the validations. NT: Non-targeting. **B)** Barplot showing differential variability changes of drugs from the compound library by log2 fold change and normalized to shRenilla. **C)** List of promising compounds identified, their commercial names and known functions.

2.2 Validations of different compounds did not show differences in MMR-defective cells

To confirm these data, a first dose-response assay was performed in MSH6-deficient cells (Figure 15A) using some of the different compounds mentioned in figure 14C. Cells were plated in quintuplicates in 96-well plates, treated with serial dilutions of each drug and proliferation was measured 72h after treatment by colorimetric assay. Regrettably, preliminary data showed that neither vincristine nor mesylate were more effective in MMR-deficient cells as compared to normal cells (Figure 15 – top panel). Other drugs were also tested in these cells with similar results.

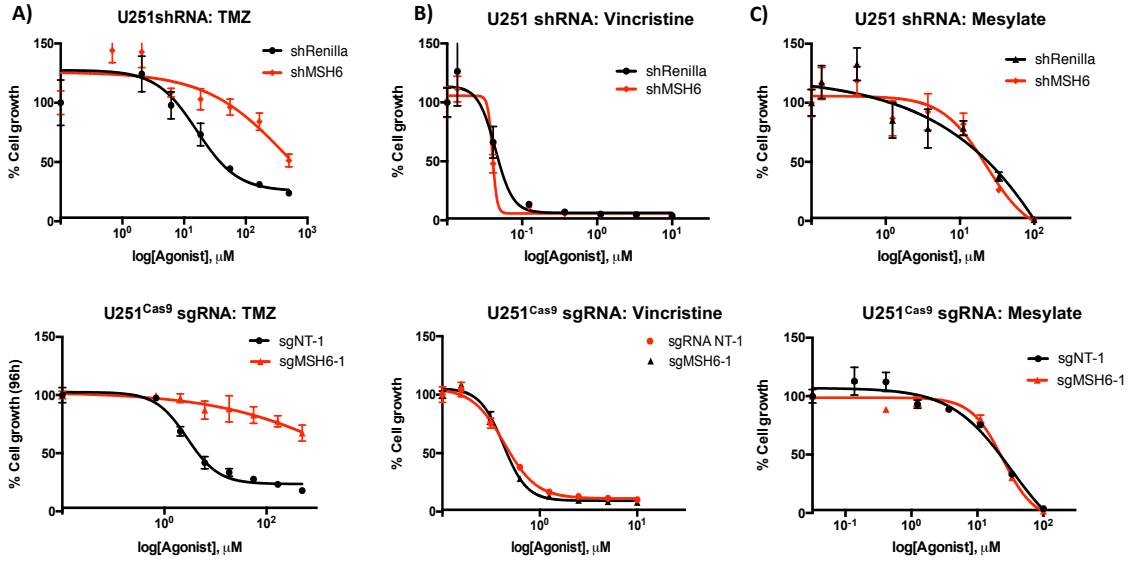

Figure 15: Example of validations of different "candidate" compounds in U251 cells transduced with RNAi (top panel) or sgRNA (bottom panel) to block the expression of MSH6. Cells were plated in 96-well plates and treated with decreasing doses of TMZ (500µM) **A)**, ETP-45338 (10µM) **B)** or ETP-51636 (100µM) **C)**. Cell growth was measured 96h after treatment by MTT assay. The results are presented as the mean and SD of five separate replicas and are expressed as the percentage relative to vehicle-treated control cells.

One drawback of the RNAi approach could be that the small levels of residual protein expression can be sufficient to avoid differences in cell viability, growth or drug response. For the compound validations we decided to generate also pure populations of MSH6-deficient cells by CRISPR/Cas9 system in U251 cells (Figure 14A). Nonetheless, we were not able to validate any of the compounds identified in this screening (Figure 15 – bottom panel). The compound screening is a technique widely-used in drug discovery (Macarron et al., 2011). We could perform a more High-Throughput Screening (HTS) using bigger compounds libraries in order to identify compounds that could sensitize more the MMR-deficient GBM cells.

3. Val-083 as a possible alternative treatment for GBM patients

The main limitation of treating GBM patients is, not only the acquisition of drug resistance which results in tumor recurrence, but also the ability of the drug to cross the BBB (Woodworth et al., 2014). It is extremely important the development and/or testing of new compounds, particularly those with different cytotoxic mechanisms of action. The aim is overcome chemoresistance, prolongs the survival and the quality of life of the patients.

One of these compounds that could help patients is the by-alkylating agent 1,2:5,6-Dianhydrogalactitol (Val-083). Val-083 is a first-in-class which means that is not an analogue or derivative of other small molecule chemotherapeutics approved for the treatment of cancer. It has shown potential antineoplastic activity, it crosses the BBB and appears to be selective for tumor cells. It does not show cross-resistance to other conventional chemotherapeutic agents and it has a long half-life in the brain being well tolerated at doses up to 40mg/m2 (Bacha et al., 2016). This compound induces interstrand crosslinks at N7-guanines generating persistent DSBs (Figure 16) and activating the homologous recombination (HR) repair pathway, which leads to cell cycle arrest in a p53 dependent or independent manner (Zhai et al., 2017). A phase III clinical trial is ongoing in order to test its efficacy in combination with Rx in patients with Newly Diagnosed GBM (unmethylated MGMT) (NCT03050736) and another phase II

clinical trial is active for patients with recurrent malignant glioma (NCT01478178). Preliminary data showed promising efficacy in GBM cells (Fouser et al., 2014).

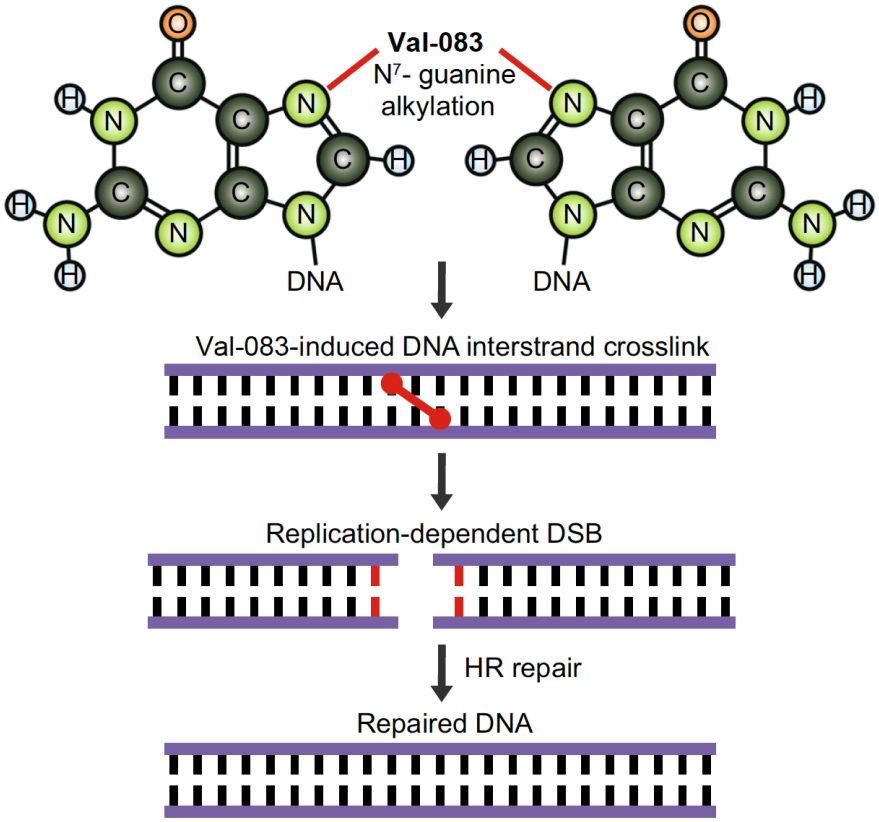

Figure 16: Mechanism of action of Val-083. Val-083 treatment induces interstrand DNA crosslinks through N7-guanine alkylation, leading to replication-dependent DSB. HR DNA repair pathway can be involved in DNA restoration (adapted from Zhai et al., 2018).

3.1 Val-083 activity is independent of MMR-status and MGMT methylation *in vitro*

We first decided to elucidate the efficacy of Val-083 as compared to TMZ in different primary human GBM cells with distinct genetic background: MGMT+ (T98G), MGMT- (U251) and MMR defective by silencing MSH6 using RNAi or CRISPR editing. Notably, we observed that, contrary to the response to TMZ (Figure17A, 17B, 17C – top panels), the various cells lines responded equally to Val-083. This suggests that its activity is not only MGMT but also MMR-independent. (Figure17A, 17B, 17C – bottom pannels).

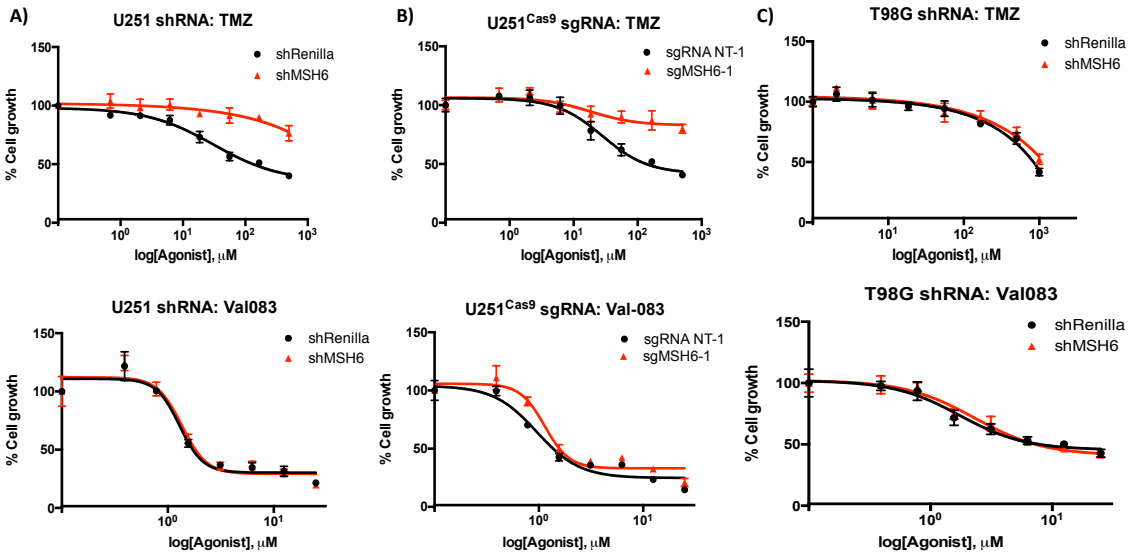

Figure 17: Val-083 is independent of MGMT or MMR status in GBM cell lines. Cells were treated with decreasing doses (dilution 1/3) of TMZ (500μM for U251 cells and 1mM for T98G cells) and Val-083 (25μM). **A)** Dose response assay in U251 cells transduced with shRNA to knockdown MSH6. **B)** Dose response assay in a pure population of U251^{Cas9} cells KO for MHS6. **C)** Dose response assay in T98G cells transduced with shRNA to knockdown MSH6. Cell growth was measured 96h after treatment by MTT assay. The results are presented as the mean and SD of five separate replicas and are expressed as the percentage relative to vehicle-treated control cells. NT: non-targeting.

3.2 Val-083 leads to cell cycle arrest at G2/M phase

Next, we carried out a cell cycle profile analysis in order to compare the effect on cell cycle progression using different doses of TMZ or Val-083. As shown in figure 18, as expected, treatment with TMZ in U251 "shRenilla" cells results in an increase of the percentage of G2/M cells, whereas this effect was not observed in MSH6 deficient cells (Top left panel). However, Val-083 produced G2/M phase arrest in both MMR-proficient and deficient cells (Figure 18, bottom left panel).

Finally, Val-083 led to a dose-dependent increase in G2/M in MGMT-positive T98G cells and this effect was also independent of MMR status (Figure 18, bottom right panel). These results confirm that the mechanism of action of Val-083 is independent of MGMT and MMR expression.

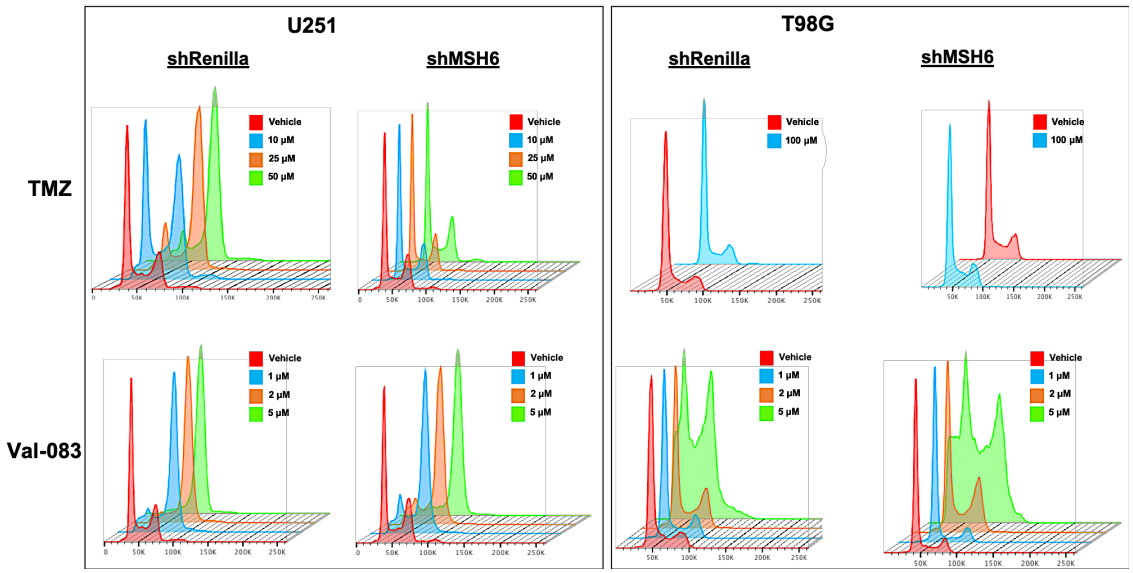

Figure 18: Val-083 promotes cell cycle arrest in G2/M phase independently of MGMT or MMR status in GBM cells. Cell cycle profile in U251 and T98G cells MSH6 proficient of deficient. Cells were treated with increasing doses of TMZ or Val-083**.** The data is representative of three independent experiments and 96h of treatment.

3.3 Combination of TMZ and Val-083 have synergistic effects in MMR-proficient and MGMT-methylated cells

For some cancers, where the current treatment is limited, combination of chemotherapies represents a promising alternative for the patients. The main objectives of using this approach are better efficacy, decreased toxicity, and reduced development of drug resistance (Foucquier & Guedj, 2015).

Because TMZ and Val-083 have independent mechanisms of toxicity, we were wondering whether Val-083 could have a synergistic effect in combination with TMZ. For this purpose, a combinatory experiment with TMZ or Val-083 was performed in U251 cells. These cells were plated and treated with increases doses of TMZ and/or Val-083 for 96 hours, cell viability was measured by MMT assay and combinatory index (CI) was measured. CI less than 0,8 shows significant synergism. 10µM of TMZ and 0,5µM of Val-08 obtained the minor CI (0,374) (Figure 19A). Additionally, more synergistic effects were observed at lower doses of TMZ and Val-083 (Figure 19A). The evaluation of drug combination effect using a Bliss independence dose-response surface model confirmed that the highest peak of synergism was produced at 10µM of TMZ and 0,5µM of Val-083 (Figure 19B).

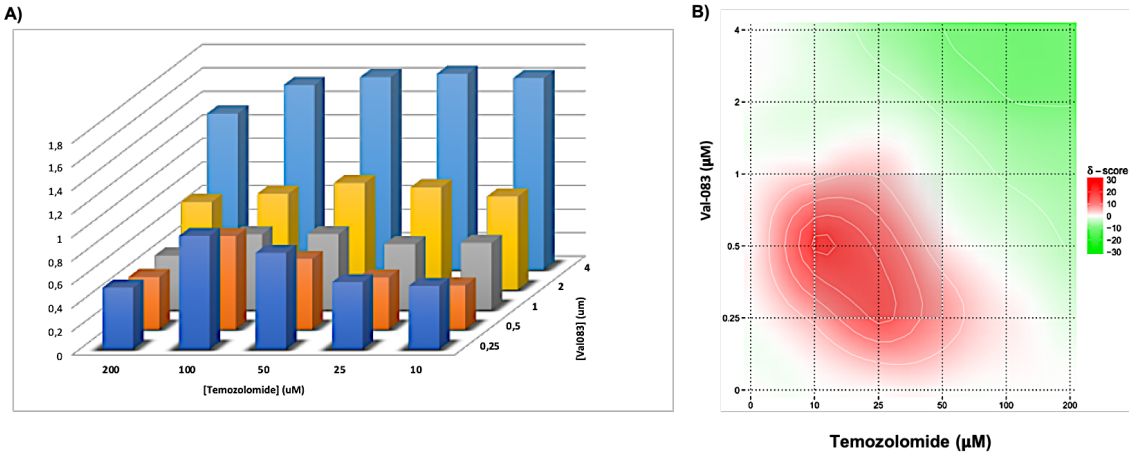

Figure 19: A drug combination data analysis. **A)** The bar graph shows the combination index (CI) of U251 cells treated 96h with TMZ, Val-083 and the combination. CI<0,8 shows synergism. **B)** A typical Bliss-plot analysis utilizes a dose-response matrix design where all possible dose combinations for a drug pair can be tested. Peak of synergism is triggered by a low dose of Val-083 (0,5 µM) and TMZ (10µM); δ: percentage of cell inhibition.

To further explore the synergistic effect of the combination of TMZ and Val-083, we performed a clonogenic assay testing 10µM or 25µM of TMZ and 0,5µM of Val-083. The results revealed the strongest effect in the combination between 10µM of TMZ and 0,5µM of Val-083 (Figure 20A). Cell cycle profile of U251 shControl cells revealed that the effect of combining TMZ and Val-083 produced an increase of G2/M arrest after 96h (Figure 20B – left panel), although each drug alone already induced a tiny effect on G2/M phase. To note that cells treated with 25µM of TMZ alone showed a marked reduction in colony formation and the addition of Val-083 did not lead to a drastic synergy in U251 shControl cells (Figure 20A; Figure 20C – left panel). As expected, we did not observe synergy of the drugs in MMR deficient cells (Figure 20B, C – right panel).

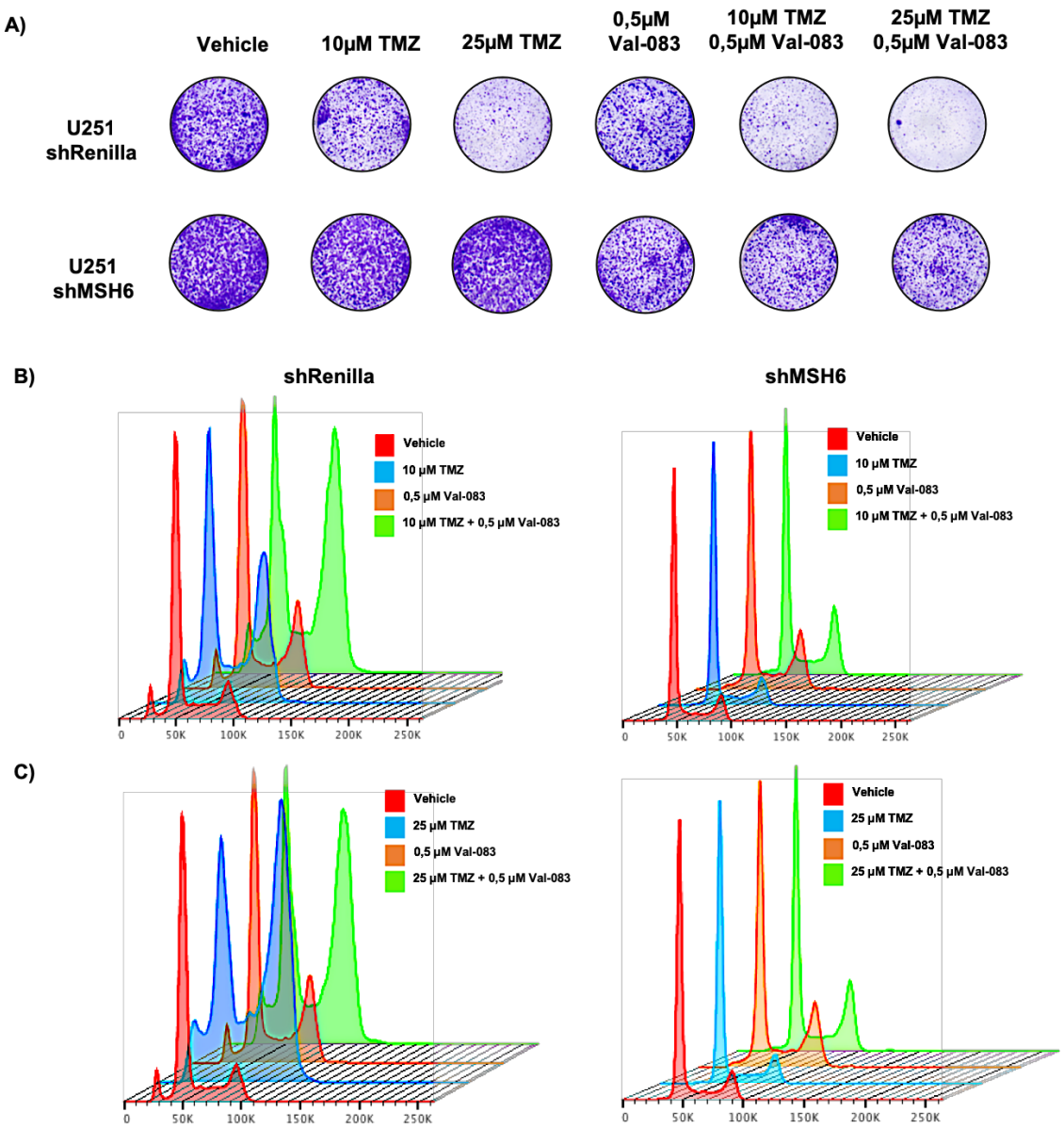

Figure 20: **Low doses of TMZ and Val-083 produce synergistic effect only in MGMT-negative U251-MG cells.** All experiments were performed in U251 control cells and MSH6-deficient U251-MG GBM cell lines. **A)** Clonogenic assay showed only a combinatory effect in U251 control cells treated with indicated doses of TMZ and Val-083 for 10 days. **B)** Cell cycle profile showed G2/M phase arrest in U251 cells treated with TMZ and Val-083 for 96h. The data is representative of three independent experiments. **C)** Cell cycle profile showed a G2/M phase arrest only in MSH6-deficient U251 cells treated with Val-083 for 96h. PI staining was performed, and cell cycle was measured and analyzed as indicated in materials and methods. The data is representative of two independent experiments.

3.4 TMZ and Val-083 treatment induces higher level of DNA damage

It is known that the TMZ treatment induces DSB when MMR pathway is active, resulting in cell death by apoptosis (Roos and Kaina, 2013). To further characterize how the synergistic effect produced by TMZ and Val-083 leads to cell cycle arrest, we examined the DNA damage status by measuring p-H2AX and 53BP1 foci formation.

Using high-throughput fluorescence microscope, we detected that the combination offered a higher activation of the DNA damage response giving rise to p-H2AX (Figure 21A – left panel;), an increase of 53BP1 foci, suggesting higher DSB-containing chromatin, and less proliferation after 72h of treatment (Figure 21A – right panel). The effect on DNA damage response of the combinatory treatment was also corroborated by flow cytometer (Figure 21B). More experiments are needed to fully elucidate the mechanism of how Val-083 in combination with TMZ induce DNA damage.

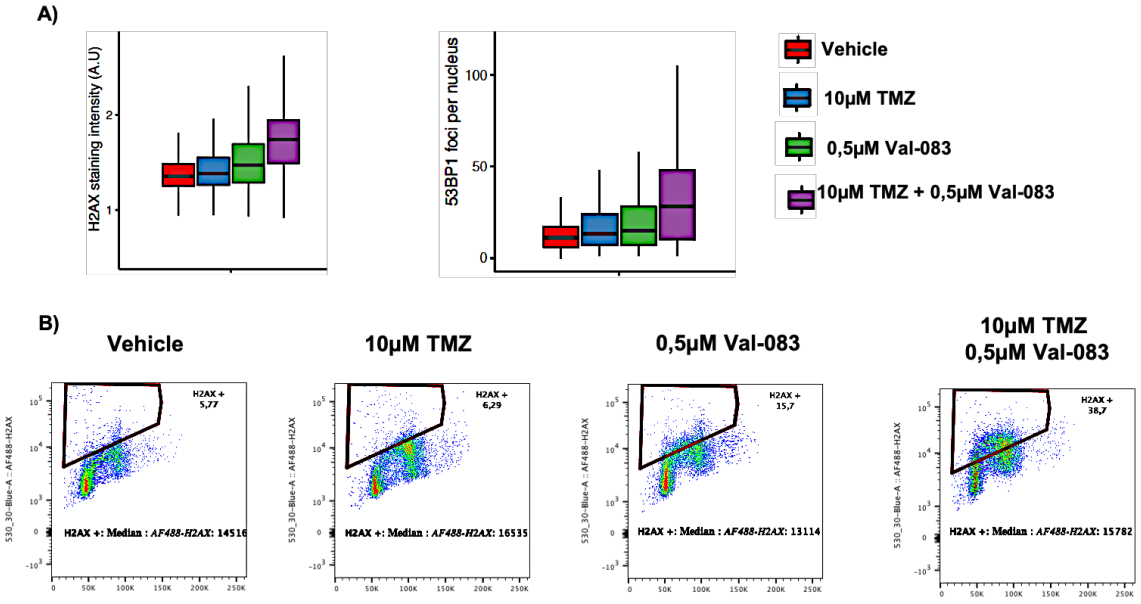

Figure 21: DNA damage is increased in combinatory treatment of Val-083 and TMZ. **A)** Measurement of different markers to evaluate DDR in U251-MG cell line after 72h with the indicated doses of Val-083, TMZ and combination of them. Then, cells were processed as indicated in material & methods and p-H2AX and 53BP1 were measured and quantified (Left and bottom panel). Val-083 and TMZ increased DNA damage in U251 cells. **B)** Flow cytometric analysis of p-H2AX after 72h of treatment. The data is representative of two independent experiments.

3.5 *Ex vivo* experiments confirm the synergistic effect between Val-083 and TMZ

Finally, to study the effect of Val-083 and its combination with TMZ under more physiological conditions we used an organotypic approach. Organ brain slices culture is a powerful tool for pharmacological studies of the CNS since it conserves the cellular structure, vessel network, and extracellular matrix of the brain (Cho et al., 2007; Fridén et al., 2009). Moreover, this procedure has been recently used to test some drugs in malignant brain tumors (Minami et al., 2017). We injected immunocompromised mice with U251 cells previously transduced with firefly luciferase (Fluc) to monitor tumor growth by IVIS spectrum. Once the mice manifested clinical symptoms of GBM development (lethargy, poor grooming, weight loss, macrocephaly), they were sacrificed, and brains were collected and processed as explained in materials and methods (Figure 22A). Brain slices were treated for 7 days with 10 and 25 μM of TMZ, 0,5 μM of Val-083 and the possible combinations (10 + 0,5μM or 25 + 0,5 μM). Luciferase activity was measured at day 0, day 4 and day 7 (Figure 22B). As observed in figure 22D single doses of TMZ or Val-083 decreased tumor growth after 7 days of treatment. Most importantly, combination of treatments resulted in a marked decrease of tumor growth confirming the synergistic effect between TMZ and Val-083. As expected, only Val-083 treatment gave a reduction in tumor growth in the MMR-defective cells (Figure 22E).

These results indicate that the TMZ and Val-083 combinatory treatment may be a promising approach for MGMT methylated patients. Moreover, our data would suggest that recurrent patients carrying defects in MMR could potentially benefits of second line treatment with Val-083.

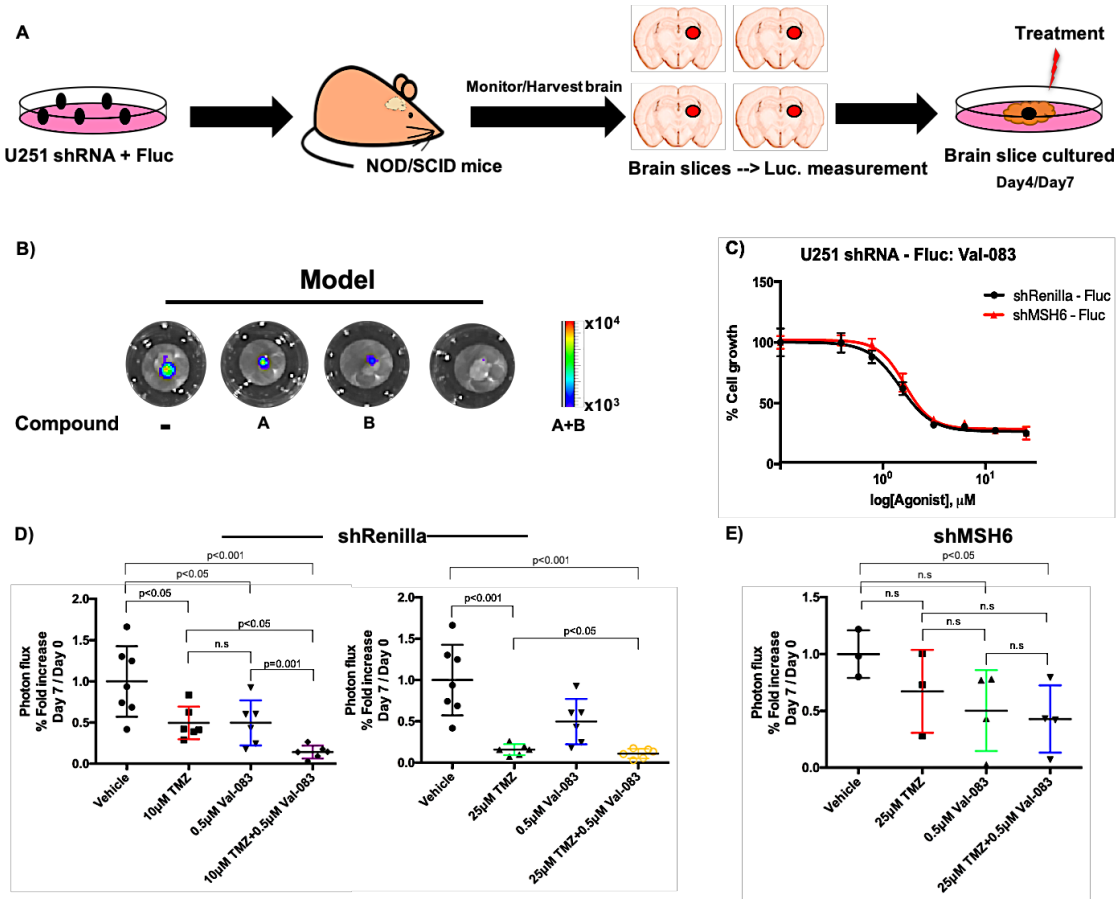

Figure 22: Orthotopic experiments showed a benefit in brain slices treated with low doses of TMZ and Val-083. A) Workflow for the orthotopic experiments. 5x10^5 U251^{Fluc}-MG cells (control or shMSH6) were injected orthotopically into nude mice and monitored 2 times/week. When the signal was optimal (>10^3 photons), brains were collected, and brains slices were processed and cultured as explained in material and methods and cultured. Treatment with Val-083 and/or TMZ was added at that point for 7 days. **B)** Representative images of brain organotypic cultures with established U251^{Fluc} cells derived tumors (luciferase^{+}) grown ex vivo for 7 days in the presence or absence of Val-083 (0,5 µM), TMZ (10/25 µM) or both. **C)** Dose response assay in U251^{Fluc} cells transduced with RNAi control or MSH6 and treated with decreasing doses (dilution 1/3) of Val-083. No differences on Val-083 response were observed. **D)** Quantification of the bioluminescence signal emitted by in U251^{Fluc} cells in each brain slice normalized by the initial value obtained at day 0 (before the addition of either DMSO, Val083, TMZ or both). **E)** Quantification of the bioluminescence signal emitted by in U251^{Fluc} shMSH6 cells in each brain slice normalized by the initial value obtained at day 0 (before the addition of either DMSO, Val083, TMZ or both). Values are shown in box-and-whisker plots and the line in the box corresponds to the median. *P* values were calculated using the two-tailed *t*-test; n.s: not significant.

4. Development of new murine model for the study of gliomas

Cancer is a heterogeneous disease characterized by multiple acquired capabilities impacting molecular, biochemical and cellular functioning. However, the function of most of these alterations is not yet known. Consequently, animal models are needed to recreate the genetic alterations that occur in patients which would help studying the biology of cancer and finding new treatment options.

As we have mentioned in the introduction, one of the most widely-used models for the study of gliomas is based on the RCAS-Tva system which is a highly reproducible, versatile and feasible model that recapitulates the high-grade glioma features (Holland & Varmus, 1998). The main aim for the last part of my project was to combine the RCAS-Tva system with the CRISPR/Cas9 genome editing technology to create a novel tool for the study of gliomas *in vivo* that could help us in cancer modelling and preclinical studies.

4.1 New Nestin/GFAP-Tva and Cas9-expressing mice

We first wanted to prove the efficacy of having a conditional and cell-type specific expression of Cas9 in brain in Nestin-Tva (NTva) or GFAP-Tva (GTva) mice. For this purpose, we used the Rosa26-LSL-Cas9 knockin mice (LSL-Cas9) (Platt et al., 2014). This mouse strain has a lox-stop-lox cassette previous the expression of the Cas9, linked via a self-cleaving P2A peptide to an enhanced green fluorescent protein (EGFP) to facilitate visualization of Cas9-expressing cells. We crossed these mice with NTva and GTva transgenic mice obtaining two different strains: NTva; Rosa26-LSL-Cas9 or GTva; Rosa26-LSL-Cas9. After crossing these mice with the tissue-specific Nestin-Cre (NCre) or hGFAP-Cre (GCre) (Tronche et al., 1999; Zhuo et al., 2001) we obtained the final strains NTv-a; NCre; LSL-Cas9 and Gtv-a; GCre; LSL-Cas9 (Figure 23A).

The second component of the RCAS/Tva system is the RCAS retroviral plasmid. We generated different RCAS-sgRNA plasmids that would allow the expression of any sgRNA of interest under the control of the human U6 promoter (Figure 23B). We also developed bicistronic RCAS-sgRNA with a driver oncogene PDGFB cassette in order to increase the efficacy of the system. In this way, all cells infected with the RCAS-sgRNA-Puro-PDGFB will contain not only the

PDGFB for tumorigenesis but also the sgRNA for the genome editing (Figure 23B). Additionally, we generated the RCAS-dualsgRNA-PuroBFP and the RCAS-sgRNA-Puro-HDR (Figure 23B) used to generate genomic rearrangements and point mutations respectively (Oldrini et al., 2018).

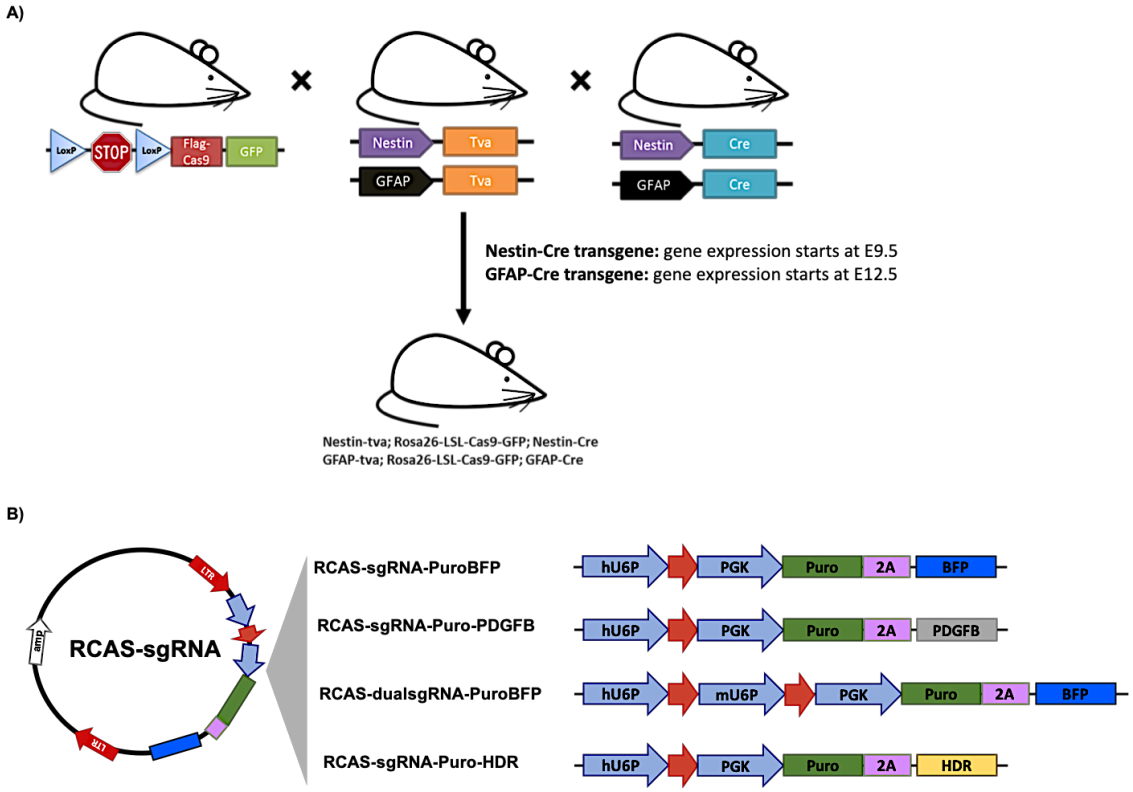

Figure 23: A) Scheme of the strains crossed for the generation of the Ntv-a; NCre; LSL-Cas9 andGtv-a; GCre; LSL-Cas9 mice. Cas9 is expressed in the TVA positive cells in both Ntv-a; NCre; LSL-Cas9 and Gtv-a; GCre; LSL-Cas9 mice. **B) Schematic illustration of the RCAS-sgRNAs plasmids developed to be used in the RCAS/Tva-CRISPR/Cas9 system.**

By using this new RCAS/Tva-CRISPR/Cas9 model, our aim was to generate precise glioma models exploiting the applicability that genome editing offered by the CRISPR/Cas9 system (KO, Knock-in, genomic rearrangements). To do so, either pups or adult mice from the strains developed can be injected with the RCAS retroviral plasmids for the generation of tumors with the desired alterations (Figure 24). Moreover, mouse neurospheres (mNSC) isolated from the strains generated in our laboratory can be infected *in vitro* with a lentiviral or retroviral plasmid that contains the sgRNA of interest. Then, the infected spheres can then

be transplanted orthotopically into nude mice to mimic glioma features (Figure 24). This strategy can help us study the biology of the tumors and, therefore, accelerate the pre-clinical testing of novel targeted therapies.

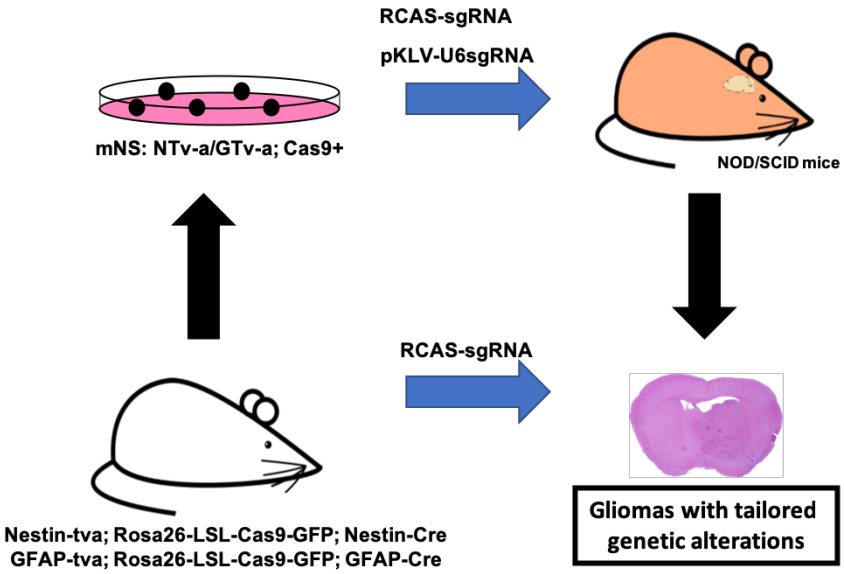

Figure 24: Workflow of the RCAS-CRISPR-Cas9 system to generate gliomas with tailored genetic alterations.

4.2 Efficient gene knockouts by RCAS-sgRNA vectors

CRISPR/Cas9 system is mostly used to generate gene knock-out (KO). Hence, in order to check whether our novel model is useful for the generation of "KO tumors" we cloned sgRNAs for tumor suppressor genes (TSGs) frequently altered in GBM: TP53, CDKN2a and PTEN, in addition to a non-targeting (sgNT) sgRNA as a control. The CDKN2A locus codes for two different proteins $p16^{INK4a}$ and $p14^{ARF}$ ($p19^{ARF}$ in mouse), both having tumor suppressor activity in gliomas (Shu et al., 2002; Weber et al., 2000). For our analysis, we have used a sgRNA targeting Cdkn2a exon 1β and therefore specific for $p19^{ARF}$.

First of all, to test the KO efficiency of the RCAS-sgRNA plasmids carrying the different guides for TSGs (RCAS-sgRNA-TSGs), we isolated and infected mNSCs from NTva; LSL-Cas9 mice with a Cre-expressing plasmid to induce Cas9 expression (mNSC-Tva-Cas9). In parallel we also generated NIH-3T3 mouse fibroblasts expressing both the Tva and the Cas9 genes (3T3Tva-Cas9).

We then infected both cell lines with the supernatant from DF1 cells transduced with the different RCAS-sgRNAs. After either drug-selection (for the mNSC-Tva-Cas9) or fluorescent-activated cell sorting (FACS) (for the BFP in the 3T3Tva-Cas9) we observed a clear reduction of Trp53, Cdkn2a and Pten by western blot analysis (Figure 25). Since NIH-3T3 cells are Cdkn2a null, we tested the Cdkn2a sgRNA efficacy only in the mNSC (Figure 25 – right panel).

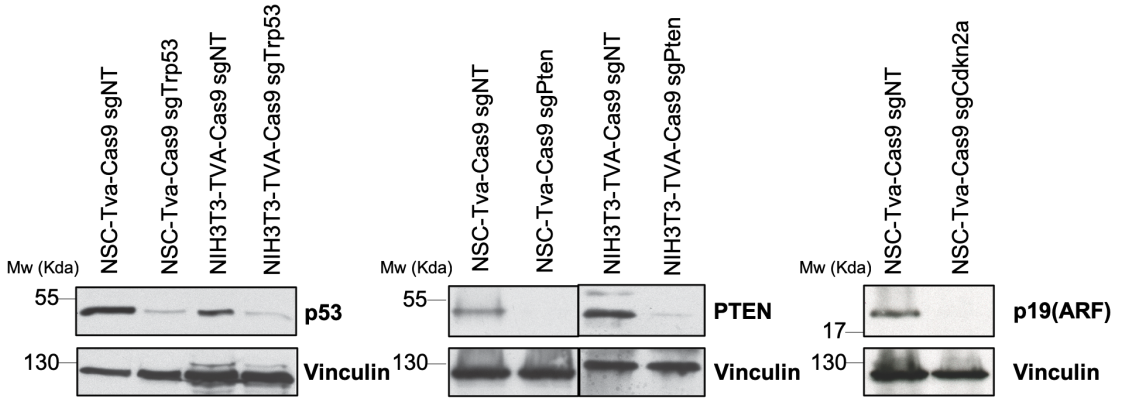

Figure 25: *In vitro* validation of the RCAS-sgRNA against Trp53, Pten, p19^{ARF} (Cdkn2a) or non-targeting control (NT). Western blot analysis, using the indicated antibodies, on whole cell extracts from 3T3Tva-Cas9 fibroblasts and mNSC-Tva-Cas9. For p53 analysis, its expression was induced by exposition to 10Gy of IR and cells were collected after 24 h.

Once we confirmed that the sgRNA worked as expected, we performed intracranial injection into NTv-a and GTv-a, either in pups or in adults, using RCAS-PDGFB as an oncogene driver to induce tumorigenesis in combination with RCAS-sgRNA vectors (either for *Trp53*, *Cdkn2a*, *Pten* or non-targeting sgRNA). Additionally, we injected the bicistronic RCAS-PDGFB construct carrying *Cdkn2a* sgRNA.

In pups, co-injections of RCAS-PDGFB and RCAS-sgRNA-TSGs both in NTva or GTva accelerated tumor formation. In addition, tumor incidence was increased when compared to co-injections RCAS-PDGFB and RCAS-sgRNA non-targeting control (NT) (Figure 26), where the tumorigenesis was very limited. In some cases, we did not even observe tumor formation in the co-injections of the RCAS-PDGFB and RCAS-sgRNA-NT. Finally, we observed similar median survival in NTva and GTva mice (Figure 26). In NTva and GTva

adult mice, the co-injections of RCAS-PDGFB and RCAS-sgRNA-TSGs also accelerated tumor formation. Mice injected with RCAS-PDGFB and RCAS-sgRNA-NT did not show tumor formation (Figure 26). We decided to have a timeframe of 120 days for the experiments (Figure 26).

A)

Strain	RCAS vectors	High grade frequency	Median survive (days)
Ntva; Ncre; LSL-Cas9 (Pups)	PDGFB + sgRNA NT	2/6(33%)	73
	PDGFB + sgRNA p53	5/5 (100%(	40
	PDGFB + sgRNA Cdkn2a	9/9 (100%)	35
	PDGFB – sgRNA Cdkn2a (bicistronic)	4/4 (100)	38,5
	PDGFB + sgRNA Pten	8/9 (88%)	33
Ntva; Ncre; LSL-Cas9 (Adults)	PDGFB + sgRNA NT	0/6 (0%)	na
	PDGFB + sgRNA p53	5/7 (71%(	46
	PDGFB + sgRNA Cdkn2a	3/6 (50%)	57
	PDGFB + sgRNA Pten	0/5 (0%)	33

B)

Strain	RCAS vectors	High grade frequency	Median survive (days)
Gtva; Gcre; LSL-Cas9 (Pups)	PDGFB + sgRNA NT	2/7 (29%)	77
	PDGFB + sgRNA p53	7/7 (100%)	42
	PDGFB + sgRNA Cdkn2a	6/6 (100%)	43,5
	PDGFB + sgRNA Pten	5/5 (100%)	33
Gtva; Gcre; LSL-Cas9 (Adults)	PDGFB + sgRNA NT	0/8 (0%)	na
	PDGFB + sgRNA p53	4/6 (67%(	53
	PDGFB + sgRNA Cdkn2a	1/4 (25%)	na
	PDGFB + sgRNA Pten	1/6 (17%)	na

C)

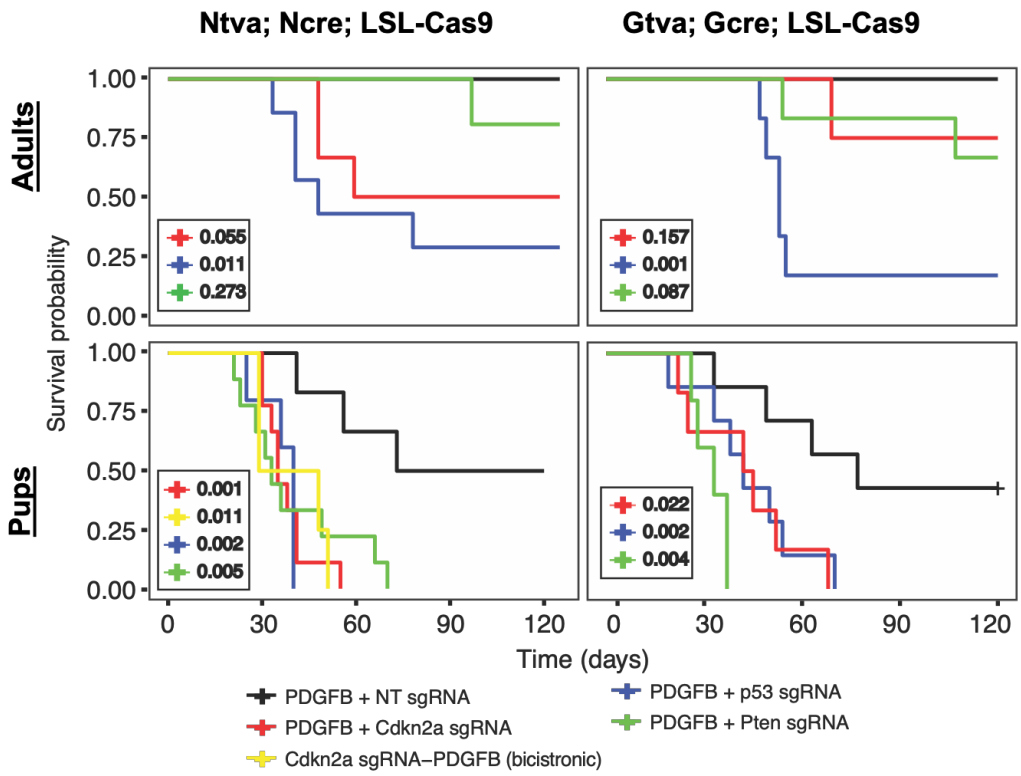

Figure 26: Coinjections with RCAS-PDGFB and RCAS-sgRNA-TSGs accelerate tumor formation and increase tumor incidence. A & B) Table summarizing the injections performed in the *Ntv-a; NCre; LSL-Cas9* and *Gtv-a; GCre; LSL-Cas9* pups and adult mice. Co-injection of RCAS-PDGFB and the RCAS-sgRNA against different tumor suppressor genes accelerate tumor formation, increases the tumor penetrance and the frequency of high-grade gliomas. **C)** Kaplan-Meier survival curves of Ntv-a; NCre; LSL-Cas9 and Gtv-a; GCre; LSL-Cas9 mice injected with the indicated RCAS plasmids.

All mice injected with the RCAS-sgRNA-TSGs displayed histological features of high-grade gliomas: microvascular proliferation and pseudopalisading necrosis (Figure 27 A). Further characterization of these tumors by immunohistochemistry (IHC) of paraffin-embedded tumor tissue showed high KI-67 positive cells and low amount of Cleaved caspase 3 positive cells (Figure 27B). To note, low grade gliomas where developed only in mice injected with RCAS-sgRNA-NT and displayed low proliferation and Cleaved caspase 3 positive cells (Figure 27B). Loss of $p19^{ARF}$ and PTEN expression in tumors injected with the corresponding RCAS-sgRNA-TSGs plasmids were verified by IHC (Figure 27A) and also by western blot in tumor-derived neurospheres (tumorspheres) (Figure 28A). Moreover, spheres derived from the PTEN KO tumors showed an increased activation of AKT signaling pathway by high phospho-AKT and phospho-S6 as compared to CDKN2a KO cells (Figure 28A). We also confirmed that the Cdkn2a sgRNA only targeted in the $p19^{ARF}$ locus and did not affect the expression of $p16^{INK4a}$ (Figure 27A, 28A). Finally, we proved the presence of deletions and/or insertions at the sgRNA target sites in tumorspheres from the various TSG models (from Pten and Cdkn2a) by sanger sequencing (Figure 28B).

In case of the RCAS-sgRNA-Trp53 induced tumors, we exposed tumor-bearing mice as well as tumorspheres to ionizing radiation (IR) in order to activate the p53 signaling pathway. As observed in figure 28A, neither p53 nor its negative regulator p21 were detectable in the Trp53 null tumors as compared to the other tumors (Figure 29A). We also detected the deletion in the p53 locus as well as the absence of p21 from the tumorspheres (Figure 29B). Additionally, real-time quantitative PCR (RT qPCR) analysis on IR treated tumorspheres showed lack of expression of a panel of p53 transcriptional targets (p21, Noxa, Mdm2 and

Puma) (Figure 29C). As before, the presence of deletions and/or insertions at the sgRNA locus in tumorspheres from p53 was verified (Figure 29D).

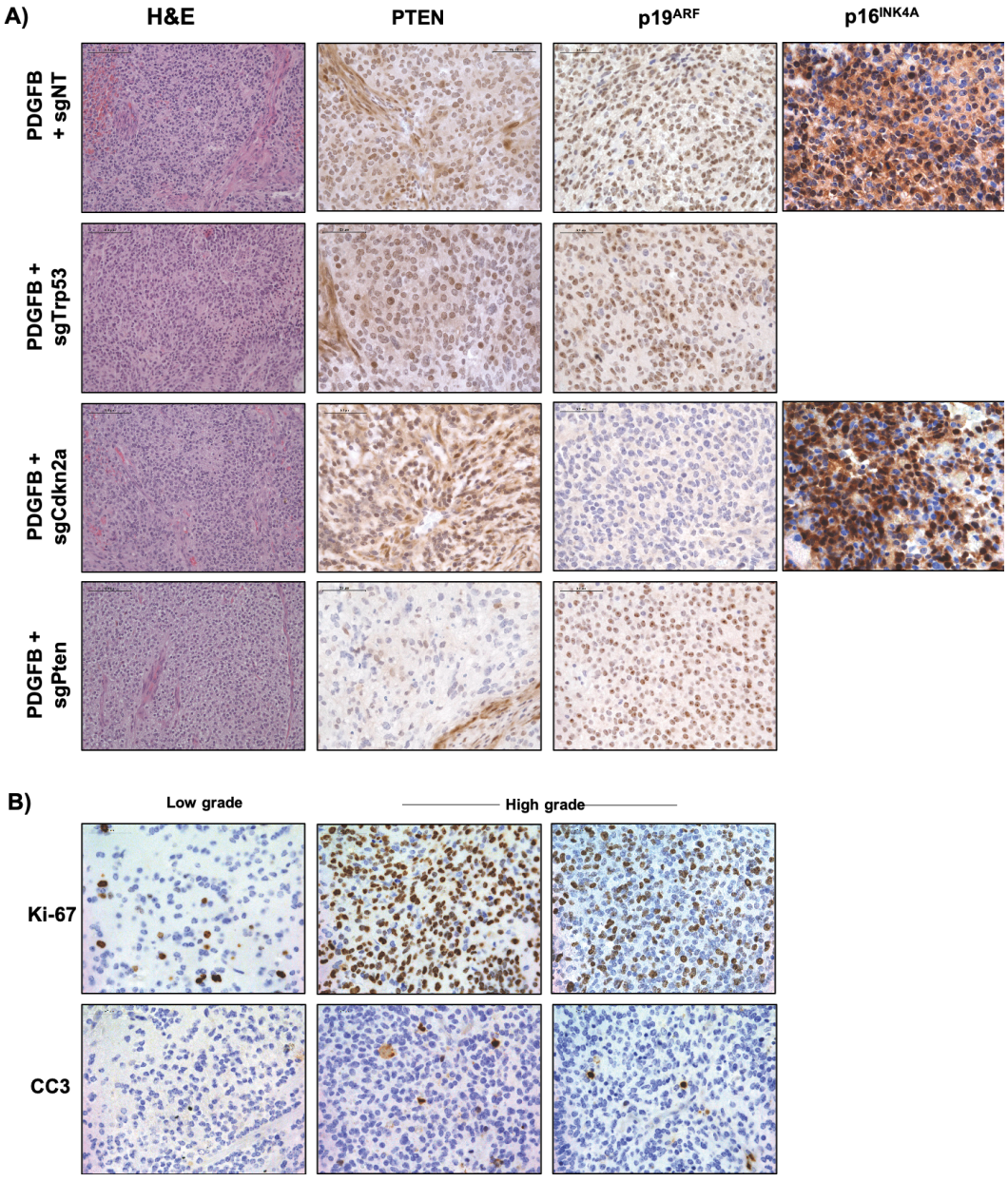

Figure 27: A) Hematoxylin and eosin (H&E) and immunohistochemical stainings (IHCs), using the indicated antibodies, of representative RCAS-PDGFB/sgRNA tumors. To note PTEN expression in the normal vasculature but not in the tumor cells of the RCAS-PDGFB + RCAS-sgRNA-Pten tumor. Scale bars: 100 µm. **B)** IHCs for Ki67 and Cleaved caspase 3 on the low- or high-grade gliomas. Scale bars:100 µm.

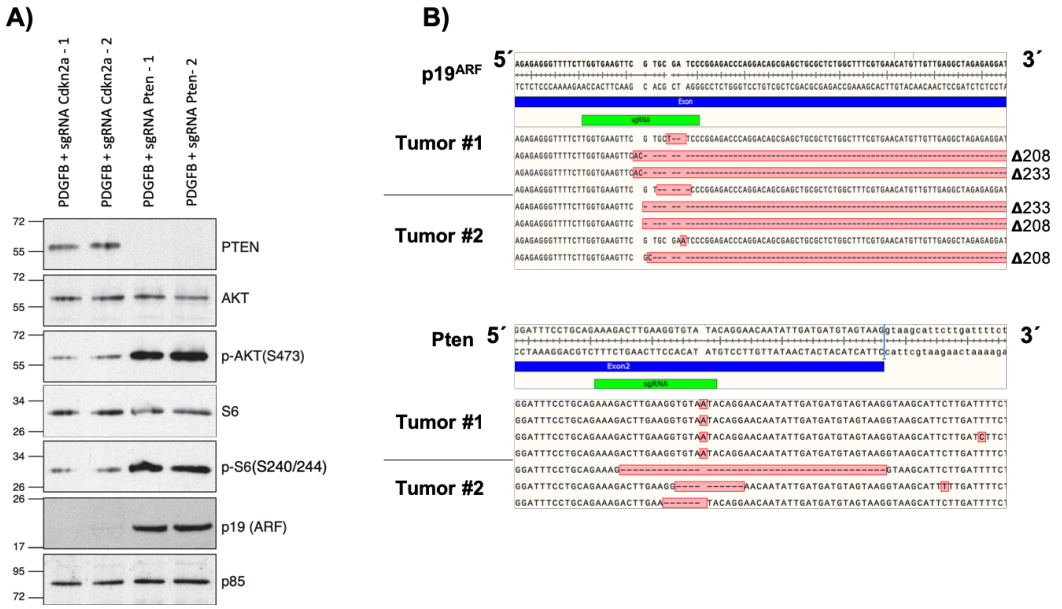

Figure 28: A) Western blot analysis, using the indicated antibodies, on whole cell extracts from tumorspheres. **B)** CRISPR/Cas9 editing in the targeted tumor suppressor genes Cdkn2a and Pten. The targeted loci were amplified from tumor-derived neurospheres. The PCR products were ligated into a cloning vector and sequenced via Sanger sequencing (n=2 tumors, 4 clones each). Deletions or insertions were found.

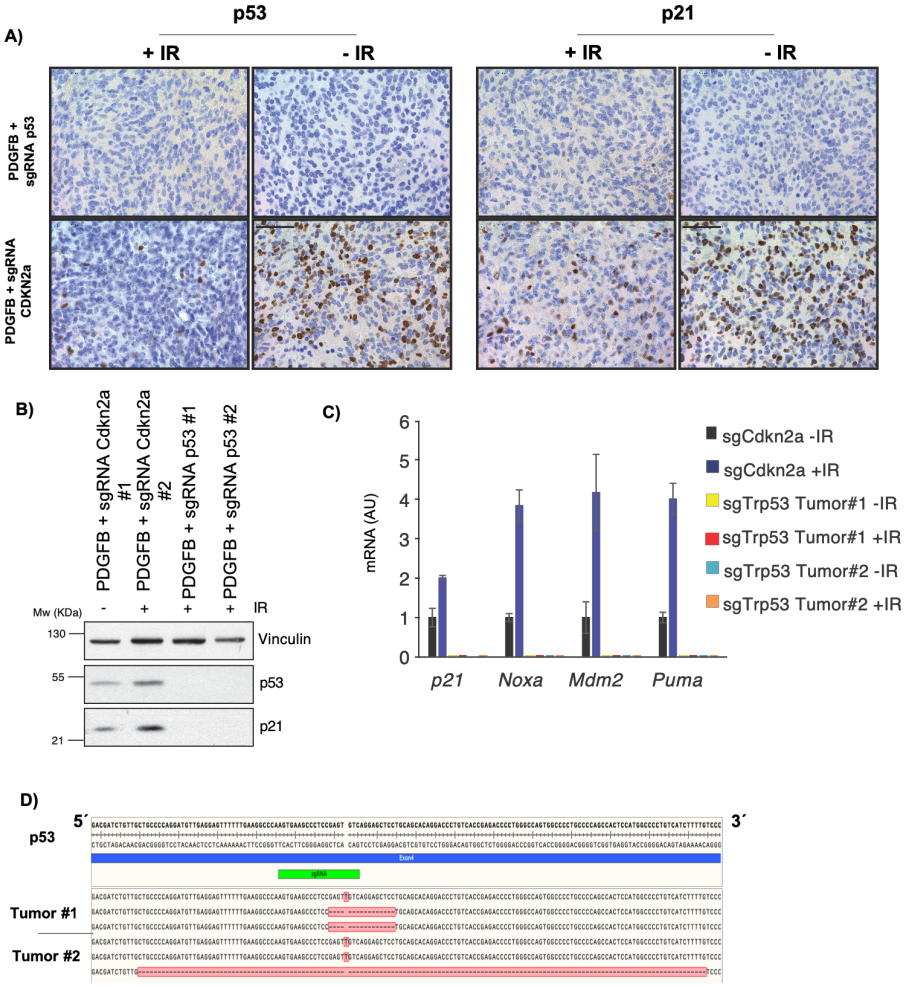

Figure 29: A) IHCs for p53 (left panel) and p21 (right panel) on the indicated tumors 1 h after exposure to 10 Gy IR. Scale bars: 50 µm. **B)** Western blot analysis, using the indicated antibodies, on whole cell extracts from tumorspheres 24 h after exposure to 10 Gy IR. **C)** Quantitative real-time PCR (qPCR) analysis on mRNA extracted from tumorspheres 3 h after exposure to 10 Gy IR. Data presented as mean ± SD (*n* = 3); A.U. arbitrary unit. **D)** CRISPR/Cas9 editing in the targeted tumor suppressor gene Trp53. The targeted loci were amplified from tumor-derived neurospheres. The PCR product was ligated into a cloning vector and sequenced via Sanger sequencing (n=2 tumors, 3 clones each). Deletions or insertions were found in all sequences and are displayed as dashes and red nucleotides, respectively. The gRNA target region is displayed in green and the 3′-PAM sequence in blue.

Altogether, all of these data demonstrate that the RCAS/Tva-CRISPR/Cas9 model is a powerful system to generates efficient KO tumors. The different TSGs cloned into the new RCAS-sgRNA plasmid induced loss of the gene of interest in an *in vivo* setting. Also, KO cells for TSGs acquired proliferative advantage that led to the generation of gene-specific null tumors that closely resemble their human features.

4.3. RCAS/Tva-CRISPR/Cas9 system allows to study the role of loss-of-funcition genes in a time-controlled manner

Besides exploring the role of TSGs genes in tumor initiation, we were also interested to check whether the RCAS/Tva-CRISPR/Cas9 model was suited to study the role of a gene of interest in tumor progression. In order to have an *in vivo* model for time-controlled gene editing, we crossed the NTva; LSL-Cas9 mice with the hUBC-CreERT2 (Ruzankina et al., 2007), that ubiquitously express a tamoxifen-regulated Cre.

Four-week-old adult NTva; LSL-Ca9; hUBC-CreERT2 mice were injected intracranially with the RCAS-PDGFB in combination with either RCAS-sgRNA-Trp53 or RCAS-sgRNA-NT. Two weeks after injection, mice were divided in two groups and treated for two weeks with either mock-treatment or tamoxifen (see Methods for details) (Figure 30A). Mice were then killed either upon sign of tumor development (seizures, lethargy, hunched posture, weight loss, …) or at the end of the experiment (90 days). All the NTva; LSL-Cas9; hUBC-CreERT2$^{+/T}$ mice injected with the RCAS-PDGFB and RCAS-sgRNA-Trp53 and treated with tamoxifen were killed at an earlier time due to high-grade gliomas (Figure 30B-

D). As for the NTva; NCre; LSL-Cas9 adult injections, none of the NTva; LSL-Cas9; hUBC-CreERT2$^{+/T}$ mice injected with the RCAS-PDGFB and RCAS-sgRNA-NT developed tumors (Figure 30C). However, Only one out of three of the mock-treated mice, injected with the RCAS-PDGFB and RCAS-sgRNA-Trp53 developed tumor, thought was a low-grade tumor (Figure 30B). Since we confirmed that this mouse had no expression of Cas9 (Figure 30B), we could exclude a possible relationship between the low-grade tumor observed and leakiness of the CreERT2 system. Although very rarely, the RCAS-PDGFB alone is sufficient to induce tumor formation in adult Ntv-a mice (Hambardzumyan et al., 2009).

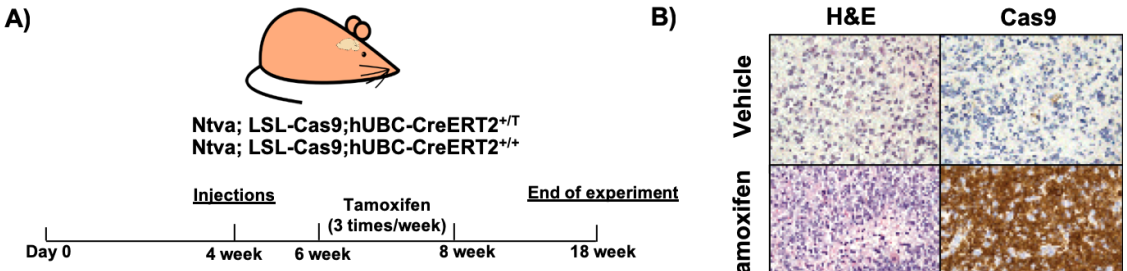

C)

Strain	Treatment	RCAS vectors	High grade frequency	Median survive (days)
Ntva; LSL-Cas9; hUBC-CreERT2 $^{+/T}$	Vehicle	PDGFB + sgRNA NT	0/4 (0%)	na
	Tamoxifen	PDGFB + sgRNA NT	0/3 (0%)	na
	Vehicle	PDGFB + sgRNA p53	0/3 (0%)	na
	Tamoxifen	PDGFB + sgRNA p53	3/3 (100%)	63

D)

Strain	hUBC-CreERT2	Treatment	RCAS vectors	High grade frequency	Median survive (days)
Ntva; LSL-Cas9;	+/+	Tamoxifen	PDGFB + sgRNA p53	0/4 (0%)	na
	+/T	Tamoxifen	PDGFB + sgRNA p53	3/4 (75%)	86

Figure 30: Ubiquitous Cas9 expression in TVA-Cas9 adult mice generates null tumors in a time-controlled manner. A) Scheme for the experiments in the *Ntv-a; LSL-Cas9*; *hUBC-CreERT2*$^{+/T}$ adult mice. **B)** H&E and Cas9 IHCs of RCAS-PDGFB + RCAS-Trp53-gRNA tumors for the indicated treatment. High-grade glioma features and Cas9 expression are present only in the tamoxifen-treated mice. Scale bars: 100 µm. **C-D)** Table summarizing the injections performed in the *Ntv-a; LSL-Cas9*; *hUBC-CreERT2*$^{+/T}$ adult mice. Mice injected with RCAS-PDGFB + RCAS-Trp53-gRNA and treated with tamoxifen to induce Cas9 expression, develop high-grade gliomas.

To complement these studies, we used NTva; LSL-Cas9 4-week-old mice, either hUBC-CreERT2+/+ or hUBC-CreERT2+/T and performed a second set of injections of the RCAS-PDGFB in combination only with the RCAS-sgRNA-Trp53. Two weeks after injection, tamoxifen was administered in the diet in all mice. Tumor formation was observed exclusively in the hUBC-CreERT2+/T genetic background (Figure 30D). These data suggest that the RCAS/Tva-CRISPR/Cas9 system would also be useful to generate KO tumors in a time-controlled manner.

Discussion

The present PhD project has been focused in the study of three important aspects:

a) Explore the mechanisms of resistance to TMZ in GBM.

The alkylating agent TMZ remains the unique option for GBM patients. Our first goal was the perform a genome-wide approach for the study the mechanisms of TMZ resistance. Because GBM patients do not respond equally to this treatment, and MGMT expression is the unique biomarker accepted so far, it is important to define novel TMZ-modulators than can be useful to predict the response.

b) Test the efficacy of a by-alkylating agent that can either substitute the current line of treatment or increase the efficacy of TMZ.

Taking into account the limitation of TMZ, there are many clinical trials trying to develop novel strategies to improve the survival in GBM patients.

c) Generation of new *in vivo* system for cancer modeling.

Recent new glioma classification based on molecular data have contributed to a better understanding of the disease. The development of precise models that recapitulate glioma alterations will help in the study of the biology of these tumors to better understand the disease and identify specific treatments for each type.

Next, we will proceed to the discussion of the results previously exposed, organizing it around the most relevant and/or controversial findings.

1) <u>Identification of potential modulators of TMZ response using a forward genetic screen approach.</u>

Forward genetic screens have been used in different studies for the identification of novel gene functions related to phenotypes of interest (Hillenmeyer et al.,2010; van Leeuwen et al., 2016). The screening in haploid cells is an unbiased approach used for genetic analysis. These cells only carry one set of chromosomes, which means that any single mutation in their genome will produce loss-of-function phenotypes (Li & Shuai, 2017). These screens are fast, cheap and reliable because the vast majority of hits obtained are very often positively validated (Carette et al., 2009; Carette et al., 2011; Elling et al., 2011). Finally, the haploid screens allow the identification of the mutations precisely by mapping the integration site. In contrast, evidence for genetic effects based on

RNAi or CRISPR methods can be biased due to off-target effects (Elling & Penninger, 2014).

The first objective of this project was to perform genome-wide libraries for the study of the TMZ resistance mechanisms. For this purpose, we have used a PB-transposon-mediated insertional mutagenesis approach in human haploid cells. Initially, we were able to identify 43 different genes related to the modulation of the TMZ response. By genome editing approach using the CRISPR/Cas9 system, all of these genes were validated in the haploid cells but only MSH6 gene was validated in the GBM context ($U251^{Cas9}$ and $U87^{Cas9}$; Figure 11). It is known that the mechanisms of chemo-resistance are not based only in one phenomenon and that many factors can be involved (Holohan et al., 2013). Although CRISPR based loss-of-function screens is a powerful strategy for unbiased phenotypic screen (Shalem et al., 2015), the number of false positive hits in samples has been reported (Sharma & Petsalaki, 2018). Therefore, it is extremely important to be aware that pooled screens are only the beginning of a study. All possible candidates have to be validated individually. Munoz and colleagues reported that the amount of false positive results is increased chromosomally unstable cancer lines, such as U251, the GBM cell line chosen for our screening (Munoz et al., 2016). These false positives could explain the identification of sgRNAs after CRISPR-sgRNA library analysis.

We have found some limitations in the course of our study. First of all, Hap1 cells are relatively resistant to TMZ due to the expression of MGMT, although MGMT levels are not as high as compared to the TMZ-resistant GBM cell line T98G (Figure 8B – bottom panel). Moreover, these cells are derived from leukaemia and the CRISPR secondary screening was performed only once in one GBM cell line which limits considerably the strength of the results.

2) Exploring synthetic lethality in MMR-deficient GBM cells.

Taking into account that the MMR status in GBM patients is very well-documented (Yip et al., 2009; Kunkel & Eurie., 2015), we decided to identify possible synthetic lethal interactions in MSH6-deficient GBM cells. Synthetic lethality occurs when alteration of two genes simultaneously results in cellular or

organismal death (Figure 12). This concept has been used for the identification of novel drugs that can cooperate with a specific genomic alteration or to explore their mechanism of action (Luo et al., 2009; Kaelin, 2009).

MMR-defective cells exhibit an “hypermutator phenotype” with a high rate of spontaneous mutations (Hunter et al., 2006), leading to an accumulation of microsatellite instability (MSI) (Strand et al., 1993). There are already described compounds that display synthetic lethality with different MMR components. For example, Hanley and colleagues showed that glioma tumor xenografts defective in MMR are hypersensitive to vinorelbine, a microtubule-targeting drug (Hanley et al., 1998). However, although anti-microtubular targeting has been shown to be cell-effective, the lack of specificity for tumor cells is translated into important side effects such as myelosuppression or neuropathy (Jordan & Wilson, 2004; Penna et al., 2017). Specifically, MSH2-mutant cancers are sensitive to methotrexate, an antimetabolite that inhibits DNA synthesis, and psoralen, a DNA crosslinking agent, but MLH1-mutant cancers are resistant to both treatments (Wu & Vasquez, 2008; Martin et al., 2009). This suggests that it is important to identify the MMR deficiency in the tumor as they differ in their therapeutic response.

In order to identify compounds that could be more effective in MSH6-defficient cells, we performed a compound screen in U251 cells with or without MSH6 deficiency (Figure 13C). The library of compounds used in this part of the project contained 120 antitumoral drugs that are FDA-approved or under clinical trials. Regrettably, we have not been able to validate any of the candidate drugs nor in the U251 cells transduced with siRNA neither in the $U251^{Cas9}$ carrying the sgRNA for MSH6 depletion (Figure 14). More precise experiments would be necessary (also in different GBM cell lines) in order to elucidate whether these candidate drugs would be interesting for preclinical assay in the MMR-deficient context.
In cancer, this strategy has allowed the identification of chemotherapies that now are in use, either alone or in combination (Mizuarai et al., 2008; Brägelmann et al., 2017). For example, cell viability with BRCA1/2-inactivating mutations was dependent on PARP for DNA-damage repair and led to the discovery of the synthetic lethality strategy using PARP inhibitors in these cells (Bryant et al.,

2005; Farmer et al., 2005; Lord & Ashworth, 2015). Thus, in order to identify promising drugs capable of sensitizing MSH6-defective tumors, we could perform other screens with bigger compound libraries.

3) Val-083 activity is independent of MGMT and MMR status.

Although the last decade highlighted enormous advances in treating other solid cancers, survival for GBM stayed nearly the same over the last 50 years, averaging 15 months from the time to diagnosis. All GBM patients receive the alkylating agent TMZ in addition to surgery and IR (Stupp et al., 2005). The main reasons for the use of this drugs in the clinics are its ability to cross BBB and possible extend of OS in patients (Figure 2A). Nevertheless, the main problems for these patients are the recurrence of the disease as well as the resistance to the current treatments with fatal results. For these reasons, many laboratories are trying to develop novel therapeutic strategies.

One of these drugs is Val-083, a “first in class” molecule able to cross the BBB and accumulate in tumor tissue (Eagan et al., 1979). Previous studies showed improved efficacy of this compound compared to TMZ in a MGMT and MMR-independent manner both *in vitro* and *in vivo* (Zhai et al., 2017). More important, this compound is already in clinical trials (in combination with radiotherapy in patients with newly diagnosed GBM (MGMT unmethylated) and in patients with recurrent malignant glioma). Our *in vitro* data confirmed that the effect of Val-083 is independent of MGMT (T98G cells) or MMR (U251 cells) status (Figure 16). Val-083 treatment led to cell cycle arrest at G2/M phase (Figure 17). This data supports the idea that they have different mechanisms of cytotoxicity, indicating non-overlapping functions between these two agents.

The mechanism of Val-083 is not well characterized. It induces interstrand crosslinks at N7-guanines generating persistent DSB and activating the HR repair pathway independent of MGMT, which leads to cell cycle arrest in a p53 dependent or independent manner (Zhai et al., 2017). There are regulatory mechanisms dependent on the cell cycle stage that are involved in the DSB repair by HR or NHEJ (Mao et al., 2008). Moreover, the G2/M phase DNA damage

signaling pathway is critical for the cellular response to DNA damage caused by chemotherapeutics having a great impact on treatment effectiveness. DNA damage activates several signaling cascades that ultimately serve to inactivate the CDK1-cyclin B1 complex, which causes G2/M cell cycle arrest (Ear et al., 2013). Our preliminary results showed an increase in DSB generation (Figure 19) at very low doses (0,5 μM) of Val-083. Further studies are necessary in order to perfectly elucidate the mechanism of action of this compound.

Single drug treatment can have poor therapeutic effect while treatment with multitarget drugs can regulate multiple network of the disease simultaneously improving the benefits and survival (Chen et al., 2013).
When the effect with a single drug is lower than that combined effect with a second drug, this combination is said to be synergistic. A synergistic interaction allows the administration of lower doses of the drug combination components, which may diminish adverse reactions such as toxicity or the development of drug resistance. This leads to an extension of life expectancy and improvement in the quality of life of the patients. Combination therapies are currently being used in the clinic for hypertension, asthma, or AIDS (Jeon et al., 2018), among other diseases. In cancer, several bioinformatic approaches have been published that identifying potential drug combinations that could be translated into the clinics (Bansal et al., 2014; Gaybert et al., 2017).

We wanted to explore the combinatory effect between Val-083 and TMZ and we observed a synergistic effect in U251 cells at lower doses for each compound (Figure 18). This effect was mediated by G2/M phase arrest with notable induction of DNA damage (Figure 19C). As discussed before, further analysis is needed to elucidate the mechanism by which Val-083 leads to G2/M phase arrest and how the combination potentiates this inhibitory effect.
In vitro and *ex vivo* models use characterized cells, replacing animal assays and facilitating the identification of the mechanism of action. *In vitro* models should mimic several features shown in human patients: proliferative capabilities and morphology of the tumor cells, cellular heterogeneity and drug response profile among others (Grotzer et al., 2016). However, some drugs may exhibit promising activity *in vitro* but may not exert similar beneficial properties *in vivo* or in patients,

due to less bioavailability or higher toxic effects on tissues and organs that were absent in an *in vitro* model (Saeidnia et al., 2015). In the context of GBM, the processes of cell dissemination, tumor recurrence and treatment resistance remain challenging. The development of novel systems where living brain tissue can be used for studying tumor cell growth, invasion and novel therapies, such as organotypic cultures, has allowed a deeper study of tumor biology (Jung et al., 2002; Grotzer et al., 2016). These research models also allow to study, not only the tumor biology, but also to explore novel therapeutic approaches.

We used an orthotopic approach in order to confirm the effect of Val-083, TMZ and their combination. As expected, *ex vivo* experiments showed a great combinatory effect between Val-083 and TMZ at low doses (Figure 22). However, preclinical models (*in vivo* experiments) are necessary to fully understand tumor biology and to evaluate drug delivery, particularly in glioblastoma where the BBB is the main obstacle to successfully treat patients. Our data could support different clinical approaches: First, Val-083 acts independently of MGMT expression. In this context, newly diagnosed GBM patients with unmethylated MGMT promoter could be treated with Val-083 alone (It is being tested under clinical trial in phase II) (Figure 31A). Second, Val-083 activity is also MMR-independent, so for those patients with recurrent GBM carrying mutations in MSH6, Val-083 could also be useful after TMZ treatment (currently under clinical trial phase III) (Figure 31B). Finally, newly diagnosed GBM patients with hypermethylated MGMT promoter could benefit from a combined treatment of Val-083 and TMZ (Figure 31C). Precise knowledge of the molecular mechanisms underlying tumor cell cytotoxicity is essential for optimal positioning of chemotherapeutic drugs in a clinical context.

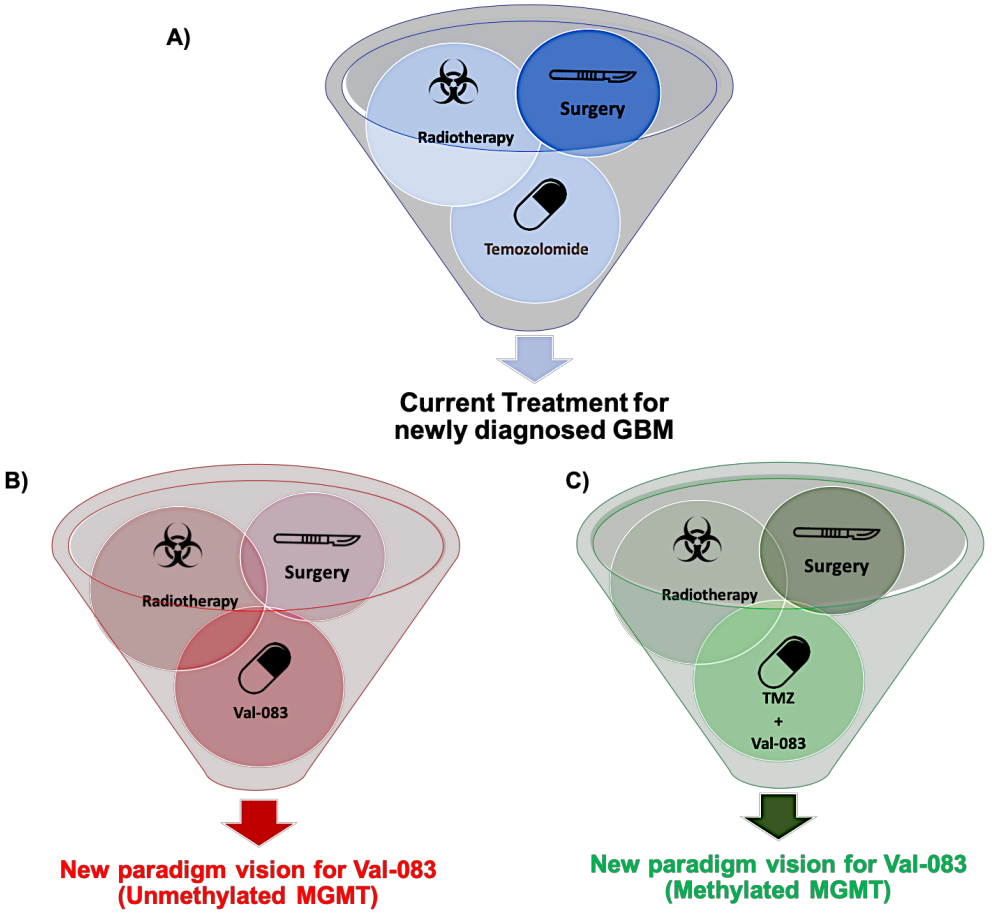

Figure 31: Schematic illustration of potential use of the compound in the clinic. A) Nowadays, patients with newly diagnosed GBM are treated with TMZ as a chemotherapy. However, cases with unmethylated MGMT promoter will not respond to TMZ. TMZ leads to self-resistance by accumulation of acquired mutations. **B)** Val-083 could be useful for patients with active MGMT in order to avoid tumor progression. **C)** Combinatory treatment with TMZ and Val-083 may be effective in patients with inactive MGMT as a first line of treatment.

4) RCAS/Tva-CRISPR/Cas9 system is an efficient tool to study the role of genes in the context of glioma initiation and glioma formation.

Different molecular alterations that occur in GBM have been identified and included in the latest glioma classification (Louis et al., 2016). This fact has highlighted the need to generate precise preclinical models for this type of tumors. Such models will be useful to study the biology of gliomas and to test novel, specific and more effective therapeutic alternatives. Few elements should be taken into consideration to properly mimic the natural history of a tumor: (a) introduction of the same mutations found in human tumors, ideally in their endogenous loci; (b) the genetic alterations should be silent during embryonic and early postnatal development (except models of familiar or pediatric tumors);

(c) the mutant genes should be expressed in particular target tissues or in specific cell types and (e) the mutations should be present in a limited number of cells (Schuhmacher & Squatrito, 2017).

Classically, to study the role of a gene of interest in cancer, a whole-body knock-out mouse is developed for *in vivo* experiments. Although this system is very well established, there are some limitations such as embryonic lethality or the modification of animal physiology which leads to adaptation and compensation mechanisms that can result in biased results (Skarnes et al., 2011). These limitations can be bypassed by applying tissue-specificity. As well as in other cancer types, for the study of gliomas, the ideal mouse glioma model has to recapitulate the human glioma features (Lenting et al., 2017) allowing for an accurate prediction of the clinical outcome of novel therapeutic strategies. The RCAS/Tva system is a well-known model used in many glioma studies that closely resembles human disease (Holland & Varmus, 1998). This system allows the incorporation of different genetic tools such as shRNA in order to study loss-of-function genes. Nowadays, the genome editing capacity by CRISPR/Cas9 system has been shown to be the best genetic tool capable of producing specific alterations (Knock-out, Knock-in and genetic rearrangements).

The last goal of this PhD project was to combine the versatile RCAS/Tva model with the CRISPR/Cas9 technology (Oldrini et al., 2018). Taking advantage of the possibilities of the genome editing and the precise murine model, the idea was to generate an accurate new model to re-create a variety of molecular alterations. For this purpose, we first generated specific mouse strains with a conditional Cas9 expression under the control of a tissue-specific promoter Nestin or GFAP (Figure 20). In addition, we adapted the RCAS vector to generate a set of plasmids for the different applications of genome editing (Figure 21).

As a proof of concept, we wanted to check the possibility of producing gliomas which lacked expression of TSGs *in vivo*. To test this, we used sgRNAs targeting specific TSGs known to cooperate with PDGFB overexpression to induce high-grade gliomas: TP53, PTEN and CDKN2A (Hambardzumyan et al., 2009; Squatrito et al., 2010). Indeed, co-injections of sgRNAs targeting those TSGs led to the formation of GBMs with high frequency in short period of time (Figure 26).

These data suggest that combining the expression of specific oncogene drivers, such as PDGFB, with sgRNAs for any gene of interest would quickly provide information on its contribution to the tumorigenesis process. Moreover, by using the hUBC-CreERT2 or other Cre-inducible strains it would be possible to exploit the RCAS-Tva/CRISPR-Cas9 system not only to study tumor initiation, but also tumor progression and maintenance.

Due to the quite recent advancement in the CRISPR-Cas9 technology, very few mouse models have been previously developed to study brain tumorigenesis (Zuckerman et al., 2015; Chen et al., 2015; Cook et al.,2017). Plasmids encoding Cas9 in combination with sgRNAs targeting Nf1, Trp53 and Pten, were able to induce highly aggressive tumors that had histopathological features of human GBMs. More recently, injections of adenoviral (Ad) vectors expressing Cas9 and the sgRNAs were used to generate the specific Bcan-Ntrk1 rearrangement in the brain of adult mice. The drawbacks of these techniques for glioma modeling would be: timing of the sgRNA delivery and lack of specificity of the targeted cells. Electroporation is normally performed at E14.5 or E15.5 and genetic alterations at this gestational stage might not be necessarily reflecting the biology of gliomas in the adult. Additionally, the expression of the Cas9 enzyme constitutively, allows the genome editing in all cell types and it could affect the resemblance of human features. This latter point is particularly relevant for proper cancer modeling, since it has been shown that the same driver mutations can lead to phenotypically and molecularly diverse glioma subtypes from different pools of adult CNS progenitor cells (Ghazi et al., 2012; Alcantara-Laguno et al., 2015). We have developed an extremely powerful and versatile mouse model that combines the somatic genome transfer ability of the RCAS-TVA system with the CRISPR-Cas9 genome editing technology. Here I only presented the characterization of the model and its use to generate KO tumors. However, the RCAS-Tva/CRISPR-Cas9 system also gives the possibility to generate specific point mutations and genomic rearrangements (Oldrini et al., 2018). Thus, this model allows mimicking these characteristics in one single model. We believe that such a flexible model will greatly expedite the generation of precise cancer models, therefore accelerating the pre-clinical testing of novel targeted therapies.

Finally, another aspect of using this novel approach is the possibility to modelling other cancer types. Seidler and colleagues have developed an LSL-TVAiLacZ knock-in mouse line that expresses TVA in a Cre recombinase-dependent manner under control of Rosa26 locus (Seidler et al., 2008; von Werder et al., 2012). By crossing with a tissue-specific Cre, we can generate specific strains that express the TVA receptor specifically in our tissue/organ. The authors then generated a specific mouse strain combining the Rosa26-LSLTVA line with the Cre-dependent pancreas specific transcription factor (Ptf1a-Cre) line. In this manner, they activated TVA expression only in pancreas (Seidler et al., 2008). Finally, they combined their Rosa26-LSLTVA; Ptf1a-Cre mouse strain with an LSL-KRAS$^{G12D/+}$ for the induction of mouse pancreatic intraepithelial neoplasia. Using this new Rosa26-LSLTVA strain, we could generate organ-specific TVA-expressing mice and by using the RCAS-sgRNA plasmids we can have used them for cancer modeling.

Conclusions

1. PiggyBac-transposon library in human haploid cells leads to the identification of 43 different genes that can modulate TMZ response. We were able to validate some candidate genes by genome editing CRISPR/Cas9 system in haploid cells

2. MSH6 gene was the unique hit validated in different GBM cells that generated resistance to TMZ

3. A pilot study based on 120 antitumor compounds did not display a better sensitivity in MSH6-deficient GBM cells

4. Val-083, currently in early clinical trials, exhibits better efficacy in different GBM cells as compared to TMZ, independently of MGMT expression and/or MMR activity

5. Val-083 shows a synergistic effect with TMZ both *in vitro* and *ex vivo*

6. We have established a novel powerful tool for precision glioma modelling by combining the versatility of the CRISPR/Cas9 methodology with the specificity of somatic gene transfer mediated by the RCAS/Tva system

7. The RCAS/Tva-CRISPR/Cas9 technology allows the generation of specific complex genetic alterations that mimics the natural history of gliomas in one single model

Conclusiones

1. La biblioteca de transposones basado en el sistema PiggyBac en células haploides humanas permitió la identificación de 43 genes diferentes que pudieran estar modulando la respuesta a TMZ. Validamos algunos de estos genes mediante el sistema de edición génica CRISPR/Cas9 en células haploides

2. El gen MSH6 fue el único gen candidato validado en diferentes líneas celulares de glioblastoma que generaba resistencia a TMZ

3. Un primer estudio utilizando 120 compuestos antitumorales no mostró una mayor sensibilidad en las líneas de glioblastoma deficientes para el gen MSH6

4. Val-083, actualmente en ensayos clínicos, presenta una major eficacia en diferentes líneas celulares de GBM en comparación con la TMZ, independientemente de la expresión de MGMT y/o la actividad de la ruta MMR

5. El Val-083 muestra un efecto sinérgico con TMZ *in vitro* y *ex vivo*

6. Hemos generado una potente herramienta para el modelaje preciso de gliomas combinando el sistema CRISPR/Cas9 con la especifificidad del sistema de tranferencia génica RCAS/Tva

7. La tecnología del RCAS/Tva-CRISPR/Cas9 permite la generación de mutaciones genéticas complejas que recapitulan la historia natural de los gliomas en un único modelo

References

ABDOLLAHI, M. & SOODABEH, S. 2012. Who plays dual role in cancerous and normal cells? natural antioxidants or free radicals or the cell environment. International Journal of Pharmacology 8, 711-712.

AGNIHOTRI, S., BURRELL, K. E., WOLF, A., JALALI, S., HAWKINS, C., RUTKA, J. T. & ZADEH, G. 2013. Glioblastoma, a brief review of history, molecular genetics, animal models and novel therapeutic strategies. Archivum Immunologiae et Therapiae Experimentalis 61, 25-41.

AHRONIAN, L. G. & LEWIS, B. C. 2014. Using the RCAS-TVA system to model human cancer in mice. Cold Spring Harbor Protocols.

ALCANTARA LLAGUNO, S. R., WANG, Z., SUN, D., CHEN, J., XU, J., KIM, E., HATANPAA, K. J., RAISANEN, J. M., BURNS, D. K., JOHNSON, J. E. & PARADA, L. F. 2015. Adult Lineage-Restricted CNS Progenitors Specify Distinct Glioblastoma Subtypes. Cancer Cell 28, 429–440.

ALIFIERIS, C. & TRAFALIS, D. T. 2015. Glioblastoma multiforme: Pathogenesis and treatment. Pharmacology and Therapeutics. 152, 63–82.

AMARAVADI, R. K., SCHUCHTER, L. M., MCDERMOTT, D. F., KRAMER, A., GILES, L., GRAMLICH, K., CARBERRY, M., TROXEL, A. B., LETRERO, R., NATHANSON, K. L., ATKINS, M. B., O'DWYER, P. J. & FLAHERTY, K. T. 2009. Phase II trial of temozolomide and sorafenib in advanced melanoma patients with or without brain metastases. Clinical Cancer Research 15, 7711–7718.

AMERICAN CANCER, S. 2017. Cancer Facts and Figures 2017. Genes and Development 21, 2525–2538.

BABASHAH, S. & SOLEIMANI, M. 2011. The oncogenic and tumour suppressive roles of microRNAs in cancer and apoptosis. European Journal of Cancer 47, 1127–1137.

BACHA, J., SCHWARTZ, R., STEINO, A., LANGLANDS, J., KANEKAL, S., LOPEZ, L. & BROWN, D. 2016. ACTR-42. CLINICAL TRIALS OF VAL-083 IN PATIENTS WITH CHEMORESISTANT GLIOBLASTOMA. Neuro-Oncology vi11.

BANSAL, M., YANG, J., KARAN, C., MENDEN, M. P., COSTELLO, J. C., TANG, H., XIAO, G., LI, Y., ALLEN, J., ZHONG, R., CHEN, B., KIM, M., WANG, T., HEISER, L. M., REALUBIT, R., MATTIOLI, M., ALVAREZ, M. J., SHEN, Y., GALLAHAN, D., SINGER, D., SAEZ-RODRIGUEZ, J., XIE, Y., STOLOVITZKY, G., CALIFANO, A., ABBUEHL, J. P., ALTMAN, R. B., BALCOME, S., BELL, A., BENDER, A., BERGER, B., BERNARD, J., BIEBERICH, A. A., BORBOUDAKIS, G., CHAN, C., CHEN, T. H., CHOI, J., COELHO, L. P., CREIGHTON, C. J., DAMPIER, W., DAVISSON, V. J., DESHPANDE, R., DIAO, L., DI CAMILLO, B., DUNDAR, M., ERTEL, A., GOSWAMI, C. P., GOTTLIEB, A., GOULD, M. N., GOYA, J., GRAU, M., GRAY, J. W., HEJASE, H. A., HOFFMANN, M. F., HOMICSKO, K., HOMILIUS, M., HWANG, W., IJZERMAN, A. P., KALLIONIEMI, O., KARACALI, B., KASKI, S., KIM, J., KRISHNAN, A., LEE, J., LEE, Y. S., LENSELINK, E. B., LENZ, P., LI, L., LI, J., LIANG, H., MPINDI, J. P., MYERS, C.

L., NEWTON, M. A., OVERINGTON, J. P., PARKKINEN, J., PRILL, R. J., PENG, J., PESTELL, R., QIU, P., RAJWA, B., SADANANDAM, A., SAMBO, F., SRIDHAR, A., SUN, W., TOFFOLO, G. M., TOZEREN, A., TROYANSKAYA, O. G., TSAMARDINOS, I., VAN VLIJMEN, H. W. T., WANG, W., WEGNER, J. K., WENNERBERG, K., VAN WESTEN, G. J. P., XIA, T., YANG, Y., YAO, V., YUAN, Y., ZENG, H., ZHANG, S., ZHAO, J. & ZHOU, J. 2014. A community computational challenge to predict the activity of pairs of compounds. Nature Biotechnology 32, 1213-1224.

BIAN, Y., KITAGAWA, R., BANSAL, P. K., FUJII, Y., STEPANOV, A. & KITAGAWA, K. 2014. Synthetic genetic array screen identifies PP2A as a therapeutic target in Mad2-overexpressing tumors. Proceedings of the National Academy of Sciences 111, 1628-1633.

BLEAU, A. M., HAMBARDZUMYAN, D., OZAWA, T., FOMCHENKO, E. I., HUSE, J. T., BRENNAN, C. W. & HOLLAND, E. C. 2009. PTEN/PI3K/Akt Pathway Regulates the Side Population Phenotype and ABCG2 Activity in Glioma Tumor Stem-like Cells. Cell Stem Cell 4, 226–235.

BORSOOK, D. 2012. Neurological diseases and pain. Brain 135; 320–344.

BRÄGELMANN, J., DAMMERT, M. A., DIETLEIN, F., HEUCKMANN, J. M., CHOIDAS, A., BÖHM, S., RICHTERS, A., BASU, D., TISCHLER, V., LORENZ, C., HABENBERGER, P., FANG, Z., ORTIZ-CUARAN, S., LEENDERS, F., EICKHOFF, J., KOCH, U., GETLIK, M., TERMATHE, M., SALLOUH, M., GREFF, Z., VARGA, Z., BALKE-WANT, H., FRENCH, C. A., PEIFER, M., REINHARDT, H. C., ÖRFI, L., KÉRI, G., ANSÉN, S., HEUKAMP, L. C., BÜTTNER, R., RAUH, D., KLEBL, B. M., THOMAS, R. K. & SOS, M. L. 2017. Systematic Kinase Inhibitor Profiling Identifies CDK9 as a Synthetic Lethal Target in NUT Midline Carcinoma. Cell Reports 20, 2833–2845.

BRENNAN, C. W., VERHAAK, R. G. W., MCKENNA, A., CAMPOS, B., NOUSHMEHR, H., SALAMA, S. R., ZHENG, S., CHAKRAVARTY, D., SANBORN, J. Z., BERMAN, S. H., BEROUKHIM, R., BERNARD, B., WU, C. J., GENOVESE, G., SHMULEVICH, I., BARNHOLTZ-SLOAN, J., ZOU, L., VEGESNA, R., SHUKLA, S. A., CIRIELLO, G., YUNG, W. K., ZHANG, W., SOUGNEZ, C., MIKKELSEN, T., ALDAPE, K., BIGNER, D. D., VAN MEIR, E. G., PRADOS, M., SLOAN, A., BLACK, K. L., ESCHBACHER, J., FINOCCHIARO, G., FRIEDMAN, W., ANDREWS, D. W., GUHA, A., IACOCCA, M., O'NEILL, B. P., FOLTZ, G., MYERS, J., WEISENBERGER, D. J., PENNY, R., KUCHERLAPATI, R., PEROU, C. M., HAYES, D. N., GIBBS, R., MARRA, M., MILLS, G. B., LANDER, E. S., SPELLMAN, P., WILSON, R., SANDER, C., WEINSTEIN, J., MEYERSON, M., GABRIEL, S., LAIRD, P. W., HAUSSLER, D., GETZ, G., CHIN, L., BENZ, C., BARRETT, W., OSTROM, Q., WOLINSKY, Y., BOSE, B., BOULOS, P. T., BOULOS, M., BROWN, J., CZERINSKI, C., EPPLEY, M., KEMPISTA, T., KITKO, T., KOYFMAN, Y., RABENO, B., RASTOGI, P., SUGARMAN, M., SWANSON, P., YALAMANCHII, K., OTEY, I. P., LIU, Y. S., XIAO, Y., AUMAN, J. T., CHEN, P. C., HADJIPANAYIS, A., LEE, E., LEE, S., PARK, P. J., SEIDMAN, J., YANG, L., KALKANIS, S., POISSON, L. M., RAGHUNATHAN, A., SCARPACE, L., BRESSLER, R., EAKIN, A., IYPE, L.,

KREISBERG, R. B., LEINONEN, K., REYNOLDS, S., ROVIRA, H., THORSSON, V., ANNALA, M. J., et al. 2013. The somatic genomic landscape of glioblastoma. Cell 155, 462–47.

BREM, H., PIANTADOSI, S., BURGER, P. C., WALKER, M., SELKER, R., VICK, N. A., BLACK, K., SISTI, M., BREM, S. & MOHR, G. 1995. Placebo-controlled trial of safety and efficacy of intraoperative controlled delivery by biodegradable polymers of chemotherapy for recurrent gliomas. The Polymer-brain Tumor Treatment Group. Lancet 345, 1008-1012.

BROCK, C. S., NEWLANDS, E. S., WEDGE, S. R., BOWER, M., EVANS, H., COLQUHOUN, I., RODDIE, M., GLASER, M., BRAMPTON, M. H. & RUSTIN, G. J. S. 1998. Phase I trial of temozolomide using an extended continuous oral schedule. Cancer Research 58, 4363-4367.

BROMBERG-WHITE, J. L., WEBB, C. P., PATACSIL, V. S., MIRANTI, C. K., WILLIAMS, B. O. & HOLMEN, S. L. 2004. Delivery of Short Hairpin RNA Sequences by Using a Replication-Competent Avian Retroviral Vector Delivery of Short Hairpin RNA Sequences by Using a Replication-Competent Avian Retroviral Vector. Journal of virology 78, 4914-4916.

BRYANT, H. E., SCHULTZ, N., THOMAS, H. D., PARKER, K. M., FLOWER, D., LOPEZ, E., KYLE, S., MEUTH, M., CURTIN, N. J. & HELLEDAY, T. 2005. Specific killing of BRCA2-deficient tumours with inhibitors of poly(ADP-ribose) polymerase. Nature 434, 913-917.

BUNTING, S. F., CALLÉN, E., WONG, N., CHEN, H. T., POLATO, F., GUNN, A., BOTHMER, A., FELDHAHN, N., FERNANDEZ-CAPETILLO, O., CAO, L., XU, X., DENG, C. X., FINKEL, T., NUSSENZWEIG, M., STARK, J. M. & NUSSENZWEIG, A. 2010. 53BP1 inhibits homologous recombination in brca1-deficient cells by blocking resection of DNA breaks. Cell 141, 243–254.

BURNET, N. G., JEFFERIES, S. J., BENSON, R. J., HUNT, D. P. & TREASURE, F. P. 2005. Years of life lost (YLL) from cancer is an important measure of population burden - And should be considered when allocating research funds. British Journal of Cancer 92, 241 – 245.

CAHILL, D. P., LEVINE, K. K., BETENSKY, R. A., CODD, P. J., ROMANY, C. A., REAVIE, L. B., BATCHELOR, T. T., FUTREAL, P. A., STRATTON, M. R., CURRY, W. T., LAFRATE, A. J. & LOUIS, D. N. 2007. Loss of the mismatch repair protein MSH6 in human glioblastomas is associated with tumor progression during temozolomide treatment. Clinical Cancer Research 13, 2038-2045.

CANCER GENOME ATLAS RESEARCH. 2015. Comprehensive, Integrative Genomic Analysis of Diffuse Lower-Grade Gliomas. N Engl J Med 372, 2481-98.

CATTANEO, R., MIEST, T., SHASHKOVA, E. V. & BARRY, M. A. 2008. Reprogrammed viruses as cancer therapeutics: targeted, armed and shielded. Nat Rev Microbiol 6, 529-40.

CARETTE, J. E., GUIMARAES, C. P., VARADARAJAN, M., PARK, A. S., WUETHRICH, I., GODAROVA, A., KOTECKI, M., COCHRAN, B. H., SPOONER, E., PLOEGH, H. L. & BRUMMELKAMP, T. R. 2009. Haploid genetic screens in human cells identify host factors used by pathogens. Science 326, 1231-1235.

CARETTE, J. E., GUIMARAES, C. P., WUETHRICH, I., BLOMEN, V. A., VARADARAJAN, M., SUN, C., BELL, G., YUAN, B., MUELLNER, M. K., NIJMAN, S. M., PLOEGH, H. L. & BRUMMELKAMP, T. R. 2011. Global gene disruption in human cells to assign genes to phenotypes by deep sequencing. Nature Biotechnology 29, 542-548.

CARSON, K. A., GROSSMAN, S. A., FISHER, J. D. & SHAW, E. G. 2007. Prognostic factors for survival in adult patients with recurrent glioma enrolled onto the new approaches to brain tumor therapy CNS consortium phase I and II clinical trials. Journal of clinical oncology: official journal of the American Society of Clinical Oncology 5, 2601-2616.

CHEN, L., KASAI, T., LI, Y., SUGII, Y., JIN, G., OKADA, M., VAIDYANATH, A., MIZUTANI, A., SATOH, A., KUDOH, T., HENDRIX, M. J. C., SALOMON, D. S., FU, L. & SENO, M. 2012. A model of cancer stem cells derived from mouse induced pluripotent stem cells. PLoS ONE 7, e33544.

CHEW, S. K., RAD, R., FUTREAL, P. A., BRADLEY, A. & LIU, P. 2011. Genetic screens using the piggyBac transposon. Methods.53, 366-371.

CHEN, Z., HAN, L., XU, M., XU, Y. & QIAN, X. 2013. Rationally Designed Multitarget Anticancer Agents. Current Medicinal Chemistry 20, 1694-1714.

CHO, S., WOOD, A. & BOWLBY, M. 2007. Brain Slices as Models for Neurodegenerative Disease and Screening Platforms to Identify Novel Therapeutics. Current Neuropharmacology 5, 19-33.

DEL VECCHIO, C. A., LI, G. & WONG, A. J. 2012. Targeting EGF receptor variant III: Tumor-specific peptide vaccination for malignant gliomas. Expert Review of Vaccines 11, 133-144.

COMBS, S. E., EDLER, L., RAUSCH, R., WELZEL, T., WICK, W. & DEBUS, J. 2013. Generation and validation of a prognostic score to predict outcome after re-irradiation of recurrent glioma. Acta Oncologica 52, 147-152.

COMBS, S. E., HEEGER, S., HASELMANN, R., EDLER, L., DEBUS, J. & SCHULZ-ERTNER, D. 2006. Treatment of primary glioblastoma multiforme with cetuximab, radiotherapy and temozolomide (GERT)--phase I/II trial: study protocol. BMC cancer 6, 133.

COOK, P. J., THOMAS, R., KANNAN, R., DE LEON, E. S., DRILON, A., ROSENBLUM, M. K., SCALTRITI, M., BENEZRA, R. & VENTURA, A. 2017. Somatic chromosomal engineering identifies BCAN-NTRK1 as a potent glioma driver and therapeutic target. Nature Communications 8, 15987.

DENNY, B. J., WHEELHOUSE, R. T., STEVENS, M. F. G., TSANG, L. L. H. & SLACK, J. A. 1994. NMR and molecular modeling investigation of the mechanism

of activation of the antitumor drug temozolomide and its interaction with DNA. Biochemistry 34, 9045–9051.

DU, Z. & LI, Y. 2007. RCAS-TVA in the mammary gland: An in vivo oncogene screen and a high fidelity model for breast transformation? Cell Cycle 67, 823-826.

DU, Z., PODSYPANINA, K., HUANG, S., MCGRATH, A., TONEFF, M. J., BOGOSLOVSKAIA, E., ZHANG, X., MORAES, R. C., FLUCK, M., ALLRED, D. C., LEWIS, M. T., VARMUS, H. E. & LI, Y. 2006. Introduction of oncogenes into mammary glands in vivo with an avian retroviral vector initiates and promotes carcinogenesis in mouse models. Proceedings of the National Academy of Sciences of the United States of America 103, 17396–17401.

EAGAN, R. T., BISEL, H. F., CHILDS, D. S., HOLBROOK, M. A., LAYTON, D. D., LAWS, E. R. & FLEMING, T. R. 1979. Dianhydrogalactitol and Radiation Therapy: Treatment of Supratentorial Glioma. JAMA: The Journal of the American Medical Association 241, 2046-2050.

EAR, P. H., BOOTH, M. J., ABD-RABBO, D., KOWARZYK MORENO, J., HALL, C., CHEN, D., VOGEL, J. & MICHNICK, S. W. 2013. Dissection of Cdk1-cyclin complexes in vivo. Proceedings of the National Academy of Sciences 100, 15716–15721.

ELICK, T. A. 1996. Excision of the piggy Bac transposable element in vitro is a precise event that is enhanced by the expression of its encoded transposase. Genetica 98, 33-41.

ELLING, U. & PENNINGER, J. M. 2014. Genome wide functional genetics in haploid cells. FEBS Letters 588, 2415–2421.

ELLING, U., TAUBENSCHMID, J., WIRNSBERGER, G., O'MALLEY, R., DEMERS, S. P., VANHAELEN, Q., SHUKALYUK, A. I., SCHMAUSS, G., SCHRAMEK, D., SCHNUETGEN, F., VON MELCHNER, H., ECKER, J. R., STANFORD, W. L., ZUBER, J., STARK, A. & PENNINGER, J. M. 2011. Forward and reverse genetics through derivation of haploid mouse embryonic stem cells. Cell Stem Cell 9, 563–574.

ESTELLER, M., GARCIA-FONCILLAS, J., ANDION, E., GOODMAN, S. N., HIDALGO, O. F., VANACLOCHA, V., BAYLIN, S. B. & HERMAN, J. G. 2000. Inactivation of the DNA-Repair Gene MGMT and the Clinical Response of Gliomas to Alkylating Agents. New England Journal of Medicine 19, 1350-1354.
EVANS, E. & ALANI, E. 2000. Roles for mismatch repair factors in regulating genetic recombination. Molecular and cellular biology 20, 7839–7844.

FISHER, G. H., ORSULIC, S., HOLLAND, E., HIVELY, W. P., LI, Y., LEWIS, B. C., WILLIAMS, B. O. & VARMUS, H. E. 1999. Development of a flexible and specific gene delivery system for production of murine tumor models. Oncogene 18, 5253-5260.

FOUCQUIER, J. & GUEDJ, M. 2015. Analysis of drug combinations: current methodological landscape Pharma Res Per 3, e00149.

FOUSE, S., STEINO, A., BUTOWSKI, N., BACHA, J., BROWN, D. & COSTELLO, J. 2014. ET-18 * VAL-083 IS A NOVEL N7 ALKYLATING AGENT THAT INHIBITS THE GROWTH OF GLIOMA STEM AND NON-STEM CULTURES, INCLUDING TEMOZOLOMIDE-RESISTANT LINES. Neuro-Oncology 16, v79–v95.

FRASER, M. J., CISZCZON, T., ELICK, T. & BAUSER, C. 1996. Precise excision of TTAA-specific lepidopteran transposons piggyBac (IFP2) and tagalong (TFP3) from the baculovirus genome in cell lines from two species of Lepidoptera. Insect Molecular Biology 5, 141-151.

FRIDÉN, M., DUCROZET, F., MIDDLETON, B., ANTONSSON, M., BREDBERG, U. & HAMMARLUND-UDENAES, M. 2009. Development of a high-throughput brain slice method for studying drug distribution in the central nervous system. Drug Metabolism and Disposition 37, 1226-1233.

FURUTA, M., WEIL, R. J., VORTMEYER, A. O., HUANG, S., LEI, J., HUANG, T. N., LEE, Y. S., BHOWMICK, D. A., LUBENSKY, I. A., OLDFIELD, E. H. & ZHUANG, Z. 2004. Protein patterns and proteins that identify subtypes of glioblastoma multiforme. Oncogene 23, 6806–6814.

GALLI, R., BINDA, E., ORFANELLI, U., CIPELLETTI, B., GRITTI, A., DE VITIS, S., FIOCCO, R., FORONI, C., DIMECO, F. & VESCOVI, A. 2004. Isolation and characterization of tumorigenic, stem-like neural precursors from human glioblastoma. Cancer Research 64, 7011–7021.

GASPAR, L. E., FISHER, B. J., MACDONALD, D. R., LEBER, D. V., HALPERIN, E. C., SCHOLD, S. C. & CAIRNCROSS, J. G. 1992. Supratentorial malignant glioma: Patterns of recurrence and implications for external beam local treatment. International Journal of Radiation Oncology, Biology, Physics 24, 55-57.

GAYVERT, K. M., ALY, O., PLATT, J., BOSENBERG, M. W., STERN, D. F. & ELEMENTO, O. 2017. A Computational Approach for Identifying Synergistic Drug Combinations. PLoS Computational Biology 13, e1005308.

GHAZI, A., ASHOORI, A., HANLEY, P. J., BRAWLEY, V. S., SHAFFER, D. R., KEW, Y., POWELL, S. Z., GROSSMAN, R., GRADA, Z., SCHEURER, M. E., HEGDE, M., LEEN, A. M., BOLLARD, C. M., ROONEY, C. M., HESLOP, H. E., GOTTSCHALK, S. & AHMED, N. 2012. Generation of polyclonal CMV-specific T cells for the adoptive immunotherapy of glioblastoma. Journal of Immunotherapy 35, 159-168.

GHOSAL, G. & CHEN, J. 2013. DNA damage tolerance: a double-edged sword guarding the genome. Translational cancer research 2, 107-129.

GONG, C., BONGIORNO, P., MARTINS, A., STEPHANOU, N. C., ZHU, H., SHUMAN, S. & GLICKMAN, M. S. 2005. Mechanism of nonhomologous end-

joining in mycobacteria: A low-fidelity repair system driven by Ku, ligase D and ligase C. Nature Structural and Molecular Biology 12, 304-312.

GROTZER, M. A., NEVE, A. & BAUMGARTNER, M. 2016. Dissecting brain tumor growth and metastasis in vitro and ex vivo. Journal of Cancer Metastasis and Treatment 2, 149-162.

GUHA, A., FELDKAMP, M. M., LAU, N., BOSS, G. & PAWSON, A. 1997. Proliferation of human malignant astrocytomas is dependent on Ras activation. Oncogene 15, 2755-2765.

GUILLOTIN, D. & MARTIN, S. A. 2014. Exploiting DNA mismatch repair deficiency as a therapeutic strategy 329, 110–115.

HAMBARDZUMYAN, D., PARADA, L. F., HOLLAND, E. C. & CHAREST, A. 2011. Genetic modeling of gliomas in mice: New tools to tackle old problems. GLIA 59, 1155–1168.

HAMID, O., ROBERT, C., DAUD, A., HODI, F. S., HWU, W.-J., KEFFORD, R., WOLCHOK, J. D., HERSEY, P., JOSEPH, R. W., WEBER, J. S., DRONCA, R., GANGADHAR, T. C., PATNAIK, A., ZAROUR, H., JOSHUA, A. M., GERGICH, K., ELASSAISS-SCHAAP, J., ALGAZI, A., MATEUS, C., BOASBERG, P., TUMEH, P. C., CHMIELOWSKI, B., EBBINGHAUS, S. W., LI, X. N., KANG, S. P. & RIBAS, A. 2013. Safety and Tumor Responses with Lambrolizumab (Anti–PD-1) in Melanoma. New England Journal of Medicine 369, 134-144.

HANLEY, M. L., ELION, G. B., COLVIN, O. M., MODRICH, P. L., KEIR, S., ADAMS, D. J., BIGNER, D. D. & FRIEDMAN, H. S. 1998. Therapeutic efficacy of vinorelbine against pediatric and adult central nervous system tumors. Cancer Chemotherapy and Pharmacology 42, 479-482.

HANSEN, R. J., NAGASUBRAMANIAN, R., DELANEY, S. M., SAMSON, L. D. & DOLAN, M. E. 2007. Role fo O6-methylguanine-DNA methyltransferase in protecting from alkylating agent-induced toxicity and mutations in mice. Carcinogenesis 28, 1111–1116.

HART, M. G., GARSIDE, R., ROGERS, G., STEIN, K. & GRANT, R. 2013. Temozolomide for high grade glioma. Cochrane Database of Systematic Reviews 30, CD007415.

HEGI, M. E., DISERENS, A.-C., GORLIA, T., HAMOU, M.-F., DE TRIBOLET, N., WELLER, M., KROS, J. M., HAINFELLNER, J. A., MASON, W., MARIANI, L., BROMBERG, J. E. C., HAU, P., MIRIMANOFF, R. O., CAIRNCROSS, J. G., JANZER, R. C. & STUPP, R. 2005. MGMT Gene Silencing and Benefit from Temozolomide in Glioblastoma. New England Journal of Medicine 352, 997-1003.

HILLENMEYER, M. E., ERICSON, E., DAVIS, R. W., NISLOW, C., KOLLER, D. & GIAEVER, G. 2010. Systematic analysis of genome-wide fitness data in yeast reveals novel gene function and drug action. Genome Biology 11:R30.

HIMLY, M., FOSTER, D. N., BOTTOLI, I., IACOVONI, J. S. & VOGT, P. K. 1998. The DF-1 chicken fibroblast cell line: Transformation induced by diverse oncogenes and cell death resulting from infection by avian leukosis viruses. Virology 248, 295–30.

HIROSE, Y., BERGER, M. S. & PIEPER, R. O. 2001. Abrogation of the Chk1-mediated G(2) checkpoint pathway potentiates temozolomide-induced toxicity in a p53-independent manner in human glioblastoma cells. Cancer Res 61, 5843-9.

HOLLAND, E. C. & VARMUS, H. E. 1998. Basic fibroblast growth factor induces cell migration and proliferation after glia-specific gene transfer in mice. Proceedings of the National Academy of Sciences of the United States of America 95, 1218–1223.

HOLOHAN, C., VAN SCHAEYBROECK, S., LONGLEY, D. B. & JOHNSTON, P. G. 2013. Cancer drug resistance: An evolving paradigm 13, 714-726.

HORTON, J. K. & WILSON, S. H. 2007. Hypersensitivity phenotypes associated with genetic and synthetic inhibitor-induced base excision repair deficiency. DNA Repair 6, 530–543.

HOU, L. C., VEERAVAGU, A., HSU, A. R. & TSE, V. C. 2006. Recurrent glioblastoma multiforme: a review of natural history and management options. Neurosurg Focus 15, 20-E5.

HUNTER, C., SMITH, R., CAHILL, D. P., STEPHENS, P., STEVENS, C., TEAGUE, J., GREENMAN, C., EDKINS, S., BIGNELL, G., DAVIES, H., O'MEARA, S., PARKER, A., AVIS, T., BARTHORPE, S., BRACKENBURY, L., BUCK, G., BUTLER, A., CLEMENTS, J., COLE, J., DICKS, E., FORBES, S., GORTON, M., GRAY, K., HALLIDAY, K., HARRISON, R., HILLS, K., HINTON, J., JENKINSON, A., JONES, D., KOSMIDOU, V., LAMAN, R., LUGG, R., MENZIES, A., PERRY, J., PETTY, R., RAINE, K., RICHARDSON, D., SHEPHERD, R., SMALL, A., SOLOMON, H., TOFTS, C., VARIAN, J., WEST, S., WIDAA, S., YATES, A., EASTON, D. F., RIGGINS, G., ROY, J. E., LEVINE, K. K., MUELLER, W., BATCHELOR, T. T., LOUIS, D. N., STRATTON, M. R., FUTREAL, P. A. & WOOSTER, R. 2006. A hypermutation phenotype and somatic MSH6 mutations in recurrent human malignant gliomas after alkylator chemotherapy. Cancer Research 66, 3987-3991.

HU, X. & ZHANG, Z. 2016. Understanding the Genetic Mechanisms of Cancer Drug Resistance Using Genomic Approaches. Trends Genet, 32, 127-137.

JEON, M., KIM, S., PARK, S., LEE, H. & KANG, J. 2018. In silico drug combination discovery for personalized cancer therapy. BMC Systems Biology 12, 59-67.

JINEK, M., CHYLINSKI, K., FONFARA, I., HAUER, M., DOUDNA, J. A. & CHARPENTIER, E. 2012. A Programmable Dual-RNA – Guided. Science 317, 816-821.

JINEK, M., JIANG, F., TAYLOR, D. W., STERNBERG, S. H., KAYA, E., MA, E., ANDERS, C., HAUER, M., ZHOU, K., LIN, S., KAPLAN, M., IAVARONE, A. T., CHARPENTIER, E., NOGALES, E. & DOUDNA, J. A. 2014. Structures of Cas9 endonucleases reveal RNA-mediated conformational activation. Science 343, 1215-1228.

JORDAN, M. A. & WILSON, L. 2004. Microtubules as a target for anticancer drugs.Nature Reviews Cancer 4, 253-265.

JUNG, S., KIM, H. W., LEE, J. H., KANG, S. S., RHU, H. H., JEONG, Y. I., YANG, S. Y., CHUNG, H. Y., BAE, C. S., CHOI, C., SHIN, B. A., KIM, K. K. & AHN, K. Y. 2002. Brain tumor invasion model system using organotypic brain-slice culture as an alternative to in vivo model. Journal of Cancer Research and Clinical Oncology 128, 469-476.

KAELIN, W. G. 2009. Synthetic lethality: A framework for the development of wiser cancer therapeutics. Genome Medicine 1, 99

KAINA, B., CHRISTMANN, M., NAUMANN, S. & ROOS, W. P. 2007. MGMT: Key node in the battle against genotoxicity, carcinogenicity and apoptosis induced by alkylating agents. DNA Repair 6, 1079–1099.

KALOSHI, G., BENOUAICH-AMIEL, A., DIAKITE, F., TAILLIBERT, S., LEJEUNE, J., LAIGLE-DONADEY, F., RENARD, M. A., IRAQI, W., IDBAIH, A., PARIS, S., CAPELLE, L., DUFFAU, H., CORNU, P., SIMON, J. M., MOKHTARI, K., POLIVKA, M., OMURO, A., CARPENTIER, A., SANSON, M., DELATTRE, J. Y. & HOANG-XUAN, K. 2007. Temozolomide for low-grade gliomas: Predictive impact of 1p/19q loss on response and outcome. Neurology 68, 1831-1836.

KAUFMANN, J. K. & CHIOCCA, E. A. 2014. Glioma virus therapies between bench and bedside. Neuro-Oncology 16, 334–351.

KERSTEN, K., DE VISSER, K. E., VAN MILTENBURG, M. H. & JONKERS, J. 2017. Genetically engineered mouse models in oncology research and cancer medicine. EMBO Molecular Medicine 9, 137-153.

KOTECKI, M., REDDY, P. S. & COCHRAN, B. H. 1999. Isolation and characterization of a near-haploid human cell line. Experimental Cell Research 252, 273–280.

KUNKEL, T. A. & ERIE, D. A. 2015. Eukaryotic Mismatch Repair in Relation to DNA Replication. Annual Review of Genetics 49, 291–313.

LAWSON, N. D. & WOLFE, S. A. 2011. Forward and Reverse Genetic Approaches for the Analysis of Vertebrate Development in the Zebrafish. Developmental Cell 21, 48-64.

LEE, S. Y. 2016. Temozolomide resistance in glioblastoma multiforme. Genes & Disease 3, 198-210.

LENTING, K., VERHAAK, R., TER LAAN, M., WESSELING, P. & LEENDERS, W. 2017. Glioma: experimental models and reality. Acta Neuropathol 133, 263–282.

LI, G.-M. 2008. Mechanisms and functions of DNA mismatch repair. Cell Research. 18, 85-98.

LI, Y. & SHUAI, L. 2017. A versatile genetic tool: Haploid cells. Cell Research & Therapy 8, 197.

LORD, C. J. & ASHWORTH, A. 2017. PARP inhibitors: Synthetic lethality in the clinic. Science 355, 1152–1158.

LOUIS, D. N., PERRY, A., REIFENBERGER, G., VON DEIMLING, A., FIGARELLA-BRANGER, D., CAVENEE, W. K., OHGAKI, H., WIESTLER, O. D., KLEIHUES, P. & ELLISON, D. W. 2016. The 2016 World Health Organization Classification of Tumors of the Central Nervous System: a summary. Acta Neuropathol 131, 803–820.

LOVELESS, A. 1969. Possible relevance of O-6 alkylation of deoxyguanosine to the mutagenicity and carcinogenicity of nitrosamines and nitrosamides. Nature 223, 206-207.

LUO, J., SOLIMINI, N. L. & ELLEDGE, S. J. 2009. Principles of Cancer Therapy: Oncogene and Non-oncogene Addiction. Cell 136, 823-837.

MACARRON, R., BANKS, M. N., BOJANIC, D., BURNS, D. J., CIROVIC, D. A., GARYANTES, T., GREEN, D. V., HERTZBERG, R. P., JANZEN, W. P., PASLAY, J. W., SCHOPFER, U. & SITTAMPALAM, G. S. 2011. Impact of high-throughput screening in biomedical research. Nat Rev Drug Discov, 10, 188-95.

MAO, Z., BOZZELLA, M., SELUANOV, A. & GORBUNOVA, V. 2008. Comparison of nonhomologous end joining and homologous recombination in human cells. DNA Repair 7, 1765–1771.

MARTIN, S. A., MCCARTHY, A., BARBER, L. J., BURGESS, D. J., PARRY, S., LORD, C. J. & ASHWORTH, A. 2009. Methotrexate induces oxidative DNA damage and is selectively lethal to tumour cells with defects in the DNA mismatch repair gene MSH2. EMBO Molecular Medicine 1, 323–337.

MEHTA, M., WEN, P., NISHIKAWA, R., REARDON, D. & PETERS, K. 2017. Critical review of the addition of tumor treating fields (TTFields) to the existing standard of care for newly diagnosed glioblastoma patients. Critical Reviews in Oncology/Hematology 111, 60–65.

MESSAOUDI, K., CLAVREUL, A. & LAGARCE, F. 2015. Toward an effective strategy in glioblastoma treatment. Part I: resistance mechanisms and strategies to overcome resistance of glioblastoma to temozolomide. Drug Discovery Today 20, 899-905.

MICHALCZYK, K. & ZIMAN, M. 2005. Nestin structure and predicted function in cellular cytoskeletal organization. Histol HIstopathol 20, 665-671.

MIDDLETON, M. R., GROB, J. J., AARONSON, N., FIERLBECK, G., TILGEN, W., SEITER, S., GORE, M., AAMDAL, S., CEBON, J., COATES, A., DRENO, B., HENZ, M., SCHADENDORF, D., KAPP, A., WEISS, J., FRAASS, U., STATKEVICH, P., MULLER, M. & THATCHER, N. 2000. Randomized phase III study of temozolomide versus dacarbazine in the treatment of patients with advanced metastatic malignant melanoma. Journal of clinical oncology: official journal of the American Society of Clinical Oncology 18, 158-166.

MINAMI, N., MAEDA, Y., SHIBAO, S., ARIMA, Y., OHKA, F., KONDO, Y., MARUYAMA, K., KUSUHARA, M., SASAYAMA, T., KOHMURA, E., SAYA, H. & SAMPETREAN, O. 2017. Organotypic brain explant culture as a drug evaluation system for malignant brain tumors. Cancer Medicine 6, 2635–2645.

MITRA, R., FAIN-THORNTON, J. & CRAIG, N. L. 2008. piggyBac can bypass DNA synthesis during cut and paste transposition. EMBO Journal 27, 1097-1109.

MIZUARAI, S., IRIE, H., SCHMATZ, D. & KOTANI, H. 2008. Integrated Genomic and Pharmacological Approaches to Identify Synthetic Lethal Genes as Cancer Therapeutic Targets. Current Molecular Medicine 8, 774-783.

MODRICH, P. & LAHUE, R. 1996. Mismatch Repair in Replication Fidelity, Genetic Recombination, and Cancer Biology. Annual Review of Biochemistry 65, 101-133.

MOODY, C. L. & WHEELHOUSE, R. T. 2014. The medicinal chemistry of imidazotetrazine prodrugs. Pharmaceuticals 7, 797-838

MUNOZ, D. M., CASSIANI, P. J., LI, L., BILLY, E., KORN, J. M., JONES, M. D., GOLJI, J., RUDDY, D. A., YU, K., MCALLISTER, G., DEWECK, A., ABRAMOWSKI, D., WAN, J., SHIRLEY, M. D., NESHAT, S. Y., RAKIEC, D., DE BEAUMONT, R., WEBER, O., KAUFFMANN, A., MCDONALD, E. R., 3RD, KEEN, N., HOFMANN, F., SELLERS, W. R., SCHMELZLE, T., STEGMEIER, F. & SCHLABACH, M. R. 2016. CRISPR Screens Provide a Comprehensive Assessment of Cancer Vulnerabilities but Generate False-Positive Hits for Highly Amplified Genomic Regions. Cancer Discov, 6, 900-13.

NAKADA, M., KITA, D., WATANABE, T., HAYASHI, Y., TENG, L., PYKO, I. V. & HAMADA, J. I. 2011. Aberrant signaling pathways in Glioma. Cancers 3, 3242-3278.

NARITA, Y., NAGANE, M., MISHIMA, K., HUANG, H. J., FURNARI, F. B. & CAVENEE, W. K. 2002. Mutant epidermal growth factor receptor signaling down-

regulates p27 through activation of the phosphatidylinositol 3-kinase/Akt pathway in glioblastomas. Cancer Research 68, 724-730.

NELSON, S. J. & CHA, S. 2003. Imaging glioblastoma multiforme. Cancer Journal 9, 134-145.

NEWLANDS, E. S., BLACKLEDGE, G. R. P., SLACK, J. A., RUSTIN, G. J. S., SMITH, D. B., STUART, N. S. A., QUARTERMAN, C. P., HOFFMAN, R., STEVENS, M. F. G., BRAMPTON, M. H. & GIBSON, A. C. 1992. Phase I trial of temozolomide (CCRG 81045: M&U 39831: NSC 362856). British Journal of Cancer 65,287-291.

NEYNS, B., SADONES, J., JOOSENS, E., BOUTTENS, F., VERBEKE, L., BAURAIN, J. F., D'HONDT, L., STRAUVEN, T., CHASKIS, C., IN'T VELD, P., MICHOTTE, A. & DE GREVE, J. 2009. Stratified phase II trial of cetuximab in patients with recurrent high-grade glioma. Annals of Oncology 20, 1596–1603.

NICKOLOFF, J. A., JONES, D., LEE, S. H., WILLIAMSON, E. A. & HROMAS, R. 2017. Drugging the Cancers Addicted to DNA Repair. JNCI J Natl Cancer Inst 109, djx059.

NISHIMASU, H., RAN, F. A., HSU, P. D., KONERMANN, S., SHEHATA, S. I., DOHMAE, N., ISHITANI, R., ZHANG, F. & NUREKI, O. 2014. Crystal structure of Cas9 in complex with guide RNA and target DNA. Cell 156, 935–949.

OBEROI, R. K., PARRISH, K. E., SIO, T. T., MITTAPALLI, R. K., ELMQUIST, W. F. & SARKARIA, J. N. 2016. Strategies to improve delivery of anticancer drugs across the blood-brain barrier to treat glioblastoma. Neuro-Oncology 18, 27–36.
OHGAKI, H., DESSEN, P., JOURDE, B., HORSTMANN, S., NISHIKAWA, T., DI PATRE, P. L., BURKHARD, C., SCHÜLER, D., PROBST-HENSCH, N. M., MAIORKA, P. C., BAEZA, N., PISANI, P., YONEKAWA, Y., YASARGIL, M. G., LÜTOLF, U. M. & KLEIHUES, P. 2004. Genetic pathways to glioblastoma: A population-based study. Cancer Research 64, 6892– 6899.

OHGAKI, H. & KLEIHUES, P. 2005. Epidemiology and etiology of gliomas. Acta Neuropathologica 109, 93-108.

OLDRINI, B., CURIEL-GARCÍA, Á., MARQUES, C., MATIA, V., ULUÇKAN, Ö., GRAÑA-CASTRO, O., TORRES-RUIZ, R., RODRIGUEZ-PERALES, S., HUSE, J. T. & SQUATRITO, M. 2018. Somatic genome editing with the RCAS-TVA-CRISPR-Cas9 system for precision tumor modeling. Nature Communications 9, 1466.

OMURO, A. & DEANGELIS, L. M. 2013. Glioblastoma and other malignant gliomas: A clinical review. Clinical Review & Education 310, Clinical Review & Education 310, 1842-1850.

OSTROM, Q. T. & BARNHOLTZ-SLOAN, J. S. 2011. Current state of our knowledge on brain tumor epidemiology. Current Neurology and Neuroscience Reports 11, 329-335.

OSTROM, Q. T., GITTLEMAN, H., LIAO, P., VECCHIONE-KOVAL, T., WOLINSKY, Y., KRUCHKO, C. & BARNHOLTZ-SLOAN, J. S. 2017. CBTRUS Statistical Report: Primary brain and other central nervous system tumors diagnosed in the United States in 2010–2014. Neuro-Oncology 19, 1-88.

OVERBALLE-PETERSEN, S., HARMS, K., ORLANDO, L. A. A., MAYAR, J. V. M., RASMUSSEN, S., DAHL, T. W., ROSING, M. T., POOLE, A. M., SICHERITZ-PONTEN, T., BRUNAK, S., INSELMANN, S., DE VRIES, J., WACKERNAGEL, W., PYBUS, O. G., NIELSEN, R., JOHNSEN, P. J., NIELSEN, K. M. & WILLERSLEV, E. 2013. Bacterial natural transformation by highly fragmented and damaged DNA. Proceedings of the National Academy of Sciences 110, 1919860-19865.

PAGLIARINI, R., SHAO, W. & SELLERS, W. R. 2015. Oncogene addiction: pathways of therapeutic response, resistance, and road maps toward a cure. EMBO reports 16, 280-296.

PANDZIC, T., LARSSON, J., HE, L., KUNDU, S., BAN, K., AKHTAR-ALI, M., HELLSTRÖM, A. R., SCHUH, A., CLIFFORD, R., BLAKEMORE, S. J., STREFFORD, J. C., BAUMANN, T., LOPEZ-GUILLERMO, A., CAMPO, E., LJUNGSTRÖM, V., MANSOURI, L., ROSENQUIST, R., SJÖBLOM, T. & HELLSTRÖM, M. 2016. Transposon mutagenesis reveals fludarabine resistance mechanisms in chronic lymphocytic leukemia. Clinical Cancer Research 22, 6217-6228.

PAOLILLO, M., BOSELLI, C. & SCHINELLI, S. 2018. Glioblastoma under siege: An overview of current therapeutic strategies. Brain Sciences 8,15.

PARATO, K. A., SENGER, D., FORSYTH, P. A. J. & BELL, J. C. 2005. Recent progress in the battle between oncolytic viruses and tumours. Nature Reviews Cancer 5, 965-976.

PARLAKIAN, A., PAULIN, D., IZMIRYAN, A., XUE, Z. & LI, Z. 2016. Intermediate filaments in peripheral nervous system: Their expression, dysfunction and diseases. Revue Neurologique (Paris) 172, 607-613.

PARRISH, K. E., POKORNY, J., MITTAPALLI, R. K., BAKKEN, K., SARKARIA, J. N. & ELMQUIST, W. F. 2015. Efflux Transporters at the Blood-Brain Barrier Limit Delivery and Efficacy of Cyclin-Dependent Kinase 4/6 Inhibitor Palbociclib (PD-0332991) in an Orthotopic Brain Tumor Model. Journal of Pharmacology and Experimental Therapeutics 355, 264–27.

PARSONS, D. W., JONES, S., ZHANG, X., LIN, J. C.-H., LEARY, R. J., ANGENENDT, P., MANKOO, P., CARTER, H., SIU, I. M., GALLIA, G. L., OLIVI, A., MCLENDON, R., RASHEED, B. A., KEIR, S., NIKOLSKAYA, T., NIKOLSKY, Y., BUSAM, D. A., TEKLEAB, H., DIAZ, L. A., HARTIGAN, J., SMITH, D. R., STRAUSBERG, R. L., MARIE, S. K. N., SHINJO, S. M. O., YAN, H., RIGGINS, G. J., BIGNER, D. D., KARCHIN, R., PAPADOPOULOS, N., PARMIGIANI, G.,

VOGELSTEIN, B., VELCULESCU, V. E. & KINZLER, K. W. 2008. An integrated genomic analysis of human glioblastoma multiforme. Science 321, 1807-1812.

PENNA, L. S., HENRIQUES, J. A. P. & BONATTO, D. 2017. Anti-mitotic agents: Are they emerging molecules for cancer treatment? Pharmacology & Therapeutics 173, 67-82.

PETROPOULOS, C. J. & HUGHES, S. H. 1991. Replication-competent retrovirus vectors for the transfer and expression of gene cassettes in avian cells. J Virol, 65, 3728-3737.

PETTITT, S. J., KRASTEV, D. B., PEMBERTON, H. N., FONTEBASSO, Y., FRANKUM, J., REHMAN, F. L., BROUGH, R., SONG, F., BAJRAMI, I., RAFIQ, R., WALLBERG, F., KOZAREWA, I., FENWICK, K., ARMISEN-GARRIDO, J., SWAIN, A., GULATI, A., CAMPBELL, J., ASHWORTH, A. & LORD, C. J. 2017. Genome-wide barcoded transposon screen for cancer drug sensitivity in haploid mouse embryonic stem cells. Scientific Data 4,170020.

PETTITT, S. J., REHMAN, F. L., BAJRAMI, I., BROUGH, R., WALLBERG, F., KOZAREWA, I., FENWICK, K., ASSIOTIS, I., CHEN, L., CAMPBELL, J., LORD, C. J. & ASHWORTH, A. 2013. A Genetic Screen Using the PiggyBac Transposon in Haploid Cells Identifies Parp1 as a Mediator of Olaparib Toxicity. PLoS ONE 8, e61520.

PICCA, A., BERZERO, G., BIELLE, F., TOUAT, M., SAVATOVSKY, J., POLIVKA, M., TRISOLINI, E., MEUNIER, S., SCHMITT, Y., IDBAIH, A., HOANG-XUAN, K., DELATTRE, J.-Y., MOKHTARI, K., DI STEFANO, A. L. & SANSON, M. 2018. FGFR1 actionable mutations, molecular specificities, and outcome of adult midline gliomas. Neurology 90, e2086-e2094.

POLLACK, I. F., JAKACKI, R. I., BUTTERFIELD, L. H., HAMILTON, R. L., PANIGRAHY, A., POTTER, D. M., CONNELLY, A. K., DIBRIDGE, S. A., WHITESIDE, T. L. & OKADA, H. 2014. Antigen-specific immune responses and clinical outcome after vaccination with glioma-associated antigen peptides and polyinosinic-polycytidylic acid stabilized by lysine and carboxymethylcellulose in children with newly diagnosed malignant brainstem and and nonbrainstem gliomas. Journal of Clinical Oncology 32, 2050-2058.

POTTER, C. J. & LUO, L. 2010. Splinkerette PCR for mapping transposable elements in Drosophila. PLoS ONE 5, e10168.

RAMASWAMY, V. & TAYLOR, M. D. 2016. Fall of the Optical Wall: Freedom from the Tyranny of the Microscope Improves Glioma Risk Stratification. Cancer Cell 29, 137-138.

RASMUSSEN, B. K., HANSEN, S., LAURSEN, R. J., KOSTELJANETZ, M., SCHULTZ, H., NØRGÅRD, B. M., GULDBERG, R. & GRADEL, K. O. 2017. Epidemiology of glioma: clinical characteristics, symptoms, and predictors of glioma patients grade I–IV in the the Danish Neuro-Oncology Registry. Journal of Neuro-Oncology 35, 571-579.

REID, J. M., STEVENS, D. C., RUBIN, J. & AMES, M. M. 1997. Pharmacokinetics of 3-methyl-(triazen-1-yl)imidazole-4-carboximide following administration of temozolomide to patients with advanced cancer. Clinical Cancer Research 3, 2393-2398.

REIFENBERGER, J., REIFENBERGER, G., LIU, L., JAMES, C. D., WECHSLER, W. & COLLINS, V. P. 1994. Molecular genetic analysis of oligodendroglial tumors shows preferential allelic deletions on 19q and 1p. Am J Pathol, 145, 1175-90.

REIFENBERGER, G., WIRSCHING, H. G., KNOBBE-THOMSEN, C. B. & WELLER, M. 2017. Advances in the molecular genetics of gliomas-implications for classification and therapy. Nature Reviews 14, 434-452.

RIZVI, N. A., HELLMANN, M. D., SNYDER, A., KVISTBORG, P., MAKAROV, V., HAVEL, J. J., LEE, W., YUAN, J., WONG, P., HO, T. S., MILLER, M. L., REKHTMAN, N., MOREIRA, A. L., IBRAHIM, F., BRUGGEMAN, C., GASMI, B., ZAPPASODI, R., MAEDA, Y., SANDER, C., GARON, E. B., MERGHOUB, T., WOLCHOK, J. D., SCHUMACHER, T. N. & CHAN, T. A. 2015. Mutational landscape determines sensitivity to PD-1 blockade in non-small cell lung cancer. Science 348, 124-128.

ROOS, W. P., BATISTA, L. F. Z., NAUMANN, S. C., WICK, W., WELLER, M., MENCK, C. F. M. & KAINA, B. 2007. Apoptosis in malignant glioma cells triggered by the temozolomide-induced DNA lesion O6-methylguanine. Oncogene 26, 186–197.

ROOS, W. P. & KAINA, B. 2013. DNA damage-induced cell death: From specific DNA lesions to the DNA damage response and apoptosis. Cancer Letters 332, 237–248.

RUZANKINA, Y., PINZON-GUZMAN, C., ASARE, A., ONG, T., PONTANO, L., COTSARELIS, G., ZEDIAK, V. P., VELEZ, M., BHANDOOLA, A. & BROWN, E. J. 2007. Deletion of the Developmentally Essential Gene ATR in Adult Mice Leads to Age-Related Phenotypes and Stem Cell Loss. Cell Stem Cell 1, 113–126.

SAEIDNIA, S., MANAYI, A. & ABDOLLAHI, M. 2016. From in vitro Experiments to in vivo and Clinical Studies; Pros and Cons. Current Drug Discovery Technologies 12, 218-224.

SANAI, N., ALVAREZ-BUYLLA, A. & BERGER, M. S. 2005. Neural Stem Cells and the Origin of Gliomas. New England Journal of Medicine 225, 811-822.

SARKARIA, J. N., HU, L. S., PARNEY, I. F., PAFUNDI, D. H., BRINKMANN, D. H., LAACK, N. N., GIANNINI, C., BURNS, T. C., KIZILBASH, S. H., LARAMY, J. K., SWANSON, K. R., KAUFMANN, T. J., BROWN, P. D., AGAR, N. Y. R., GALANIS, E., BUCKNER, J. C. & ELMQUIST, W. F. 2018. Is the blood-brain barrier really disrupted in all glioblastomas? A critical assessment of existing clinical data. Neuro-Oncology 20, 184–191.

SCHAEFER-KLEIN, J., GIVOL, I., BARSOV, E. V., WHITCOMB, J. M., VANBROCKLIN, M., FOSTER, D. N., FEDERSPIEL, M. J. & HUGHES, S. H. 1998. The EV-O-derived cell line DF-1 supports the efficient replication of avian leukosis-sarcoma viruses and vectors. Virology 248, 305–311.

SCHWARTZENTRUBER, J., KORSHUNOV, A., LIU, X. Y., JONES, D. T., PFAFF, E., JACOB, K., STURM, D., FONTEBASSO, A. M., QUANG, D. A., TONJES, M., HOVESTADT, V., ALBRECHT, S., KOOL, M., NANTEL, A., KONERMANN, C., LINDROTH, A., JAGER, N., RAUSCH, T., RYZHOVA, M., KORBEL, J. O., HIELSCHER, T., HAUSER, P., GARAMI, M., KLEKNER, A., BOGNAR, L., EBINGER, M., SCHUHMANN, M. U., SCHEURLEN, W., PEKRUN, A., FRUHWALD, M. C., ROGGENDORF, W., KRAMM, C., DURKEN, M., ATKINSON, J., LEPAGE, P., MONTPETIT, A., ZAKRZEWSKA, M., ZAKRZEWSKI, K., LIBERSKI, P. P., DONG, Z., SIEGEL, P., KULOZIK, A. E., ZAPATKA, M., GUHA, A., MALKIN, D., FELSBERG, J., REIFENBERGER, G., VON DEIMLING, A., ICHIMURA, K., COLLINS, V. P., WITT, H., MILDE, T., WITT, O., ZHANG, C., CASTELO-BRANCO, P., LICHTER, P., FAURY, D., TABORI, U., PLASS, C., MAJEWSKI, J., PFISTER, S. M. & JABADO, N. 2012. Driver mutations in histone H3.3 and chromatin remodelling genes in paediatric glioblastoma. Nature, 482, 226-31.

SEIDLER, B., SCHMIDT, A., MAYR, U., NAKHAI, H., SCHMID, R. M., SCHNEIDER, G. & SAUR, D. 2008. A Cre-loxP-based mouse model for conditional somatic gene expression and knockdown in vivo by using avian retroviral vectors. Proceedings of the National Academy of Sciences 105, 10137–10142.

SEOM 2017. La cifras del cáncer en España. Seom. M-2172-2017.

SHALEM, O., SANJANA, N. E., HARTENIAN, E., SHI, X., SCOTT, D. A., MIKKELSON, T., HECKL, D., EBERT, B. L., ROOT, D. E., DOENCH, J. G. & ZHANG, F. 2014. Genome-scale CRISPR-Cas9 knockout screening in human cells. Science, 343, 84-87.

SHAO, H., LI, X., NOLAN, T. J., MASSEY, H. C., PEARCE, E. J. & LOK, J. B. 2012. Transposon-mediated Chromosomal Integration of Transgenes in the Parasitic Nematode Strongyloides ratti and Establishment of Stable Transgenic Lines. PLoS Pathogens 8, e1002871.

SHARMA, S. & PETSALAKI, E. 2018. Application of CRISPR-Cas9 Based Genome-Wide Screening Approaches to Study Cellular Signalling Mechanisms. Int J Mol Sci, 19.

SHENG, Z., LI, L., ZHU, L. J., SMITH, T. W., DEMERS, A., ROSS, A. H., MOSER, R. P. & GREEN, M. R. 2010. A genome-wide RNA interference screen reveals an essential CREB3L2-ATF5-MCL1 survival pathway in malignant glioma with therapeutic implications. Nature Medicine 16, 671-678.

SHERGALIS, A., BANKHEAD, A., LUESAKUL, U., MUANGSIN, N. & NEAMATI, N. 2018. Current Challenges and Opportunities in Treating Glioblastoma. Pharmacological Reviews 70, 412-445.
SIEGEL, R. L., MILLER, K. D. & JEMAL, A. 2018. Cancer statistics, 2018. CA: A Cancer Journal for Clinicians 68, 7-30.

SILBER, J. R., BOBOLA, M., BLANK, A. & CHAMBERLAIN, M. C. 2012. O6-Methylguanine-DNA methyltransferase in glioma therapy: Promise and problems. Biochimica et Biophysica Acta - Reviews on Cancer 1826, 71-82.

SINGH, S. K., HAWKINS, C., CLARKE, I. D., SQUIRE, J. A., BAYANI, J., HIDE, T., HENKELMAN, R. M., CUSIMANO, M. D. & DIRKS, P. B. 2004. Identification of human brain tumour initiating cells. Nature 432, 396-401.

SKARNES, W. C., ROSEN, B., WEST, A. P., KOUTSOURAKIS, M., BUSHELL, W., IYER, V., MUJICA, A. O., THOMAS, M., HARROW, J., COX, T., JACKSON, D., SEVERIN, J., BIGGS, P., FU, J., NEFEDOV, M., DE JONG, P. J., STEWART, A. F. & BRADLEY, A. 2011. A conditional knockout resource for the genome-wide study of mouse gene function. Nature 474, 337-344.

SMITH, C. & IRONSIDE, J. W. 2007. Diagnosis and pathogenesis of gliomas. Current Diagnostic Pathology 13, 180-192.

SNITKOVSKY, S., NIEDERMAN, T. M., CARTER, B. S., MULLIGAN, R. C. & YOUNG, J. A. 2000. A TVA-single-chain antibody fusion protein mediates specific targeting of a subgroup A avian leukosis virus vector to cells expressing a tumor-specific form of epidermal growth factor receptor. Journal of virology 74, 9540–9545.

SQUATRITO, M., BRENNAN, C. W., HELMY, K., HUSE, J. T., PETRINI, J. H. & HOLLAND, E. C. 2010. Loss of ATM/Chk2/p53 Pathway Components Accelerates Tumor Development and Contributes to Radiation Resistance in Gliomas. Cancer Cell 18, 619–629.

STERNBERG, S. H., LAFRANCE, B., KAPLAN, M. & DOUDNA, J. A. 2015. Conformational control of DNA target cleavage by CRISPR-Cas9. Nature 527, 110-123.

STERNBERG, S. H., REDDING, S., JINEK, M., GREENE, E. C. & DOUDNA, J. A. 2014. DNA interrogation by the CRISPR RNA-guided endonuclease Cas9. Nature 507, 62-73.

STRAND, M., PROLLA, T. A., LISKAY, R. M. & PETES, T. D. 1993. Destabilization of tracts of simple repetitive DNA in yeast by mutations affecting DNA mismatch repair. Nature 365, 274-276.

STUPP, R., MASON, W., VAN DEN BENT, M. J., WELLER, M., FISHER, B. M., TAPHOORN, M. J. B., BELANGER, K., BRANDES, A. A., MAROSI, C., BOGDAHN, U., CURSCHMANN, J., JANZER, R. C., LUDWIN, S. K., GORLIA, T., ALLGEIER, A., LACOMBE, D., CAIRNCROSS, G., EISENHAUER, E. &

MIRIMANOFF, R. O. 2005. Radiotherapy plus Concomitant\nand Adjuvant Temozolomide for Glioblastoma. The New England Journal of Medicine 352, 987-996.

STUPP, R., TAILLIBERT, S., KANNER, A. A., KESARI, S., STEINBERG, D. M., TOMS, S. A., TAYLOR, L. P., LIEBERMAN, F., SILVANI, A., FINK, K. L., BARNETT, G. H., ZHU, J. J., HENSON, J. W., ENGELHARD, H. H., CHEN, T. C., TRAN, D. D., SROUBEK, J., TRAN, N. D., HOTTINGER, A. F., LANDOLFI, J., DESAI, R., CAROLI, M., KEW, Y., HONNORAT, J., IDBAIH, A., KIRSON, E. D., WEINBERG, U., PALTI, Y., HEGI, M. E. & RAM, Z. 2015. Maintenance therapy with tumor-Treating fields plus temozolomide vs temozolomide alone for glioblastoma a randomized clinical trial. JAMA - Journal of the American Medical Association 314, 2535-2543.

STUPP, R., WONG, E. T., KANNER, A. A., STEINBERG, D., ENGELHARD, H., HEIDECKE, V., KIRSON, E. D., TAILLIBERT, S., LIEBERMANN, F., DBALÝ, V., RAM, Z., VILLANO, J. L., RAINOV, N., WEINBERG, U., SCHIFF, D., KUNSCHNER, L., RAIZER, J., HONNORAT, J., SLOAN, A., MALKIN, M., LANDOLFI, J. C., PAYER, F., MEHDORN, M., WEIL, R. J., PANNULLO, S. C., WESTPHAL, M., SMRCKA, M., CHIN, L., KOSTRON, H., HOFER, S., BRUCE, J., COSGROVE, R., PALEOLOGOUS, N., PALTI, Y. & GUTIN, P. H. 2012. NovoTTF-100A versus physician's choice chemotherapy in recurrent glioblastoma: A randomised phase III trial of a novel treatment modality. European Journal of Cancer 48, 2192– 2202.

TEJADA, S., DIEZ-VALLE, R., DOMINGUEZ, P. D., PATINO-GARCIA, A., GONZALEZ-HUARRIZ, M., FUEYO, J., GOMEZ-MANZANO, C., IDOATE, M. A., PETERKIN, J. & ALONSO, M. M. 2018. DNX-2401, an Oncolytic Virus, for the Treatment of Newly Diagnosed Diffuse Intrinsic Pontine Gliomas: A Case Report. Front Oncol, 8, 61.

TERASAKI, M., SHIBUI, S., NARITA, Y., FUJIMAKI, T., AOKI, T., KAJIWARA, K., SAWAMURA, Y., KURISU, K., MINETA, T., YAMADA, A. & ITOH, K. 2011. Phase I trial of a personalized peptide vaccine for patients positive for human leukocyte antigen-A24 with recurrent or progressive glioblastoma multiforme. Journal of Clinical Oncology 29, 337-44.

THEELER, B. J. & GROVES, M. D. 2011. High-grade gliomas. Current Treatment Options in Neurology 13, 386-399.

TRONCHE, F., KELLENDONK, C., KRETZ, O., GASS, P., ANLAG, K., ORBAN, P. C., BOCK, R., KLEIN, R. & SCHÜTZ, G. 1999. Disruption of the glucocorticoid receptor gene in the nervous system results in reduced anxiety. Nature Genetics 22, 99-103.

TSAI, S. Q. & JOUNG, J. K. 2016. Defining and improving the genome-wide specificities of CRISPR-Cas9 nucleases. Nat Rev Genet, 17, 300-12.

VALIENTE, M., OBENAUF, A. C., JIN, X., CHEN, Q., ZHANG, X. H. F., LEE, D. J., CHAFT, J. E., KRIS, M. G., HUSE, J. T., BROGI, E. & MASSAGUÉ, J. 2014.

Serpins promote cancer cell survival and vascular Co-option in brain metastasis. Cell 156, 1002–1016.

VAN LEEUWEN, J., PONS, C., MELLOR, J. C., YAMAGUCHI, T. N., FRIESEN, H., KOSCHWANEZ, J., UŠAJ, M. M., PECHLANER, M., TAKAR, M., UŠAJ, M., VANDER SLUIS, B., ANDRUSIAK, K., BANSAL, P., BARYSHNIKOVA, A., BOONE, C. E., CAO, J., COTE, A., GEBBIA, M., HORECKA, G., HORECKA, I., KUZMIN, E., LEGRO, N., LIANG, W., VAN LIESHOUT, N., MCNEE, M., SAN LUIS, B. J., SHAERI, F., SHUTERIQI, E., SUN, S., YANG, L., YOUN, J. Y., YUEN, M., COSTANZO, M., GINGRAS, A. C., ALOY, P., OOSTENBRINK, C., MURRAY, A., GRAHAM, T. R., MYERS, C. L., ANDREWS, B. J., ROTH, F. P. & BOONE, C. 2016. Exploring genetic suppression interactions on a global scale. Science 354, 599-611.

VAN TELLINGEN, O., YETKIN-ARIK, B., DE GOOIJER, M. C., WESSELING, P., WURDINGER, T. & DE VRIES, H. E. 2015. Overcoming the blood-brain tumor barrier for effective glioblastoma treatment. Drug Resistance Updates 19, 1-12.

VERBEEK, B., SOUTHGATE, T. D., GILHAM, D. E. & MARGISON, G. P. 2008. O6-Methylguanine-DNA methyltransferase inactivation and chemotherapy. British Medical Bulletin 85, 17–33.

VERHAAK, R. G. W., HOADLEY, K. A., PURDOM, E., WANG, V., QI, Y., WILKERSON, M. D., MILLER, C. R., DING, L., GOLUB, T., MESIROV, J. P., ALEXE, G., LAWRENCE, M., O'KELLY, M., TAMAYO, P., WEIR, B. A., GABRIEL, S., WINCKLER, W., GUPTA, S., JAKKULA, L., FEILER, H. S., HODGSON, J. G., JAMES, C. D., SARKARIA, J. N., BRENNAN, C., KAHN, A., SPELLMAN, P. T., WILSON, R. K., SPEED, T. P., GRAY, J. W., MEYERSON, M., GETZ, G., PEROU, C. M. & HAYES, D. N. 2010. Integrated Genomic Analysis Identifies Clinically Relevant Subtypes of Glioblastoma Characterized by Abnormalities in PDGFRA, IDH1, EGFR, and NF1. Cancer Cell 17, 98–110.

VREDENBURGH, J. J., DESJARDINS, A., HERNDON, J. E., MARCELLO, J., REARDON, D. A., QUINN, J. A., RICH, J. N., SATHORNSUMETEE, S., GURURANGAN, S., SAMPSON, J., WAGNER, M., BAILEY, L., BIGNER, D. D., FRIEDMAN, A. H. & FRIEDMAN, H. S. 2007. Bevacizumab plus irinotecan in recurrent glioblastoma multiforme. Journal of clinical oncology: official journal of the American Society of Clinical Oncology. Journal of Clinical Oncology 25, 4722-4729.

WANG, J., CAZZATO, E., LADEWIG, E., FRATTINI, V., ROSENBLOOM, D. I., ZAIRIS, S., ABATE, F., LIU, Z., ELLIOTT, O., SHIN, Y. J., LEE, J. K., LEE, I. H., PARK, W. Y., EOLI, M., BLUMBERG, A. J., LASORELLA, A., NAM, D. H., FINOCCHIARO, G., IAVARONE, A. & RABADAN, R. 2016. Clonal evolution of glioblastoma under therapy. Nat Genet, 48, 768-76.

WANG, H., XU, T., JIANG, Y., XU, H., YAN, Y., FU, D. & CHEN, J. 2015. The challenges and the promise of molecular targeted therapy in malignant gliomas. Neoplasia (New York, N.Y.) 17, 239-255.

WELLER, M., BUTOWSKI, N., TRAN, D. D., RECHT, L. D., LIM, M., HIRTE, H., ASHBY, L., MECHTLER, L., GOLDLUST, S. A., IWAMOTO, F., DRAPPATZ, J., O'ROURKE, D. M., WONG, M., HAMILTON, M. G., FINOCCHIARO, G., PERRY, J., WICK, W., GREEN, J., HE, Y., TURNER, C. D., YELLIN, M. J., KELER, T., DAVIS, T. A., STUPP, R., SAMPSON, J. H., BUTOWSKI, N., CAMPIAN, J., RECHT, L., LIM, M., ASHBY, L., DRAPPATZ, J., HIRTE, H., IWAMOTO, F., MECHTLER, L., GOLDLUST, S., BECKER, K., BARNETT, G., NICHOLAS, G., DESJARDINS, A., BENKERS, T., WAGLE, N., GROVES, M., KESARI, S., HORVATH, Z., MERRELL, R., CURRY, R., O'ROURKE, J., SCHUSTER, D., WONG, M., MRUGALA, M., JENSEN, R., TRUSHEIM, J., LESSER, G., BELANGER, K., SLOAN, A., PUROW, B., FINK, K., RAIZER, J., SCHULDER, M., NAIR, S., PEAK, S., PERRY, J., BRANDES, A., WELLER, M., MOHILE, N., LANDOLFI, J., OLSON, J., FINOCCHIARO, G., JENNENS, R., DESOUZA, P., ROBINSON, B., CRITTENDEN, M., SHIH, K., FLOWERS, A., ONG, S., CONNELLY, J., HADJIPANAYIS, C., GIGLIO, P., MOTT, F., MATHIEU, D., LESSARD, N., SEPULVEDA, S. J., LÖVEY, J., WHEELER, H., INGLIS, P. L., HARDIE, C., BOTA, D., LESNIAK, M., PORTNOW, J., FRANKEL, B., JUNCK, L., THOMPSON, R., BERK, L., MCGHIE, J., MACDONALD, D., SARAN, F., SOFFIETTI, R., BLUMENTHAL, D., ANDRÉ DE, S. B. C. M., NOWAK, A., et al. 2017. Rindopepimut with temozolomide for patients with newly diagnosed, EGFRvIII-expressing glioblastoma (ACT IV): a randomised, double-blind, international phase 3 trial. The Lancet Oncology 18, 1373-1385.

WELLER, M., WICK, W., ALDAPE, K., BRADA, M., BERGER, M., PFISTER, S. M., NISHIKAWA, R., ROSENTHAL, M., WEN, P. Y., STUPP, R. & REIFENBERGER, G. 2015. Glioma. Nature Reviews Disease Primers 1, 1-18.

WERDER, A. V., SEIDLER, B., SCHMID, R. M., SCHNEIDER, G. & SAUR, D. 2012. Production of avian retroviruses and tissue-specific somatic retroviral gene transfer in vivo using the RCAS/TVA system. Nature Protocols 7, 1167-1183.

WICK, W., WELLER, M., VAN DEN BENT, M. & STUPP, R. 2010. Bevacizumab and recurrent malignant gliomas: A European perspective. Journal of Clinical Oncololy 28, e188-189.

WIEDENHEFT, B., STERNBERG, S. H. & DOUDNA, J. A. 2012. RNA-guided genetic silencing systems in bacteria and archaea. Nature 482, 331-338.

WIESTLER, B., CAPPER, D., HOLLAND-LETZ, T., KORSHUNOV, A., VON DEIMLING, A., PFISTER, S. M., PLATTEN, M., WELLER, M. & WICK, W. 2013. ATRX loss refines the classification of anaplastic gliomas and identifies a subgroup of IDH mutant astrocytic tumors with better prognosis. Acta Neuropathol, 126, 443-51.

WILSON, T. A., KARAJANNIS, M. A. & HARTER, D. H. 2014. Glioblastoma multiforme: State of the art and future therapeutics. Surgical neurology international 5, 64.

WINOGRAD, E. K., CIESIELSKI, M. J. & FENSTERMAKER, R. A. 2016. Novel vaccines for glioblastoma: Clinical update and perspective. Immunotherapy 8, 1293-1308.

WOODWORTH, G. F., DUNN, G. P., NANCE, E. A., HANES, J. & BREM, H. 2014. Emerging Insights into Barriers to Effective Brain Tumor Therapeutics. Frontiers in Oncology 4,126.

WU, Q. & VASQUEZ, K. M. 2008. Human MLH1 protein participates in genomic damage checkpoint signaling in response to DNA interstrand crosslinks, while MSH2 functions in DNA repair. PLoS Genetics 4, e1000189.

WU, S. C. Y., MEIR, Y. J. J., COATES, C. J., HANDLER, A. M., PELCZAR, P., MOISYADI, S. & KAMINSKI, J. M. 2006. piggyBac is a flexible and highly active transposon as compared to Sleeping Beauty, Tol2, and Mos1 in mammalian cells. Proceedings of the National Academy of Sciences 103, 15008–15013.

XUE, S., HU, M., IYER, V. & YU, J. 2017. Blocking the PD-1/PD-L1 pathway in glioma: A potential new treatment strategy. Journal of Hematology & Oncology 10, 81.

YAN, Y., XU, Z., DAI, S., QIAN, L., SUN, L. & GONG, Z. 2016. Targeting autophagy to sensitive glioma to temozolomide treatment. J Exp Clin Cancer Res, 35, 23.

YANG, Z. & WANG, K. K. W. 2015. Glial fibrillary acidic protein: from intermediate filament assembly and gliosis to neurobiomarker. Trends in neurosciences 38, 364-374.

YIP, S., IAFRATE, A. J. & LOUIS, D. N. 2008. Molecular diagnostic testing in malignant gliomas: A practical update on predictive markers. J Neuropathol Exp Neurol 67, 1-14.

YIP, S., MIAO, J., CAHILL, D. P., IAFRATE, A. J., ALDAPE, K., NUTT, C. L. & LOUIS, D. N. 2009. MSH6 mutations arise in glioblastomas during temozolomide therapy and mediate temozolomide resistance. Clinical Cancer Research 15, 4622-4629.

YOUNG, R. M., JAMSHIDI, A., DAVIS, G. & SHERMAN, J. H. 2015. Current trends in the surgical management and treatment of adult glioblastoma. Annals of translational medicine 9, 121.

YUNG, W. K. A., PRADOS, M. D., YAYA-TUR, R., ROSENFELD, S. S., BRADA, M., FRIEDMAN, H. S., ALBRIGHT, R., OLSON, J., CHANG, S. M., O'NEILL, A. M., FRIEDMAN, A. H., BRUNER, J., YUE, N., DUGAN, M., ZAKNOEN, S. & LEVIN, V. A. 1999. Multicenter phase II trial of temozolomide in patients with anaplastic astrocytoma or anaplastic oligoastrocytoma at first relapse. Journal of Clinical Oncology 17, 2762-2771.

ZHAI, B., GOBIELEWSKA, A., STEINO, A., BACHA, J. A., BROWN, D. M., NICLOU, S. & DAUGAARD, M. 2017. Abstract 2483: Molecular mechanisms of dianhydrogalactitol (VAL-083) in overcoming chemoresistance in glioblastoma. Cancer Research 77(13 Suppl).

ZHANG, J., F.G. STEVENS, M. & D. BRADSHAW, T. 2012. Temozolomide: Mechanisms of Action, Repair and Resistance. Current Molecular Pharmacology 5, 102-114.

ZHAO, S., JIANG, E., CHEN, S., GU, Y., SHANGGUAN, A. J., LV, T., LUO, L. & YU, Z. 2016. PiggyBac transposon vectors: the tools of the human gene encoding. Transl Lung Cancer Res 5, 120-125.

ZHU, Z., GORMAN, M. J., MCKENZIE, L. D., CHAI, J. N., HUBERT, C. G., PRAGER, B. C., FERNANDEZ, E., RICHNER, J. M., ZHANG, R., SHAN, C., WANG, X., SHI, P.-Y., DIAMOND, M. S., RICH, J. N. & CHHEDA, M. G. 2017. Zika virus has oncolytic activity against glioblastoma stem cells. The Journal of Experimental Medicine 214, 2843–2857.

ZHUO, L., THEIS, M., ALVAREZ-MAYA, I., BRENNER, M., WILLECKE, K. & MESSING, A. 2001. hGFAP-cre transgenic mice for manipulation of glial and neuronal function in vivo. Genesis 31, 85–94.

ZUCKERMANN, M., HOVESTADT, V., KNOBBE-THOMSEN, C. B., ZAPATKA, M., NORTHCOTT, P. A., SCHRAMM, K., BELIC, J., JONES, D. T. W., TSCHIDA, B., MORIARITY, B., LARGAESPADA, D., ROUSSEL, M. F., KORSHUNOV, A., REIFENBERGER, G., PFISTER, S. M., LICHTER, P., KAWAUCHI, D. & GRONYCH, J. 2015. Somatic CRISPR/Cas9-mediated tumour suppressor disruption enables versatile brain tumour modelling. Nature Communications 6,7391.